Dissertation zur Erlangung des Doktorgrades
der Fakultät für Chemie und Pharmazie
der Ludwigs-Maximilians-Universität München

Utilizing different PAT tools to improve scale-up and process transfer for freeze drying

---

Marco Carfagna

aus

Frosinone, Italien

2023

Erklärung

Diese Dissertation wurde im Sinne von §7 der Promotionsordnung vom 28. November 2011 von Herrn Prof. Dr. Wolfgang Frieß betreut.

Eidesstattliche Versicherung

Diese Dissertation wurde eigenständig und ohne unerlaubte Hilfe erarbeitet.

München, 6 September 2023

_____

Marco Carfagna

Dissertation eingereicht am:	15 September 2023
1. Gutachter:	Prof. Dr. Wolfgang Frieß
2. Gutachter:	Prof. Dr. Gerhard Winter
Mündliche Prüfung am:	7 November 2023

Alla mia famiglia e alla mia determinazione.

Acknowledgements

The presented thesis was prepared between September 2016 and December 2020 at the facilities of Coriolis Pharma in Martinsried in collaboration with the Department of Pharmacy, Pharmaceutical Technology and Biopharmaceutics at the Ludwig-Maximilians-University (LMU) Munich under the supervision of Dr. Andrea Hawe from Coriolis Pharma and Prof. Dr. Wolfgang Frieß from the LMU

First and foremost, I want to express my deepest gratitude to my supervisors Prof. Dr. Wolfgang Frieß and Dr. Andrea Hawe who gave me the opportunity to further develop in the fascinating field of the lyophilization.

This project would not have been possible without Dr. Andrea Hawe that provided the most innovative research environment for it. Additionally, her scientific mindset and constructive feedbacks were a constant reference along this "journey".

I am extremely grateful to Prof. Dr. Wolfgang Frieß for the opportunity to join his research group and the guidance of this work. His inspiring approach and tireless enthusiasm have encouraged my research and shaped this thesis.

Dr. Monica Rosa and Dr. Matthias Lucke deserve a huge thank for all the valuable discussions, the wise words and the encouragements especially during the most challenging phases of this project.

A special thanks goes to Dr. Thomas Bosch for his example in term of critical thinking, outstanding management style and his trust in my potential. Working with him has inspired my professional and personal development.

Moreover, Dr. Ahmad Abdul-Fattah and Zarah Schaal are kindly acknowledged for his advice and efforts in the first phase of the project and for her contribution during her internship time, respectively.

Many thanks to all the Coriolis Pharma colleagues for the moments spent together. My office mates Dr. Adam Grabarek, Dr. Wendelin Kranz, Dr. Constanze Helbig and Dr. Marina Guehlke. As it is difficult to mention someone in particular, but I want to express special thanks to Karim Lechgar,

Matthias Wurm, Mirjam Salazar, Benjamin Pevestorf, Dr. Lorenzo Gentiluomo, Dr. Mara Leone, Dr. Eleonora Corrradini, Dr. Julia Baumgartner, Dr. Randy Wanner, Orhan Causevic, Dr. Stefan Heindl, Dr. Tim Menzen, Dr. Georg Schuster and Ivana Ognenoska. Last but not least, I want to thank Dr. Michael and Thomas Wiggenhorn as founders and board representatives of such innovative company. I would like to mention also the colleagues at the Ludwig Maximilian University of Munich. Even if limited, I did appreciate the time spent together.

I would like to express my deepest gratitude to my family and friends for their endless support through the years. Foremost, I want to thank my parents, Giulia and Giampaolo, my sister, Annasilvia, together with her husband Daniele, my parents-in-law, Stefania and Antonio.

Most importantly, I thank my wife Anita, for her continuous support, patience and unconditional love. Our children and the family we created are an infinite source of smiles and happiness.

Table of Contents

Chapter I: Introduction

1. Freeze-drying

Freeze-drying is a common industrial process in which, as indicated in the name, the product is converted in the solid state, during the freezing, and then the solvent, typically water, is removed under vacuum conditions, during the drying phase [1,2]. The alternative name, lyophilization, derives from two ancient Greek words, λύος and φιλέιν and it refers to the high solvent affinity of the product which readily re-dissolves in the solvent [3].

Freeze-drying found broad application in the pharmaceuticals field due to the stabilizing effect and the possibility to extend the shelf life of the labile-molecules [4]. Three main steps are part of the freeze-drying process: (a) freezing (b) primary and (c) secondary drying [3]. As shown in Figure 1, the principal components of a freeze-dryer are represented by the chamber where the process is performed, a condenser used as vapor trap, and the vacuum pump [5]. The chamber holds shelves where the product to be dried is placed. A fluid circulates inside the shelves to regulate the temperature according to the defined parameters.

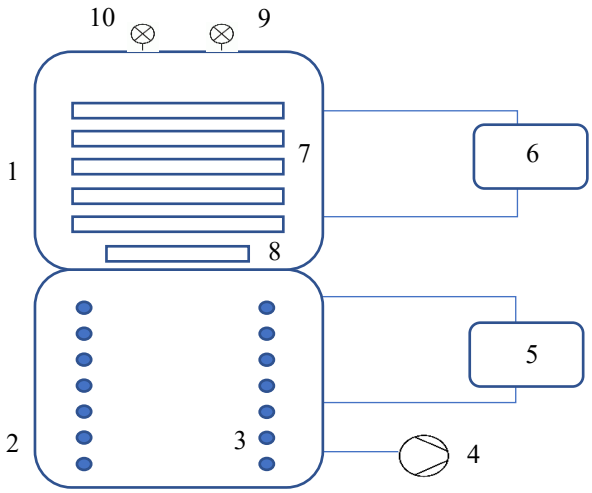

Figure 1 Main components of a typical freeze-dryer: chamber (1), condenser (2), condenser coil (3), vacuum pump (4), cooling condenser system (5), heating / cooling shelf system (6), shelves (7), isolation shelf (8), capacitance manometer (9) and Pirani gauge (10)

The pressure inside the chamber s usually monitored and controlled by a capacitance manometer [6]. Additionally, a conductivity gauge (Pirani gauge) is often applied because, in combination with the capacitance manometer, it can indicate the primary drying endpoint [7]. Product temperature is usually monitored with T-type copper-constantan thermocouples (TCs) or platinum resistance temperature detectors (RTDs) [6] placed inside the

product. Further process analytical technology (PAT) tools to monitor the lyophilization are discussed in paragraph 3.

1.1 The Freezing Phase

After the filling the liquid into a glass vial, the vial is partially stoppered and placed on the shelf [8]. As the shelf temperature is decreased, the product temperature (T_p) becomes lower until ice nucleation takes place at T_n (Figure 2) [8]. The exothermic phenomenon of nucleation causes a temperature rise to the equilibrium freezing point; this delta is considered as the degree of supercooling [9]. Subsequently a temperature plateau establishes as the nucleation heat balances the heat removal by the colder shelf and lastly T_p decreases following the temperature of the fluid circulating in the shelf (T_{fluid}) as ice formation comes to completion.

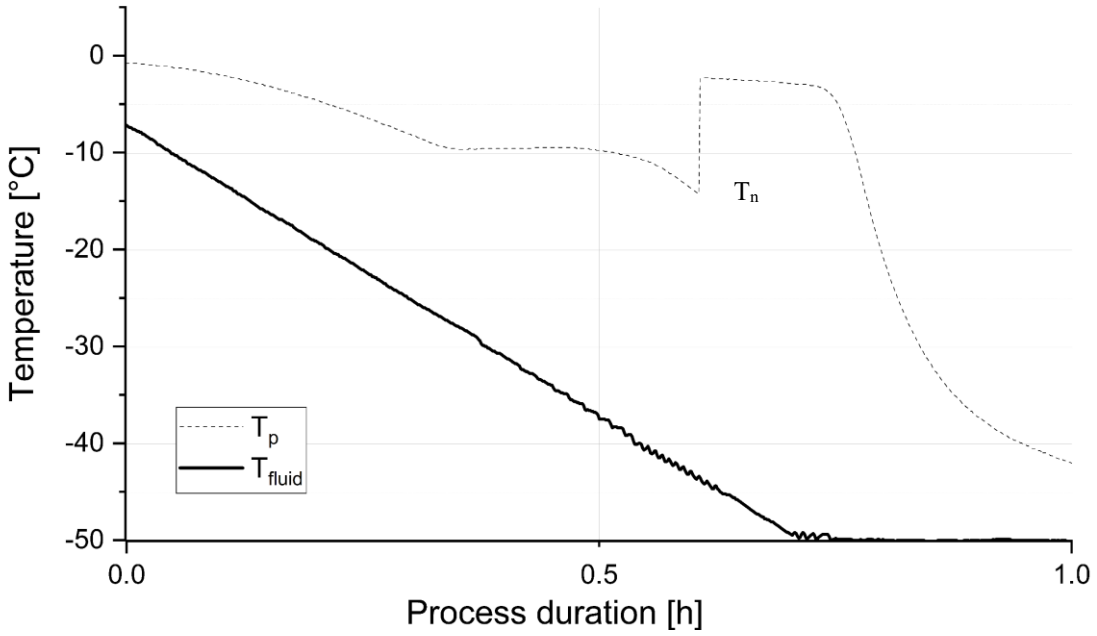

Figure 2 Exemplary temperature of the product (T_P) and of the fluid circulating in the shelf (T_{fluid}) in the freezing phase - Product formulation BSA 150 mg / ml according description in Chapter V – cooling rate 1°C/min

As the ice formation proceeds the remaining solution becomes up-concentrated (freeze-concentration) [3]. This increase in solute concentration comes with a viscosity increase that ends with the product solidification. Formation of a crystalline matrix takes place below the eutectic temperature (T_{eu}). The glass formation of amorphous systems occurs at the glass transition temperature of the maximally freeze-concentrated solution (T_g') [10].

Generally, ice nucleation is a stochastic event that can be influenced by various factors [11]. The temperature at which it takes place (T_n) and the degree of supercooling represent key factors in the ice crystal formation, and

consequently in the morphology of the resulting lyophilizate. Less supercooling typically results in larger ice crystals on formation of larger pores generation as the ice is removed [12]. This in turn leads to a lower resistance to the water vapor removal, a higher mass transfer rate, and a shorter drying time. Thus, the freezing process is of key importance [13,14].

1.2 The Primary Drying Phase

The longest and most critical step of a freeze-drying process is the primary drying phase [7,15]. In this phase, ice is removed by sublimation under vacuum [3]. The chamber pressure is set to the saturation vapor pressure at the target ice temperature. As sublimation is an endothermic process, heat is provided through the fluid circulating in the shelfs [15]. Thus, the primary drying phase is coined by the chamber pressure (P_c) and T_{fluid}. Heat (Q) and mass flux (J_w), which are key can be described by equations 1 and 2 [16,17]:

$$Q = K_v \left(T_{fluid} - T_p\right) \quad (1)$$

$$J_w = (P_i - P_c) \left(R_p\right)^{-1} \quad (2)$$

Q is directly proportional to heat transfer coefficient (K_v) and the difference between T_{fluid} and T_p. The mass flux of water removal is proportional to the difference of between the pressure between at the sublimation interface (P_i) and P_c as well as to the product resistance (R_p) that increases during the process with the thickness of the dried layer [18]. Once the last ice crystal is sublimed, the primary drying phase can be considered completed and the last step, the secondary drying phase, can start.

1.3 The Secondary Drying Phase

At the end of primary drying, water is still present in the product as part of the partially dried freeze-concentrate [3]. The final desired product water content, secondary drying is applied. T_{fluid} is raised while the Pc is kept low or further reduced compared to primary drying [19]. Typically, the target moisture level of the product is 1% or less for an appropriate shelf life [20].

2. The Quality by Design Approach

For many years, the approach to quality aspects in the pharmaceutical field was focused, as indicated in the guideline issued by the Food and Drug Administration (FDA) in 1987, to establish “documented evidence which provides a high degree of assurance that a specific process will consistently produce a product meeting its predetermined specifications and quality attributes” [21]. This quality by testing approach (QbT) was based on data-intensive submission with high relevance of batch history and a quality assurance relying on in-process tests and offline analysis with slow response [24][22]. It is assumed that a validated process will produce always a constant product quality if the same input parameters are applied [23]. In this context, process changes were discouraged as the focus was on reproducibility of historic data. Thus, industry was hesitant to implement new technologies as it was unclear how they were perceived from regulatory bodies [24]. In addition, understanding of

the process was frequently incomplete and scale-up, transfer or troubleshooting were difficult and time-consuming [23]. To mitigate these constraints, in 2002 FDA announced the initiative of the Pharmaceutical Current Good Manufacturing Practices (CGMPs) for the 21st Century and, in 2004, issued a final report on the topic [25]. The aim of this document was to encourage an early adoption of new technologies and to enhance implementation of a risk-based approach [26]. The international conference of harmonization (ICH) with four guidelines provided a framework for an approach where the product quality is ensured based on in-depth scientific understanding [27]. This shift in the quality paradigm to quality by design (QbD) is defined as "a systematic approach to development that begins with predefined objectives and emphasizes product and process understanding and process control, based on sound science and quality risk management" [28]. Starting from predefined goals, it relies on a full process control and understanding based on scientific evidences. QbD is formed from product-related and process-related key elements [29]. The product properties, defined as quality target product profile (QTPP), and subsequent identification of the critical quality attributes (CQAs) through risk assessment, are related to product design. Process-wise, the design space defined as "established multidimensional combination and interaction of material attributes and/or process parameters demonstrated to provide assurance of quality" is of pivotal importance [24].
To understand and define which variation affects the product quality and to which extent, it is necessary that a technology support is effective and efficient in all the phases of product lifecycle. FDA encouraged the application of new technologies by issuing in 2004 the guidance for industry "PAT — A Framework for Innovative Pharmaceutical Development, Manufacturing, and Quality Assurance" [30]. PAT is the acronym of Process Analytical Technology and is defined as "a system for designing, analyzing, and controlling manufacturing through timely measurements (i.e., during processing) of critical quality and performance attributes of raw and in-process materials and processes, with the goal of ensuring final product quality". Four categories of PAT tools are considered in this framework: process analyzers, multivariate tools for design, data acquisition and analysis, process control tools, continuous improvements and knowledge management tools [30]. Among the first category, depending on the place and the timing of analysis, measurements can be: i) at-line whereby sample is removed from the process and analyzed in close proximity to the process stream; ii) on-line whereby sample is diverted by the process line measured and may return into the process line; iii) in-line whereby sample is not removed from the process stream and the analysis can be invasive o noninvasive [30]. All these options are in contrast with the traditional approach "offline" whereby the sample is withdrawn and the measurement takes place in a second moment with delayed results, if real-time decisions are critical [31].

3. PAT tools in lyophilization

General recommendations on an ideal PAT tool were highlighted in literature [32,33]:

a) Available and practical on each freeze-dryer scale to allow smooth transfer /scale-up; in case necessary, retrofitting with minimum modifications
b) Good reproducibility and sensitivity
c) Capable to obtain representative measurement of the selected CQA
d) Ability to withstand steam sterilization

The PAT tools in lyophilization are commonly classified in two broad categories based on the focus of the monitoring, vial(s)- and batch techniques [34,35]. The monitoring tools are in turn classified based on which parameter is measured.

3.1.Vial(s)-monitoring PAT tools

3.1.1 Temperature-based PAT tools

A thermocouple (TC) is one the most common tool in the field [6]. It consists of two wires made of dissimilar electrical conductors. This electrical junction produces a voltage temperature-dependent based on the Seebeck effect. T-type copper-constantan TCs are the most commonly used in the freeze drying [6,36]. The TC tip is placed in the vial and the measurement is considered reliable in the primary drying until the output signal increases abruptly when the tip loses contact to the surrounding dried product [19,39]. Their broad working range, low cost and rapidity of response make TCs a highly valuable support for freeze-drying specialists [6]. However, the uncertainty of the measurement, the incompatibility to automatic loading/unloading system and the invasiveness represent relevant limitations in manufacturing phases.

Usually bulkier than TCs, resistance thermal detectors (RTDs) are another commonly available tool. Their working principle is based on a change in electric resistance when temperature changes [37]. They present better accuracy, robustness and repeatability compared to TC but due to the wire materials, Pt / Ni or Cu, they usually are more expensive than TCs besides the above-mentioned cons of handling and the invasiveness [37,38].

Nowadays, newer technology to measure product temperature wireless gained attention due to compatibility with sterilization and automatic loading / unloading systems. The technology is based on the excitation of a quartz crystal in the sensor placed in the product through an electromagnetic signal. The resonance of the sensor depends on the temperature and the signal is transduced by an external unit [39].

A solution introduced by Kasper et al is an optical fiber sensor (OFS). It consists of an optical fiber irradiated equipped with a fiber Bragg grating (FBG). The change of refractive index is temperature dependent and the value can be determined by the light received post fiber irradiation. An alternative for T_p determination is the soft sensor. This device combines a temperature sensor external to the vial and a mathematical model to establish the temperature profile at the sublimating interface [37].

3.1.2 Heat flux-based PAT tools

As mentioned in paragraph 1.2, the heat flux is one of the key pieces of information to describe the primary drying. After application in many sectors before, heat flux sensors (HFSs) have been introduced in lyophilization [40]. The technology relies on thermocouples (40-50) connected in series and embedded in Kapton layer, a few µm thick. The HFS is placed between the shelf surface and the bottom of the vial. It was applied for checking the freezing phase, detecting end of primary drying and monitoring T_p based on a previous knowledge of K_v [40]. As the potential of this PAT tool was investigated in this PhD thesis, further information can be found in Chapter III, IV and V.

3.1.3 Spectroscopy-based PAT tools

Both, Raman and infrared (IR) spectroscopy have been applied for monitor lyophilization processes. Raman spectroscopy is based on inelastic scattering when a sample is hit by a mono-chromatic light. As water is a weak Raman scatterer, this non-destructive technique is useful, initially offline and later as in-line PAT tools [41,42]. The applications are mainly qualitative to semi-quantitative and range from investigation of solid-state during freezing to structural changes in protein formulations. The only weak spectrum, the risk of heat input and the necessity of close proximity between probe and sample represent still open challenges for application in GMP freeze-dryers [33,43]. Infrared (IR) spectroscopy can be applied as near infrared (NIR) or Fourier-Transform infrared (FTIR) in lyophilization on laboratory-scale freeze-dryer and mainly for qualitative analysis [35]. It is applied for in-line measurement to understand the freezing step, to obtain T_p and to determine sublimation flow. The complex data interpretation, the highly formulation- and process-dependency of the spectrum and the incompatibility with the GMP application limited this technology [35,44].

3.1.4 Sublimation flow-based PAT tools

Micro-balances can be used to analyze the sublimation flow rate, by lifting a single vial during primary drying [45]. In this way it is possible to determine also the product resistance R_p. It was proposed to weigh up to 15 vials simultaneously but the set-up interferes with the hexagonal array influencing the heat exchange compared to the

rest of the batch [46]. Additionally, micro-balances are incompatible with loading/unloading system, with hydraulic closure of the vials based on shelf compression and with GMP environment for sterility reasons [35].

3.2.Batch-monitoring PAT tools

3.2.1 Pressure-based PAT tools

A capacitance manometer measures the absolute pressure independently of the gas in the system. The electrical output is proportional to the capacitance between an electrode and a thin metallic diaphragm. The degree of deflection is caused by the pressure difference between outside of the system to be measured and the inside which is sealed and kept under a low pressure. Capacitance manometers are mostly used to control the chamber pressure [6].

Another common pressure measurement system is the Pirani gauge which measures the pressure based on the thermal conductivity of a hot wire. The heat exchange with the surrounding atmosphere depends on the frequency of collisions which is related to the pressure, and the molecular weight of the gas involved. The Pirani gauge is calibrated with nitrogen and presents a limited reliable pressure range [46].

The combination of capacitance manometer and Pirani gauge allows to detect the end point of primary drying and to follow secondary drying. The thermal conductivity of the water molecules is 60% higher than that of nitrogen molecules. During primary drying, the freeze-dryer chamber exclusively holds water molecules and thus the Pirani gauge shows higher values than the capacitance manometer. Once sublimation ends, the predominant gas in the chamber is nitrogen and the convergence of the two pressure values indicates the primary drying endpoint [47]. An increase in the Pirani gauge readout can be observed as water molecules desorb during secondary drying.

Another widespread PAT tool for batch monitoring is the Pressure rise test. The method relies on the pressure rise in case of temporary closure of the valve between the drying chamber and the condenser [48]. The pressure increase is fitted to sublimation models and the sublimation flow can be estimated [49]. The technique can be applied on many different machines, including equipment with automatic loading/unloading, if a fast-closing valve between condenser and drying chamber is built in [50]. The manometric temperature measurement (MTM) was introduced by Pikal and consists of valve closure for 25 seconds every 60 minutes during which pressure rise is measured. The conceived algorithm, which assumes the same thermal behavior within the batch, estimates the vapor pressure over the ice, product and stopper resistance and a fitting parameter X [51]. It allows an on-line evaluation of the ice content and to measure T_p without further components. But MTM reliably covers only the first 2/3 of primary drying [52] as the sublimation area decreases along the process as edge vials dry faster. Furthermore, it is no applicable to highly concentrated protein or high amorphous content formulations potentially due the water re-adsorption [53]. Chouvenc et al. proposed the pressure rise analysis as a viable alternative [54]. It also takes the thermal capacity of the glass and the re-adsorption heat into account. Additionally, it was applied in case of a slow-

closing valve but with unreliable parameters in early phase of drying based on T_p assumption [54]. A similar approach was presented by Velardi et al [55]. Initial key variables are estimated by the algorithm to then predict the outputs by minimizing the difference to measured values. This model is applicable also in the last part of the drying phase due to the introduction of a corrective factor of the sublimating interface [56].

3.2.2 Composition- or flow-based

A rather suitable but expensive technique is tunable diode laser absorption spectroscopy (TDLAS) which measures the vapor flow and concentration in the duct connecting chamber to condenser [57]. K_v and R_p can obtained in real time and the end point both of primary and secondary drying are easily detectable [57,58]. The necessity of a linear duct of adequate length and the difficult calibration represent limitation to its applicability [23].

Another technique used to detect the gas composition is the residual gas analyzer. A quadrupole mass spectrometer analyzes the molecules in the chamber atmosphere. It can determine the drying endpoint but it also used to detect leakage of silicone oil circulating in the shelf [33]. It requires complex and individual calibration for quantitative analysis [49].

4. Transfer and scale-up and of freeze-drying cycle

The transfer of a freeze-drying cycle from one equipment to another is often challenging [59]. Usually, this step takes place from an R&D to a pilot /industrial freeze-dryer as the batch size is increased. The aim of each transfer is to obtain the same thermal history for the product [60]. The main challenges are related to (a) a different geometry / material in the equipment that can influence heat transfer, or an alternative duct and condenser that influence the chamber pressure (b) dissimilar systems / strategies to control shelf temperature, and (c) environmental conditions such as the particulate level difference between a GMP room and R&D lab [61].

Different strategies were applied to transfer or to scale up a lyophilization cycle. In the past, due the lack of many current in-process tools, the simplest solution was a “trial and error” approach that resulted in an extremely resources- and time-consuming experimental campaign in which the results were limited to the studied configuration (formulation /primary packaging/ involved equipment) [62]. When the freeze-drying cycle is applied in the larger scale as it is in the laboratory equipment, the outcome depends on the technical similarities and designing of the cycle. Nevertheless, this strategy can imply premature end of primary drying with consequent impact on dried matrix and on CQAs (e.g., water content) [63]. When parameters adjustment is implemented, expertise is key but without numeric process evaluations, in many cases, the lyophilization cycles were suboptimal.

A second option is to focus on an initial lyophilization cycle robust enough to be applied in both freeze-dryers despite systematic differences. Therefore, experiments in the lab-scale equipment are carried out to assess the impact on the final product of variations of shelf temperature and chamber pressure compared to the target values. In recent years the trend to apply mathematical models to design and characterize the lyophilization cycle is increasing. The aim is a transfer and scale up with just a limited number of experiments based on the QbD approach [59]. These mathematical models are usually based on description of heat and mass transfers in the primary drying. Initially, the proposals were focused on a detailed description of the phenomena with the drawback of multi-dimensional algorithms including parameters difficult to obtain. Recently, the attention was addressed to simplified model capable to support researchers in parameters selection [59]. A milestone was focused on introducing parameters describing the heat and the mass transfer by K_v and R, respectively [64]. The first parameter is a sum of three main heat mechanisms coefficients (contact between vial and shelf, gas conduction between vial and shelf, irradiation from surrounding to vial) while the second considers the resistance to the sublimation flow. Further mono-dimensional model was proposed by Velardi and Barresi where the mass transfer resistance is indicated by the overall R_p coefficient that takes in consideration product, stopper and drying chamber contributions [65]. Additionally, to describe the heat transfer between shelf temperature and sublimating interface temperature, a sum of two heat resistances was introduced. More specifically, the heat loss is described from shelf to vial by the inverse of K_v while in the product by the ratio between thickness of the frozen layer and thermal conductivity of the frozen layer [66].

Once the cycle is described mathematically, it is possible to predict the cycle in the receiving equipment of the transfer based on K_v and R_p. As well-known, the heat transfer coefficient differs even considering the vial position in a same freeze-dryer [67]. Therefore, R_p is the most relevant as describes the product implications in the model. There are two potential scenarios: either same product resistance achievable or not in the two freeze-dryers. The first case is the simplest case where the shelf temperature is calculated and adjusted based on product temperature obtained in the first freeze-dryer used. Afterwards, drying time and temperature profile in the receiving freeze-dryer can be easily calculated by mathematical model [59]. When it is impossible to replicate the product resistance, it is necessary to decide to obtain either same product temperature or same sublimation flow, and consequently, drying time.

From these considerations, it appears of paramount importance having PAT tools / equipment able to provide information to conceive and control the lyophilization cycle and, ideally, to estimate in-silico the design space of the receiving unit so to obtain an efficient process and a smooth transfer.

5. References

[1] F. Franks, T. Auffret, Freeze-drying of Pharmaceuticals and Biopharmaceuticals, (2008). https://books.google.com/books?hl=it&lr=&id=-0gkSrMyyNAC&oi=fnd&pg=PA59&dq=Freeze-drying+of+Pharmaceuticals+and+Biopharmaceuticals&ots=i3VWZvgXeE&sig=qzGZTlRBpa0Zh3wGMXPSqeqvbQQ (accessed May 20, 2023).

[2] D. Varshney, M. Singh, History of Lyophilization, Lyophilized Biologics and Vaccines. (2015) 3–10. https://doi.org/10.1007/978-1-4939-2383-0_1.

[3] L. Rey, J.C. May, Freeze-Drying/Lyophilization Of Pharmaceutical & Biological Products, Revised and Expanded, CRC Press, 2004.

[4] A. Shanley, Modernizing lyophilization, Biopharm Int. 30 (2017) 50–52.

[5] A.G. Renteria Gamiz, P.J. Van Bockstal, S. De Meester, T. De Beer, J. Corver, J. Dewulf, Analysis of a pharmaceutical batch freeze dryer: resource consumption, hotspots, and factors for potential improvement, Https://Doi.Org/10.1080/07373937.2018.1518916. 37 (2019) 1563–1582. https://doi.org/10.1080/07373937.2018.1518916.

[6] S. Nail, S. Tchessalov, E. Shalaev, A. Ganguly, E. Renzi, F. Dimarco, L. Wegiel, S. Ferris, W. Kessler, M. Pikal, G. Sacha, A. Alexeenko, T.N. Thompson, C. Reiter, J. Searles, P. Coiteux, Recommended Best Practices for Process Monitoring Instrumentation in Pharmaceutical Freeze Drying—2017, AAPS PharmSciTech. 18 (2017) 2379–2393. https://doi.org/10.1208/S12249-017-0733-1/FIGURES/12.

[7] S.M. Patel, T. Doen, M.J. Pikal, Determination of End Point of Primary Drying in Freeze-Drying Process Control, AAPS PharmSciTech. 11 (2010) 73–84. https://doi.org/10.1208/s12249-009-9362-7.

[8] J.C. Kasper, W. Friess, The freezing step in lyophilization: Physico-chemical fundamentals, freezing methods and consequences on process performance and quality attributes of biopharmaceuticals, European Journal of Pharmaceutics and Biopharmaceutics. 78 (2011) 248–263. https://doi.org/10.1016/j.ejpb.2011.03.010.

[9] M. Akyurt, G. Zaki, B. Habeebullah, Freezing phenomena in ice–water systems, Energy Convers Manag. 43 (2002) 1773–1789.

[10] S.K. Pansare, S.M. Patel, Practical Considerations for Determination of Glass Transition Temperature of a Maximally Freeze Concentrated Solution, AAPS PharmSciTech. 17 (2016) 805–819. https://doi.org/10.1208/S12249-016-0551-X.

[11] L.T. Deck, D.R. Ochsenbein, M. Mazzotti, Stochastic ice nucleation governs the freezing process of biopharmaceuticals in vials, Int J Pharm. 625 (2022) 122051. https://doi.org/10.1016/J.IJPHARM.2022.122051.

[12] A. Hottot, S. Vessot, J. Andrieu, Freeze drying of pharmaceuticals in vials: Influence of freezing protocol and sample configuration on ice morphology and freeze-dried cake texture, Chemical Engineering and Processing: Process Intensification. 46 (2007) 666–674. https://doi.org/10.1016/J.CEP.2006.09.003.

[13] A. Hottot, S. Vessot, J. Andrieu, A direct characterization method of the ice morphology. Relationship between mean crystals size and primary drying times of freeze-drying processes, Drying Technology. 22 (2004) 2009–2021. https://doi.org/10.1081/DRT-200032717.

[14] A.K. Konstantinidis, W. Kuu, L. Otten, S.L. Nail, R.R. Sever, Controlled nucleation in freeze-drying: Effects on pore size in the dried product layer, mass transfer resistance, and primary drying rate, J Pharm Sci. 100 (2011) 3453–3470.

[15] X. Tang, M.P.-P. research, undefined 2004, Design of freeze-drying processes for pharmaceuticals: practical advice, Springer. 21 (2004) 191–200. https://doi.org/10.1023/B:PHAM.0000016234.73023.75.

[16] M.J. Pikal, M.L. Roy, S. Shah, Mass and heat transfer in vial freeze-drying of pharmaceuticals: Role of the vial, J Pharm Sci. 73 (1984) 1224–1237. https://doi.org/10.1002/JPS.2600730910.

[17] S. Bosca, A.A. Barresi, D. Fissore, Use of a soft sensor for the fast estimation of dried cake resistance during a freeze-drying cycle, Int J Pharm. 451 (2013) 23–33.

[18] W.Y. Kuu, L.M. Hardwick, M.J. Akers, Rapid determination of dry layer mass transfer resistance for various pharmaceutical formulations during primary drying using product temperature profiles, Int J Pharm. 313 (2006) 99–113.

[19] M.J. Pikal, S. Shah, M.L. Roy, R. Putman, The secondary drying stage of freeze drying: drying kinetics as a function of temperature and chamber pressure, Int J Pharm. 60 (1990) 203–207. https://doi.org/https://doi.org/10.1016/0378-5173(90)90074-E.

[20] C.C. Hsu, C.A. Ward, R. Pearlman, H.M. Nguyen, D.A. Yeung, J.G. Curley, Determining the optimum residual moisture in lyophilized protein pharmaceuticals., Dev Biol Stand. 74 (1992) 255–270.

[21] U.S. FDA, Guideline on general principles of process validation, Guide Indus May. (1987).

[22] A.S. Patil, A.M. Pethe, Quality by Design (QbD): A new concept for development of quality pharmaceuticals, International Journal of Pharmaceutical Quality Assurance. 4 (2013) 13–19.

[23] M. Galan, Monitoring and control of industrial freeze-drying operations: The challenge of implementing Quality-by-Design (QbD), in: Freeze-Drying/Lyophilization of Pharmaceutical and Biological Products, CRC Press, 2016: pp. 455–473.

[24] A.S. Rathore, H. Winkle, Quality by design for biopharmaceuticals, Nat Biotechnol. 27 (2009) 26–34. https://doi.org/10.1038/nbt0109-26.

[25] J. Woodcock, The concept of pharmaceutical quality, Am Pharm Rev. 7 (2004) 10–15.

[26] K.T. Patel, N.P. Chotai, Pharmaceutical GMP: past, present, and future–a review, Die Pharmazie-An International Journal of Pharmaceutical Sciences. 63 (2008) 251–255.

[27] M. Schweitzer, M. Pohl, M. Hanna-Brown, P. Nethercote, P. Borman, G. Hansen, K. Smith, J. Larew, Implications and opportunities of applying QbD principles to analytical measurements, Pharmaceutical Technology. 34 (2010) 52–59.

[28] D.M. Zagalo, B.M.A. Silva, C. Silva, S. Simões, J.J. Sousa, A quality by design (QbD) approach in pharmaceutical development of lipid-based nanosystems: A systematic review, J Drug Deliv Sci Technol. 70 (2022) 103207. https://doi.org/https://doi.org/10.1016/j.jddst.2022.103207.

[29] V. Mishra, S. Thakur, A. Patil, A. Shukla, Quality by design (QbD) approaches in current pharmaceutical set-up, Expert Opin Drug Deliv. 15 (2018) 737–758. https://doi.org/10.1080/17425247.2018.1504768.

[30] FDA, Guidance for Industry Guidance for Industry PAT — A Framework for Innovative Pharmaceutical, (2004). http://www.fda.gov/cvm/guidance/published.html (accessed May 21, 2023).

[31] M.A.P. McAuliffe, G.E. O'Mahony, C.A. Blackshields, J.A. Collins, D.P. Egan, L. Kiernan, E. O'Neill, S. Lenihan, G.M. Walker, A.M. Crean, The Use of PAT and Off-line Methods for Monitoring of Roller Compacted

Ribbon and Granule Properties with a View to Continuous Processing, Org Process Res Dev. 19 (2015) 158–166. https://doi.org/10.1021/op5000013.

[32] T.R.M. De Beer, M. Wiggenhorn, A. Hawe, J.C. Kasper, A. Almeida, T. Quinten, W. Friess, G. Winter, C. Vervaet, J.P. Remon, Optimization of a pharmaceutical freeze-dried product and its process using an experimental design approach and innovative process analyzers, Talanta. 83 (2011) 1623–1633.

[33] S.M. Patel, M. Pikal, Process analytical technologies (PAT) in freeze-drying of parenteral products, Pharm Dev Technol. 14 (2009) 567–587. https://doi.org/10.3109/10837450903295116.

[34] H. Kawasaki, T. Shimanouchi, Y. Kimura, Recent Development of Optimization of Lyophilization Process, J Chem. 2019 (2019) 9502856. https://doi.org/10.1155/2019/9502856.

[35] A. Kauppinen, Raman and near-infrared spectroscopic methods for in-line monitoring of freeze-drying process, (2015).

[36] K. Nakagawa, A. Hottot, S. Vessot, J. Andrieu, Modeling of freezing step during freeze-drying of drugs in vials, AIChE Journal. 53 (2007) 1362–1372.

[37] J.C. Kasper, M. Wiggenhorn, M. Resch, W. Friess, Implementation and evaluation of an optical fiber system as novel process monitoring tool during lyophilization, European Journal of Pharmaceutics and Biopharmaceutics. 83 (2013) 449–459.

[38] F. Jameel, W.J. Kessler, S. Schneid, Application of PAT in real-time monitoring and controlling of lyophilization process, in: Principles and Practices of Lyophilization in Product Development and Manufacturing, Springer, 2023: pp. 333–361.

[39] S. Schneid, H. Gieseler, Evaluation of a new wireless temperature remote interrogation system (TEMPRIS) to measure product temperature during freeze drying, AAPS PharmSciTech. 9 (2008) 729–739.

[40] I. Vollrath, V. Pauli, W. Friess, A. Freitag, A. Hawe, G. Winter, Evaluation of Heat Flux Measurement as a New Process Analytical Technology Monitoring Tool in Freeze Drying, J Pharm Sci. 106 (2017) 1249–1257. https://doi.org/10.1016/j.xphs.2016.12.030.

[41] H. Grohganz, D. Gildemyn, E. Skibsted, J.M. Flink, J. Rantanen, Rapid solid-state analysis of freeze-dried protein formulations using NIR and Raman spectroscopies, J Pharm Sci. 100 (2011) 2871–2875.

[42] A. Hedoux, L. Paccou, S. Achir, Y. Guinet, Mechanism of protein stabilization by trehalose during freeze-drying analyzed by in situ micro-raman spectroscopy, J Pharm Sci. 102 (2013) 2484–2494.

[43] T. De Beer, A. Burggraeve, M. Fonteyne, L. Saerens, J.P. Remon, C. Vervaet, Near infrared and Raman spectroscopy for the in-process monitoring of pharmaceutical production processes, Int J Pharm. 417 (2011) 32–47.

[44] S.A. Barker, M.D. Antonijevic, Thermal analysis-dielectric techniques, (2011).

[45] C. Roth, G. Winter, G. Lee, Continuous measurement of drying rate of crystalline and amorphous systems during freeze-drying using an in situ microbalance technique, J Pharm Sci. 90 (2001) 1345–1355.

[46] A.A. Barresi, R. Pisano, D. Fissore, V. Rasetto, S.A. Velardi, A. Vallan, M. Parvis, M. Galan, Monitoring of the primary drying of a lyophilization process in vials, Chemical Engineering and Processing: Process Intensification. 48 (2009) 408–423.

[47] A. Juckers, P. Knerr, F. Harms, J.S.- Processes, undefined 2022, Emerging PAT for Freeze-Drying Processes for Advanced Process Control, Mdpi.Com. (2022). https://doi.org/10.3390/pr10102059.

[48] D. Fissore, R. Pisano, A.A. Barresi, On the methods based on the Pressure Rise Test for monitoring a freeze-drying process, Drying Technology. 29 (2010) 73–90.

[49] A. Barresi, D. Fissore, In-line product quality control in FD, Modern Drying Technology. 3 (2011) 91–113.

[50] D. Fissore, R. Pisano, A.A. Barresi, Process analytical technology for monitoring pharmaceuticals freeze-drying–A comprehensive review, Drying Technology. 36 (2018) 1839–1865. https://doi.org/10.1080/07373937.2018.1440590.

[51] X.C. Tang, S.L. Nail, M.J. Pikal, Evaluation of manometric temperature measurement (MTM), a process analytical technology tool in freeze drying, part III: heat and mass transfer measurement, AAPS PharmSciTech. 7 (2006) E105–E111.

[52] X. Tang, S.L. Nail, M.J. Pikal, Freeze-drying process design by manometric temperature measurement: design of a smart freeze-dryer, Pharm Res. 22 (2005) 685–700.

[53] H. Gieseler, T. Kramer, M.J. Pikal, Use of manometric temperature measurement (MTM) and SMART™ freeze dryer technology for development of an optimized freeze-drying cycle, J Pharm Sci. 96 (2007) 3402–3418.

[54] P. Chouvenc, S. Vessot, J. Andrieu, P. Vacus, Optimization of the freeze-drying cycle: a new model for pressure rise analysis, Drying Technology. 22 (2004) 1577–1601.

[55] S.A. Velardi, V. Rasetto, A.A. Barresi, Dynamic parameters estimation method: Advanced manometric temperature measurement approach for freeze-drying monitoring of pharmaceutical solutions, Ind Eng Chem Res. 47 (2008) 8445–8457. https://doi.org/10.1021/ie7017433.

[56] A.A. Barresi, R. Pisano, V. Rasetto, D. Fissore, D.L. Marchisio, Model-based monitoring and control of industrial freeze-drying processes: effect of batch nonuniformity, Drying Technology. 28 (2010) 577–590.

[57] W.J. Kessler, E. Gong, Tunable diode laser absorption spectroscopy in lyophilization, Lyophilization of Pharmaceuticals and Biologicals: New Technologies and Approaches. (2019) 113–141.

[58] H. Gieseler, W.J. Kessler, M. Finson, S.J. Davis, P.A. Mulhall, V. Bons, D.J. Debo, M.J. Pikal, Evaluation of tunable diode laser absorption spectroscopy for in-process water vapor mass flux measurements during freeze drying, J Pharm Sci. 96 (2007) 1776–1793.

[59] D. Fissore, A.A. Barresi, Scale-up and process transfer of freeze-drying recipes, Drying Technology. 29 (2011) 1673–1684. https://doi.org/10.1080/07373937.2011.597059.

[60] S.M. Patel, M.J. Pikal, Emerging freeze-drying process development and scale-up issues, AAPS PharmSciTech. 12 (2011) 372–378. https://doi.org/10.1208/S12249-011-9599-9.

[61] R. Pisano, D. Fissore, A.A. Barresi, M. Rastelli, Quality by design: Scale-up of freeze-drying cycles in pharmaceutical industry, AAPS PharmSciTech. 14 (2013) 1137–1149. https://doi.org/10.1208/s12249-013-0003-9.

[62] H. Kawasaki, T. Shimanouchi, M. Yamamoto, K. Takahashi, Y. Kimura, Scale-up procedure for primary drying process in lyophilizer by using the vial heat transfer and the drying resistance, Chem Pharm Bull (Tokyo). 66 (2018) 1048–1056. https://doi.org/10.1248/cpb.c18-00516.

[63] S. Tchessalov, E. Shalaev, B. Bhatnagar, S. Nail, A. Alexeenko, F. Jameel, J. Srinivasan, M. Dekner, E. Sahni, S. Schneid, Best Practices and guidelines (2022) for Scale-up and Tech transfer in Freeze-Drying based on Case Studies. Part 1: challenges during Scale up and transfer, AAPS PharmSciTech. 24 (2022) 11.

[64] M.J. Pikal, M.L. Roy, S. Shah, Mass and heat transfer in vial freeze-drying of pharmaceuticals: Role of the vial, J Pharm Sci. 73 (1984) 1224–1237. https://doi.org/10.1002/jps.2600730910.

[65] D. Fissore, R. Pisano, A.A. Barresi, Advanced approach to build the design space for the primary drying of a pharmaceutical freeze-drying process, J Pharm Sci. 100 (2011) 4922–4933. https://doi.org/10.1002/jps.22668.

[66] S.A. Velardi, A.A. Barresi, Development of simplified models for the freeze-drying process and investigation of the optimal operating conditions, Chemical Engineering Research and Design. 86 (2008) 9–22. https://doi.org/10.1016/j.cherd.2007.10.007.

[67] A. Hottot, S. Vessot, J. Andrieu, Determination of mass and heat transfer parameters during freeze-drying cycles of pharmaceutical products, PDA J Pharm Sci Technol. 59 (2005) 138–153.

Chapter II: Aim and outline of thesis

The overall aim of this thesis was to investigate different PAT tools / equipment to conceive optimized freeze-drying cycles ready for scale-up / transfer with minimized material and time invest. Throughout the thesis, the combination of HFS, mathematical models and miniaturized equipment was extensively investigated. The question arose whether a design space fed by HFS-based inputs in a MicroFD allows to understand quickly the impact of operating parameters on product quality and process efficiency by optimization of the drying time.

In lyophilization it is key to balance heat provided by the shelf and the heat removed by sublimation during primary drying. A surplus of energy could impair the product quality by collapse whereas an energy deficit leads to extended expensive processes. Key input parameters are T_{fluid}, P_c, K_v and R_p. This work focused to combine different PAT tools to create a design space for primary drying. In particular, the focus was on the heat flux sensor (HFS), a quite recent PAT tool in lyophilization, in combination with a mathematical model (**Chapter III**). We performed a study on a laboratory-scale freeze-dryer comparing the classic gravimetric method to the HFS-based technique. Additionally, a freeze-drying cycle was designed and transferred to another equipment to verify the HSF / in-silico model developed. These data highlight the applicability of the HFS-based approach to substantially accelerate the design of freeze-drying cycles.

We further investigated the HFS in a miniaturized freeze-dryer, named MicroFD, to highlight the potential and the drawbacks of this PAT tool using only a very limited number of vials for process design (**Chapter IV**). In the first phase it was necessary to characterize the peculiar and innovative setup of the MicroFD including the LyoSIM, a temperature-controlled ring surrounding the product vials. Subsequently, the chapter considers the Kv obtained via the HFS for two exemplary types of formulations (amorphous and crystalline) and two different freezing protocols. Finally, the role of atypical radiation in the HFS output was investigated.

The aim of **Chapter V** was to clarify whether HFS / MicroFD can be applied for high concentration protein formulations and to check the potential for design space creation. To this end, we determined K_v and R_p of the formulations in the MicroFD. Subsequently, we generated a design space for the primary drying process and confirmed its validity experimentally considering the estimate of primary drying time and product temperature profile and characterizing cake appearance and water content.

Chapter III: Heat flux sensor to create a design space for freeze-drying development

Marco Carfagna[1, 2], Monica Rosa[1], Matthias Lucke[1], Andrea Hawe[1]*, Wolfgang Frieß[2]

[1] Coriolis Pharma Research GmbH, D-82152 Planegg, Germany;

[2] Department of Pharmacy, Pharmaceutical Technology and Biopharmaceutics, Ludwig Maximilian University, D-81377 Munich, Germany;

* Corresponding author: Andrea Hawe, Coriolis Pharma Research GmbH, Fraunhoferstraße 18B, D-82152 Planegg, Germany; e-mail: andrea.hawe@coriolis-pharma.com; Tel.: +49(0)89 41 77 60 -251;

The following chapter has been published in the European Journal of Pharmaceutics and Biopharmaceutics as:

Heat flux sensor to create a design space for freeze-drying development

Marco Carfagna, Monica Rosa, Matthias Lucke, Andrea Hawe, Wolfgang Frieß,

European Journal of Pharmaceutics and Biopharmaceutics,

Volume 153,2020, Pages 84-94, ISSN 0939-6411, https://doi.org/10.1016/j.ejpb.2020.05.028.

Abstract

Freeze-drying methodology requires an in-depth understanding and characterization for optimal processing of biopharmaceuticals. Particularly the primary drying phase, the longest and most expensive stage of the process, is of interest for optimization. The currently used process analytical technology (PAT) tools give highly valuable insights but come with limitations. Our study describes, for the first time, the application of a heat flux sensor (HFS) to build a primary drying design space and predict the process evolution. First, the heat transfer coefficient (K_v) generated by HFS and by the most accurate, but time-consuming and invasive, gravimetric method were compared. Second, the applicability to generate a design space was tested and verified. Obtained results revealed a good agreement of the values generated from this new and fast HFS compared to the gravimetric determination. Additionally, residual moisture assessed by Karl-Fischer titration and frequency modulated spectroscopy (FMS) support the quality of the obtained predictions. Thus, the HFS approach can substantially accelerate evaluation, development and transfer of a freeze-drying cycle.

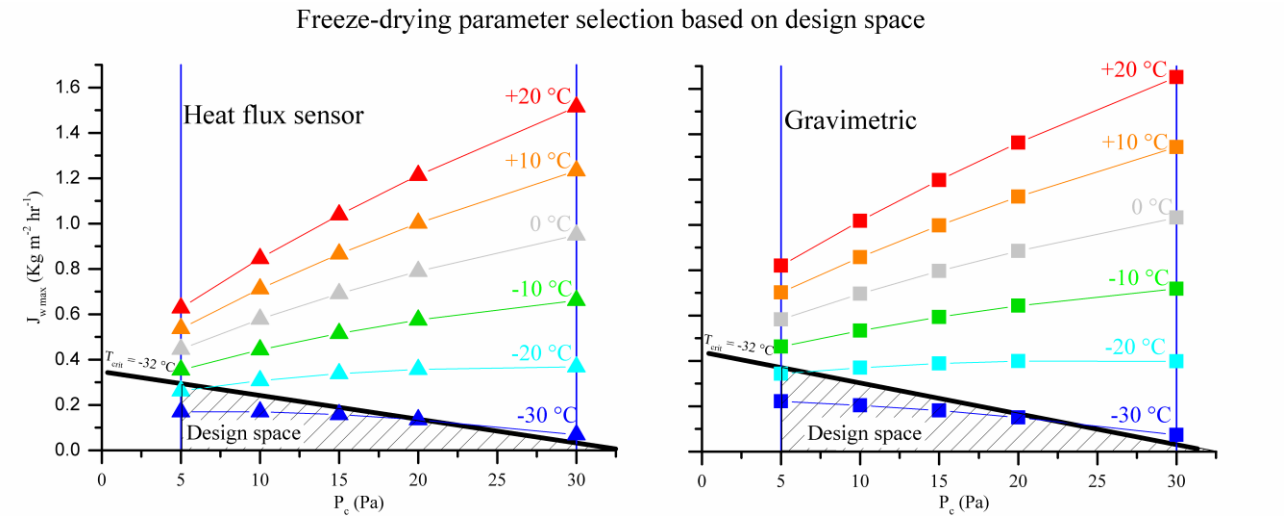

1. Introduction

Biopharmaceuticals represent extremely important therapeutics with an estimated market worth of 445 billion dollars in 2019 [1]. Many of these products need conversion from solution to a solid-state through lyophilization to achieve an adequately stable drug product [2]. This process is complex, cost- and time-consuming, and can – if not optimized – impair the quality of the pharmaceutical product [3-6].

The primary drying step is the longest and most challenging step of the freeze-drying process [7]. Its aim is the sublimation of the frozen water in the product by using energy provided by the shelves in the shortest possible time. However, supplying an energy surplus to the product during primary drying can lead to a partial or total change in structure of the dried material (micro- or macro-collapse). Collapse can result in a higher water content within the product, which could affect product stability [8, 9]. Shelf fluid temperature (T_{fluid}) and chamber pressure (P_c) are the parameters to control the water sublimation rate (mass transfer) and the product temperature (T_p) during primary drying. Both, P_c and T_{fluid}, must be selected in such a way that are adequate to keep primary drying short but at the same time to prevent T_p to exceed the critical thermal properties of the formulation (collapse temperature or temperature of eutectic melting). Unfortunately, T_p is also influenced by receiving energy via uncontrolled radiation [10]. Therefore, it is essential to know the relation between T_{fluid} and the total heat received (Q_{total}) by a particular vial:

$$K_v = Q_{total} \left(T_{fluid} - T_p\right)^{-1} \quad (1)$$

K_v is the heat transfer coefficient, a parameter introduced by Pikal [11] and applied to describe the role of the vial and of the equipment in the process for a specific position in the dryer [12, 13].

To consider the effect of the formulation composition and freezing conditions on sublimation, the product resistance (R_p) was introduced [14]:

$$R_p = (P_i - P_c)\ (J_w)^{-1} \quad (2)$$

with P_i being the pressure at the sublimating interface and J_w the sublimation flux.

The characterization of a freeze-drying process, potentially also through the above-mentioned equations, allows to understand the influence of process parameters on defined critical quality attributes (CQAs) [15, 16]. CQAs often considered in for freeze-dried products are visual appearance, residual water content, reconstitution time, preservation of biological activity, stability and sterility [16].

The approach towards quality evolves from testing-driven (quality by testing – QbT) to design-driven (quality by design – QbD) point of view in order to transform product and process assessment to a science-based

methodology [17]. Essential elements of this are the above-mentioned CQAs, the risk assessment to define limits to those attributes and the design space [18]. The latter, defined by the "ICH Q8 Pharmaceutical Development Guideline" as a "multidimensional combination of input variables and process parameters that have been demonstrated to provide assurance of quality" [19] can be of extreme interest not only from quality but also economic perspective [20]. Building a design space requires an extensive experimental campaign, but this process can be streamlined with the support of mathematical modelling [21, 22]. For establishing the design space, a certain number of experiments are necessary to obtain the required parameters (i.e. K_v and R_p) to describe and predict the freeze-drying cycles.

K_v can be used to obtain the mass of sublimed ice and R_p [14]. Knowing heat and mass transfer as a function of T_{fluid} and P_c allows the generation of a design space. K_v and R_p can be obtained by different techniques, which can be classified in vial- and batch-. The most accurate technique is the gravimetric method (vial-based) in which the vials are weighed before and after the experiment to determine the amount of sublimed solvent. However, the method is invasive because the process has to be stopped in order to obtain a reliable product temperature measurement over the considered primary drying. If the type of vial is changed or the effect of P_c on the heat transfer is considered, repetitions (at least three) are necessary leading to an extremely time-consuming method. The most frequently used batch techniques, pressure rise test (PRT) and the tunable diode laser absorption spectroscopy (TDLAS) [9, 23-26], enable to monitor an ongoing process in "real-time". Unfortunately, they are not applicable to every equipment type and they provide only an average K_v for all vials in the freeze-dryer without the possibility for differentiation of vial location (e.g., center or edge vials) [18, 27-31]. Ideally a fast, non-invasive technique applicable to any sort of freeze-dryer, would be necessary to enable the characterization of a given lyophilization process.

Heat flux sensors (HFSs) have recently been introduced as novel PAT tool to monitor and develop freeze-drying processes. The temperature difference above and below the sensor is converted in a voltage, resulting from the Seebeck effect and then transduced in the proportional heat flux [32]. In the current set-up, the energy measured for a defined vial population positioned on the HFS (Q_{HFS}) is positive when the heat flux is provided by the shelf. Further, HFSs are useful to obtain insights into the freezing steps i.e., to follow nucleation events, to identify the end of primary drying, and to estimate T_p if K_v is known [33].

While the focus of previous work on HFS was mainly on applicability and endpoint detection, the scope of our current work was to create a fast and reliable methodology to obtain key process parameters like K_v and R_p generated from HFS measurements. Subsequently, a single experiment to generate multiple K_v and R_p by HFS was

assessed by varying parameters during the cycle. This should ultimately provide an option to substantially accelerate understanding and development of the process.

Our work was divided in three parts:

a. Investigation of K_v and R_p obtained by HFS compared to the gravimetric methodology in a laboratory-scale freeze-dryer.
b. Assessment of a single HFS experiment to create a primary drying design space
c. Demonstration of the feasibility to predict a rational freeze-drying cycle including a transfer to a different lyophilization equipment based on a fast procedure using the HFS.

2. Materials and Methods

2.1 Formulations and primary packaging

Sucrose (Ph. Eur. grade) from Merck (Darmstadt, Germany) and highly purified water (Milli-Q integral water purification system, Merck Millipore, Hertfordshire, United Kingdom) were used to prepare 10% w/V solutions for all the tests performed. The solutions were filtered by using 0.22 µm PVDF (polyvinylidene difluoride) membrane filters (Merck, Darmstadt, Germany) prior to filling.

A volume of 5 ml sucrose solution was filled in 6R TopLyo glass vials (Schott, Müllheim-Hügelheim, Germany) and the vials were partially closed with 20-mm bromobutyl single vent lyophilization stoppers (Westar RS, FluoroTec B2-40 coating; West, Eschweiler, Germany).

In case of two supplementary experiments, 2R and 20R glass vials (Schott, Müllheim-Hügelheim, Germany) were filled with 2 ml (2R) and 5 ml (20R), respectively. The vials were partially closed with 13-mm and 20-mm bromobutyl single vent lyophilization stoppers (Westar RS, FluoroTec B2-40 coating; West, Eschweiler, Germany).

2.2 Freeze-drying equipment and heat flux sensor (HFS)

Freeze-drying experiments were performed on a Revo freeze-dryer (Millrock Technology, Kingston, New York, USA), named as FD01 through the manuscript. The verification of the predicted time and design space parameters was performed on an Epsilon 2-12D freeze-dryer (Martin Christ, Osterode, Germany) indicated as FD02 in the rest of this work.

FD01 was equipped with three shelves, presenting a total area of 0.55 m^2. Pressure was controlled by a capacitance manometer and additionally monitored with a Pirani gauge. T-type copper-constantan thermocouples

were used. An HFS is in the center of the bottom shelf. From the HFS readout (Q_{HFS}), a HFS-based K_v (K_v HFS) was calculated:

$$K_v\ HFS = Q_{HFS}\left(T_{shelf\ surface} - T_p\right)^{-1} \quad (3)$$

where $T_{shelf\ surface}$ is the temperature of the shelf surface as measured from thermocouple built-in the HFS and T_p is the product temperature measured at the vial bottom. In our manuscript we refer to the term T_{fluid} to indicate the shelf fluid temperature set in the freeze-dryer and to differentiate it from the $T_{shelf\ surface}$, which is the temperature measured from thermocouple embedded in the HFS. In the K_v HFS calculations, the temperature recorded from the sensor indicated as $T_{shelf\ surface}$ was applied instead of T_{fluid}. The detection area of the sensor was 6.68 * 6.35 cm with a thickness of 0.178 mm. A thin frame (named shim) made of stainless steel surrounded the sensor to provide an even stand for the vials placed in the freeze-dryer.

FD02 was equipped with four shelves, presenting a total area of 0.63 m^2, and an individual shelf closure mechanism. T_p was monitored by resistance temperature detectors. Vacuum was controlled by a capacitance manometer and additionally monitored with a Pirani gauge.

2.3 Determination of K_v and R_p: gravimetric and HFS experiments

Each of the three shelves in the freeze-dryer (FD01) was loaded with 91 filled vials. The 91 filled vials equal 27% of the maximum freeze-dryer capacity. 19 vials were placed on the heat flux sensor and 72 on the surrounding area. Three gravimetric experiments were carried out at chamber pressures of 5.3 Pa, 10.7 Pa and 16.0 Pa with a cycle as outlined in Table 1.

Table 1. Freeze-drying parameters used for gravimetric experiments.

No.	Step	Time [hh:mm:ss]	T_{fluid} [°C]	P_c [Pa]			Ramp [°C/min]
1	Loading	00:00:00	20	100,000			
2	Freezing	00:46:00	-3	100,000			0.50
3	Freezing	01:00:00	-3	100,000			
4	Freezing	00:47:00	-50	100,000			1.0
5	Freezing	02:00:00	-50	100,000			
6	Primary drying	00:15:00	-50	5.3	10.7	16.0	
7	Primary drying	01:00:00	-20	5.3	10.7	16.0	0.50
8	Primary drying	09:00:00	-20	5.3	10.7	16.0	

5.3 and 16.0 Pascal were selected to cover a representative chamber pressure in pharmaceutical freeze-drying [34]. Additionally, 5.3 Pa is usually the minimum chamber pressure attainable in a manufacturing freeze-dryer. Furthermore, at 16.0 Pa gas conduction mechanism accounts for almost half of the total heat transfer [35] and our study wanted to highlight potential differences between the gravimetric and the HFS method potentially affected by the mode of energy transfer. Water loss (Δm) was measured by weighing the 19 vials placed on the HFS by using an analytical balance (Genius ME – Sartorius, Gottingen, Germany) before the start of the process and after circa 10 hours of primary drying time (steps 6-7-8 in Table 1). The reason of a premature freeze-drying cycle interruption is to obtain reliable product temperature through the entire process. K_v was calculated according to the following equation:

$$K_v\ grav = \frac{\Delta m\ \Delta H_s}{A_v \int_0^{\Delta t} \left(T_{fluid} - T_p\right) dt} \tag{4}$$

where ΔH_s is the sublimation heat of ice and A_v is the cross-sectional area of the vial. R_p was calculated according to equation (2).

Three additional cycles were performed and stopped after step 7 (Table 1) to determine the water loss during the primary drying ramp. The gravimetric procedure described for FD01 was applied also to FD02 to obtain the corresponding K_v data.

Two additional tests with 20R and 2R vials were carried out to verify the offset between the gravimetric and the HFS methodology. Each of the three shelves in FD01 was loaded with 91 (20R) or 169 (2R) filled vials. 7 20 R vials or 61 2R vials resp. were placed on the heat flux sensor and 84 20R vials or 108 2R vials resp. on the surrounding area. In both the experiments, the cycle was performed as described in Table 1 for 5.3 Pa cycle. In order to assess the effect of the freeze-dryer load on the HFS output, two additional tests at the maximum freeze-dryer capacity were carried out in FD01 at chamber pressures of 5.3 and 10.7 Pa.

The feasibility test of a fast method to generate K_v at three different chamber pressures was named 3-pressure experiment (3PE). P_c was set first at 5.3 Pa to obtain also R_p and then increased at 10.7 and later to 16.0 Pa (T_{fluid} kept at -20°C).

2.4 Mathematical model for HFS-based design space generation

Non-linear fitting of K_v and R_p was performed by applying the Levenberg–Marquardt algorithm with Origin 2016 (OriginLab Corporation, Northampton, Massachusetts, USA). For K_v calculation, the following equation was used:

$$K_v = A_{Kv} + \frac{B_{Kv}\, P_C}{1 + l_v \frac{B_{Kv}}{\lambda_0}\, P_C} \quad (5)$$

The first term of the equation (A_{Kv}) represents the sum of the heat contributions of vial-to-shelf contact and uncontrolled radiation. The second term of the equation represents the gas conduction according the Smoluchowsky theory. B_{Kv} is a coefficient proportional to the temperature of the gas and to the gas composition in the chamber. l_v indicates the average distance between vial bottom to the shelf and λ_0 the thermal conductivity of the gas at ambient pressure [36, 37]. l_v was estimated using the imprint test described in section 2.6 while λ_0 was taken from literature ($1.8\ 10^{-2}$ $Wm^{-1}K^{-1}$) [11].

For R_p calculation, the following equation was used [37]:

$$R_p = R_{p0} + \frac{A_{Rp}\, L_{dried}}{1 + B_{Rp}\, L_{dried}} \quad (6)$$

R_{p0}, A_{Rp} and B_{Rp} are obtained from the best fit of R_p vs. dried layer (L_{dried}) evolution. T_p profiles and K_v were used to calculate R_p [14]. The mathematical model proposed by Velardi and Barresi was applied to estimate evolution of dried material, temperature at the sublimating interface (T_i) and primary drying time [21]. A design space was created for both HFS and gravimetric data.

2.5 Transfer of cycle from FD01 to FD02

The obtained HFS-based design space was verified with a cycle transfer from FD01 to FD02 for a 2 ml fill. This change in the filling volume from 5 ml (applied in previous experiment) to 2 ml does not affect the product resistance, according the obtained R_p curve. Process parameters are listed in Table 2.

Table 2. Freeze-drying parameters used for FD02 predicted by using HFS data in FD01.

No.	Step	Time [hh:mm:ss]	T_{fluid} [°C]	P_c [Pa]	Ramp [°C/min]
1	Loading	00:00:00	20	100,000	
2	Freezing	00:46:00	-3	100,000	0.50
3	Freezing	01:00:00	-3	100,000	
4	Freezing	00:47:00	-50	100,000	1.0
5	Freezing	02:00:00	-50	100,000	
6	Primary drying	00:15:00	-50	5.3	
7	Primary drying	00:58:00	-21	5.3	0.50
8	Primary drying	42:40:00	-21	5.3	0.50
9	Secondary drying	08:30:00	30	5.3	0.50
10	Secondary drying	06:00:00	30	5.3	0.50
11	Closing			80,000	

The fluid temperature in FD02 ($T_{fluid\ FD02}$) was selected to match the product evolution of the product in FD01 (ice thickness $L_{frozen\ FD01}$ and pressure at the sublimating interface $T_{i\ FD01}$) according to K_v HFS and R_p HFS). The following equation was used to select the T_{fluid} of FD02 [38]:

$$T_{fluid\ FD02} = \frac{K_{v\ FD02}\left(\frac{1}{K_{v\ FD02}} + \frac{L_{frozen\ FD01}}{k_{frozen}}\right)T_{p\ FD01} + T_{i\ FD01}}{K_{v\ FD02}\left(\frac{1}{K_{v\ FD02}} + \frac{L_{frozen\ FD01}}{k_{frozen}}\right) - 1} \quad (7)$$

where k_{frozen} indicates the ice thermal conductivity.

2.6 Determination of vial-to-shelf contact area (imprint test)

The bottom of five vials was dyed on an inkpad and then transferred to a piece of paper. The paper was scanned with a CFI 60 bright-field/dark-field microscope (Nikon Corporation, Japan) and the composite picture was processed with ImageJ (Fiji – open-source package) to obtain the contact area. l_v was obtained as described from Pikal et al. [11]. In brief, vials were carefully cut in their axial direction, dyed on the inkpad and placed on a piece of paper with a moderate pressure. The imprint was scanned and the picture processed with ImageJ. The maximum distance from the vial to the horizontal plane was measured and equal to 2.7 10^{-4} m.

2.7 Analytical methods

2.7.1 Differential scanning calorimetry

Differential scanning calorimetry (DSC) was performed in a Mettler Toledo DSC 1 (Mettler Toledo, Columbus, Ohio, USA) to determine the glass transition temperature of the maximally freeze-concentrated solution (Tg') for our formulation. Approximately 10 µl of the formulation were analyzed in crimped Al-crucibles. The samples were twice cooled to -50 °C (cooling rate of 1 °C/min) and reheated to 10 °C with a scanning rate of 5 °C/min. The midpoint of the endothermic shift of the baseline during the heating scan was taken as Tg'.

2.7.2 Karl Fischer titration

The residual moisture content of the freeze-dried samples was analyzed by direct injection using a coulometric Karl Fischer (KF) titrator Aqua 40.00 (Analytik Jena, Jena, Germany). The samples were prepared in a glovebox at ≤ 10% relative humidity. Approximately 30 – 50 mg freeze-dried material was weighed into an empty vial, dissolved in about 1.5 ml of titrant solvent, and sonicated for 5 minutes. Approx. 1 ml was analyzed with exact mass control of the injected sample.

2.7.3 Frequency modulating spectroscopy

The partial pressure of water vapor in the vial headspace was determined using a FMS-1400 Headspace Pressure / Moisture Analyzer (Lighthouse Instruments, Charlottesville, Virginia, USA). All samples were measured in triplicates and the mean and standard deviation of the partial pressure of water vapor is reported in Pa.

2.8 Data analysis

Throughout the manuscript, K_v gravimetric values represent the experimental mean (calculated on n = 19) ± standard deviation. For K_v HFS values are the mean of the calculated data over the primary drying phase ± standard deviation. In KF and FMS charts, each bar represents the experimental mean (calculated for KF data on n=3, for FMS data on n=50) ± standard deviation. A z-test was applied to assess statistically significant difference between two considered groups ($p < 0.05$).

3. Results and Discussion

3.1. Comparison of K_v based on HFS with K_v gravimetric

The first goal was to compare K_v derived from HFS to the well-established gravimetric K_v determination [39]. A primary drying model based on the assumption of a "pseudo steady state" (PSS) implies that all the heat received by the product in the vial is equal to the heat removed by sublimation (i.e., no heat dispersion) [40]. Therefore, the K_v grav PSS was determined excluding the perturbation by the T_{fluid} ramp phase [41] via subtraction of the water loss during the temperature ramp. In addition, we included the K_v grav in non-steady state condition for comparison because of its pragmatic aspect. Non-steady state data often are the only available information for process scientists but in this situation no extra lyophilization cycles are required.

Our K_v results for 10% w/V sucrose are in good agreement with previous work conducted with water [42]. Considering the K_v grav non-PSS data in the primary drying evolution may cause a K_v underestimation with impact on product quality, especially for freeze-drying cycles where T_p is close to the critical product temperature. Nevertheless, in our case of 9 hours primary drying (holding phase) the difference is subtle and the discrepancy between the K_v gravimetric PSS and non-PSS are less than 6.5%. A statistical test confirmed the impossibility to distinguish PSS from non-PSS data in the considered P_c range. On the basis of our evaluation, we can conclude that in case of an adequate experiment time and fast temperature ramping both, the non-PSS and PSS data, are acceptable.T_p and K_v of vials placed on the sensor or not on the sensor directly on the shelf were comparable (data in Figure A 1 and Table A 1).

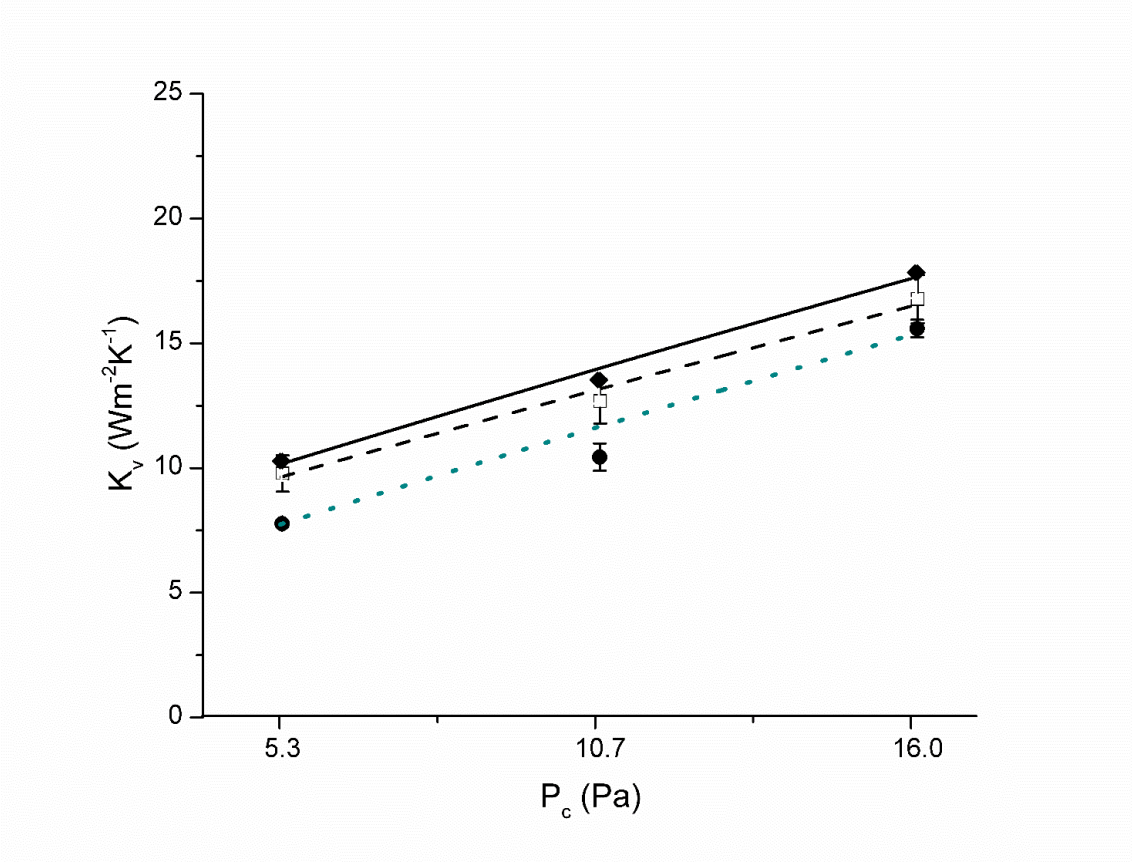

Figure 1. K_v HFS (•), K_v grav PSS (♦) and K_v grav non-PSS (□) as a function of P_c. The lines indicate the fit of the data sets (for all fits $R^2 > 0.985$). [K_v HFS (…) K_v grav PSS (—) K_v grav non-PSS (---)]

Based on equation (3), K_v HFS is on average 2.6 $Wm^{-2}K^{-1}$ lower than K_v grav PSS (Figure 1). Whereas the gravimetric approach assesses the total heat received by the vials, the HFS approach measures only a part of it. The heat transfer during primary drying is ascribed to three mechanisms: direct contact of the vial bottom with the shelf, radiation coming from the surrounding of the vial (i.e., walls and door) and gas conduction. These mechanisms are considered in equation (5), which can be used to extrapolate K_v data [43]. Contact and radiation are gas-independent and their sum is described by A_{Kv}. The second term of the equation is influenced by P_c and related to B_{Kv}. Mathematical fitting (equation (4)) [43] enabled us to distinguish between the gas-dependent and the gas-independent contributions. The pressure dependency of K_v HFS and K_v grav PSS show a similar evolution (Figure 1), reflected by the B_{Kv} values (Table 3). This means that both ways of K_v determination have the same pressure dependency. Looking at the results in Table 3, the difference of gas-independent contribution (A_{Kv} term) between the different data sets is noticeable. The A_{Kv} value of the HFS is 2.4 $Wm^{-2}K^{-1}$ lower than the value obtained for the K_vs grav PSS. In other words, the sum of radiative heat plus heat received by direct contact shows a difference of 38.7% between K_v HFS and K_v grav PSS at an assumed P_c of 0 Pa. In previous work, the relative importance of the A_{Kv} term varies from ca. 70% at 4 Pa (40% contact / 30% radiation) to ca. 45% at 15 Pa (25%

contact / 20% radiation) [35]. Due to the fact HFS is placed below the vial, we assume that the discrepancy between the HFS and the gravimetric method is related to the radiative heat. However, this hypothesis allows for an own study and is beyond the aim of this work.

Subsequently, 2R and 20R vials were considered and same offset between K_v grav and K_v HFS was obtained applying same drying conditions (data in Figure A 2). The HFS output was checked also in relation to the freeze-dryer load (Table 4). The freeze-dryer load did not affect the HFS output. This result corresponds to the available gravimetric K_v data [44].

3.2.R_p derived from K_v grav and HFS

Applying the approach suggested by Kuu et al. [14], the evolution of R_p as a function of dried layer thickness derived from the HFS and the gravimetric analysis was compared.

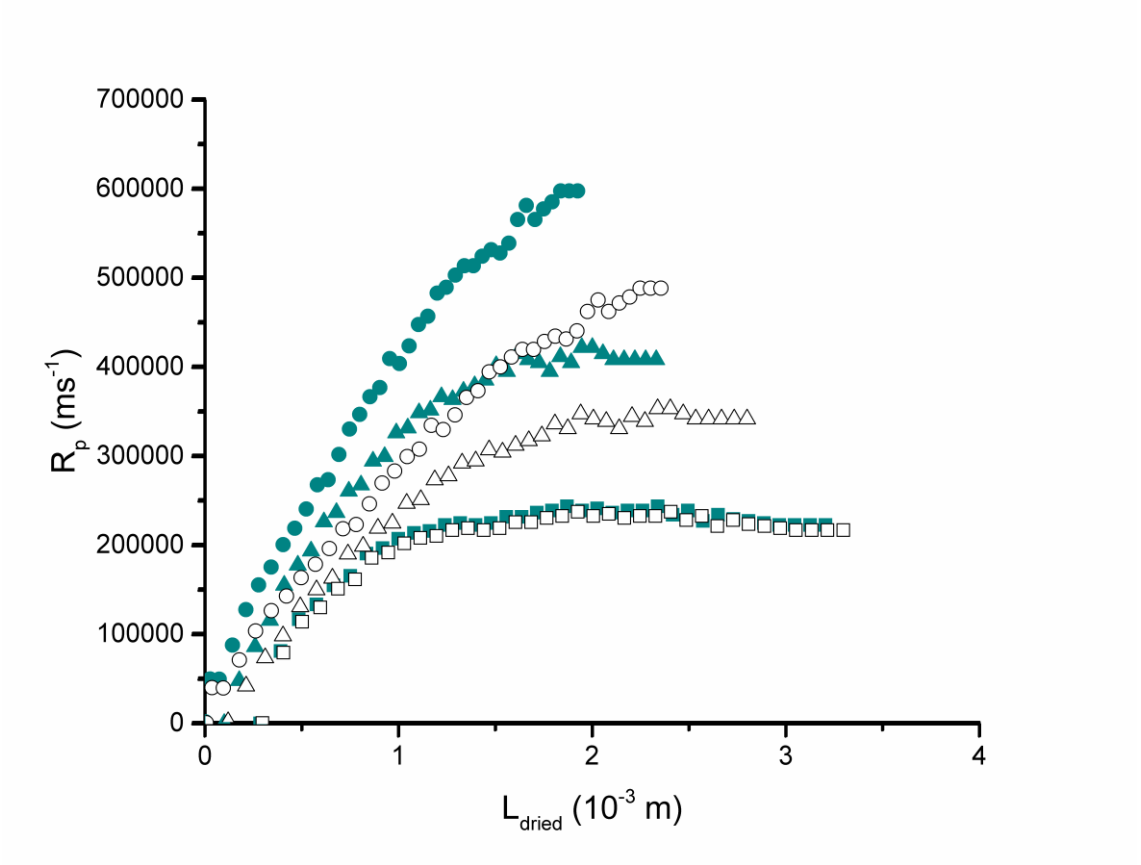

Figure 2. R_p as a function of dried layer thickness derived from K_v grav (empty symbols) and K_v HFS (filled symbols) at 5.3 Pa (circles), 10.7 Pa (triangles) and 16.0 Pa (squares).

As displayed in Figure 2, decreasing of R_p values were found with increasing of chamber pressures, irrespective whether the gravimetric or the HFS-based data were evaluated. This phenomenon may be explained by a progressing extent of micro-collapse [45, 46]. A confirmation of this hypothesis can be found from the observation

of the product temperature profiles at 10.7 and 16.0 Pa and the considered Tg' (data in Figure A 3). R_p calculated from K_v HFS data was higher compared to R_p obtained from K_v grav at P_c of 5.3 and 10.7 Pa. The two R_p evolutions matched at 16.0 Pa and compare well to the values presented by Scutellá et al. [47]. This observation can be explained by the offset between the two K_v methods (Figure 1), which has a higher relative importance at low to mid P_c than at high P_c. The R_p in design space is of extreme importance, because it accounts for product composition, freezing conditions [45]. The R_p increases as primary drying continues since the dried layer gains in thickness and its evolution can be described empirically (equation (7)). The mathematical descriptions of R_p vs. dried layer thickness were applied to define the design spaces originated according the HFS and the gravimetric methods.

3.3.Assessment of a single HFS experiment procedure to create a design space

In order to accelerate the development of a freeze-drying cycle, we examined the possibility to obtain all the data necessary to create a design space in a single experiment.

We verified that K_v HFS is barely affected by the T_{fluid} in a pre-test (data shown in Figure A 4). Afterwards we conducted the 3-pressure experiment (3-PE) to reduce time and effort for generating a design space. This freeze-drying cycle was conceived to obtain three K_v HFS and the corresponding R_p for our formulation. The first segment of the experiment was designed to obtain R_p and was performed at 5.3 Pa for two main reasons: i) minimizing the dry layer formation and ii) reducing the probability of micro-collapse of the sucrose formulation. The other two primary drying segments (10.7 – 16.0 Pa) were sufficiently long to ensure that PSS was established.

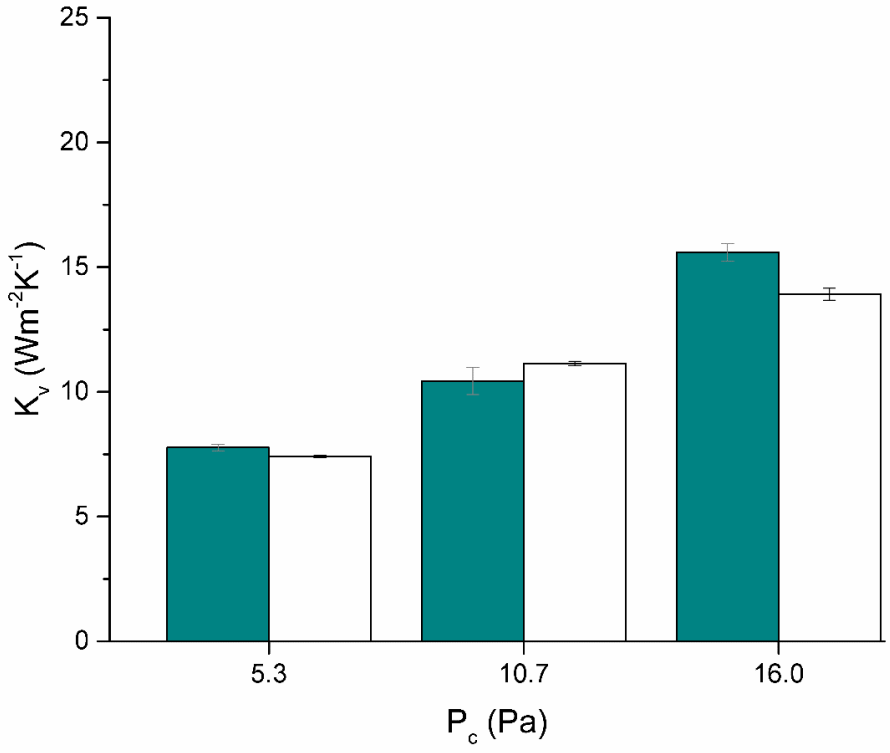

Figure 3. K_v HFS comparing single test (green) and 3-PE cycle (white).

Figure 3 illustrates the comparison between the K_v HFS values obtained in the single pressure experiments and the 3-PE. The two data sets are in good agreement for P_c of 5.3 and 10.7 Pa. At 16.0 Pa, the 3-PE K_v HFS was 1.7 $Wm^{-2}K^{-1}$ below the K_v HFS of the individual test. This difference might be explained by the progression of the cycle as P_c increases K_v and in turn affects R_p. As stated earlier in the section 3.2, the heat flux increment reduces the vapor flow resistance of the dried matrix. According to our calculations for the 16.0 Pa conditions at the 3-PE, R_p was ca. 5% higher than for the single experiment. Accordingly, T_p was 1.65 °C higher in the 3-PE. The drawback of a less accurate measurement at high P_c is compensated by the possibility to obtain quickly multiple K_v values and R_p during the low P_c phase, the 5.3 Pa segment. Results obtained for the 3-PE experiment were in fair agreement with the single experiment values. From that perspective, we consider the 3-PE as an attractive way to accelerate the cycle development by lowering the effort and shortening the time to obtain reliable K_v data at low and moderate P_c. Therefore, we considered obtained R_p and K_vs (at 5.3 – 10.7 Pa) for the following phase.

3.4.Design space and freeze-drying cycle transfer

Finally, we evaluated the possibility to use a design space derived from HFS data for a cycle transfer to a pilot-scale freeze-dryer (FD02). Once the mathematical descriptions of K_v and R_p were obtained, a mono-dimensional model was applied to estimate primary drying duration, maximum temperature at the sublimating interface (T_i) and sublimation flow rate (J_w) for each selected T_{fluid} and P_c value. The primary drying design spaces were created from HFS and gravimetric determination (Figure 4 and Figure 5).

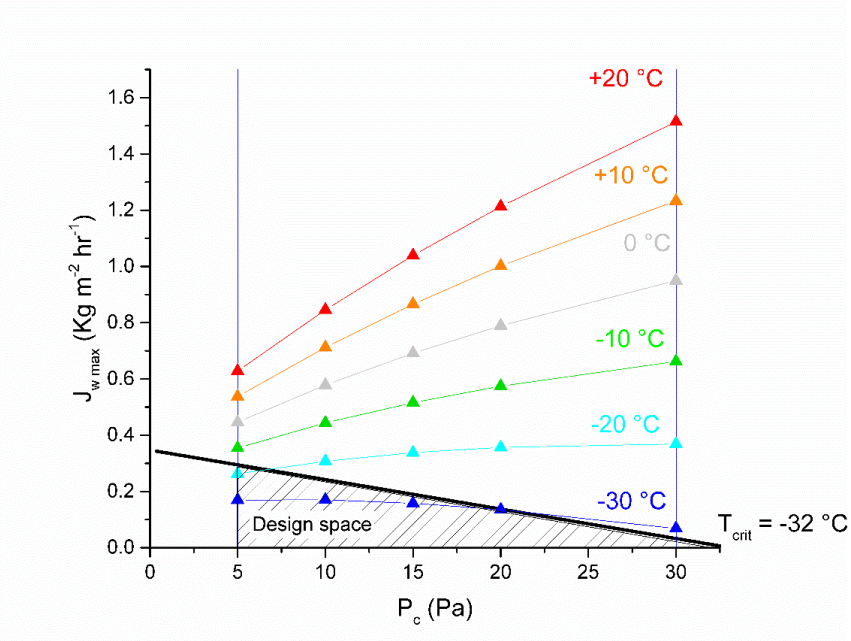

Figure 4. Design space generated using HFS data. [R_P obtained at 5.3 Pa].

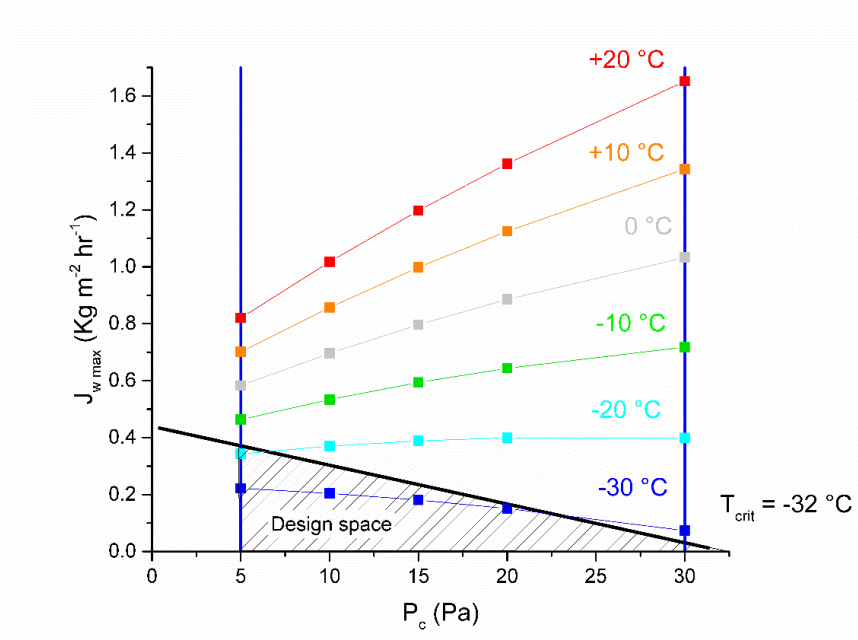

Figure 5. Design space generated using gravimetric data. [R_P obtained at 5.3 Pa].

The sublimation flow rates were plotted against P_c for 30 performed simulations. Each line connecting the data points depicts the isotherm of T_{fluid}. The black line indicates the critical product temperature (T_{crit}) of -32 °C, which was determined by DSC and confirmed by collapse temperature data from literature [48]. The triangular area defined from the T_{crit} and the vertical lines represents the design space and a combination of process variables (T_{fluid} and P_c) that give a temperature at the sublimating interface $T_i < T_{crit}$ falls in this region. The boundaries in terms of allowable T_{fluid} and P_c are the same for the two design spaces at 5.3 Pa. As a direct consequence of the previously described offset between the two techniques, the sublimation flow rates are lower for the HFS-based calculations. This aspect must be considered for freeze-dryers prone to choked flow, where an underestimation of the real sublimation flow rate can cause a loss of pressure control and consequent product impairment. The R_p change with P_c did not affect the sublimation flow but led to a decrease of the area representing the allowable T_{fluid} and P_c (Figure A 5 and Figure A 6) as evidenced in previous work [45]. The application of K_v and R_p from HFS data to conceive a freeze-drying cycle leads to a result comparable to the one derived from gravimetric data for the selection of T_{fluid} and P_c. There is a mathematical compensation for the K_v underestimation and the R_p overestimation obtained from HFS data for low and moderate chamber pressures (as shown in the Appendix – Calculation of T_i). This leads to an overlapping temperature profile for both the methods. The estimated drying time is related to the calculated heat: primary drying HFS-based is longer than the gravimetric-based. To minimize the predicted time HFS-based, it is necessary to reduce it of a percentage equal to the relative importance of the offset between the two methods.

From the established HFS-based design space a T_{fluid} of -20 °C and a P_c of 5.3 Pa were selected to reduce the primary drying time (to maximize J_w) while maintaining T_i below the T_{crit}. The verification of the estimated primary drying time and product dynamics was performed in FD02 with R_p as obtained from the HFS and gravimetric data (5.3 Pa). By using equation (7) the T_{fluid} was adjusted from -20 °C at FD01 to -21 °C at FD02. The end of sublimation was calculated as 43:40 (h : min) (1:00 ramp + 42:40 h : min) for the HFS approach and at 42:40 (h : min) (1:00 ramp + 41:40 h : min) for the gravimetric approach. The overestimated time equal to circa + 2.4% from HFS is due to already mentioned differences between the two methods.

As shown in Figure 6 (and also in Figure A 7), the comparative pressure measurement (Pirani-capacitance pressure ratio) indicated the end of primary drying after approx. 42 hours in FD02, which is in agreement with our gravimetric prediction and slightly earlier than the HFS-based prediction.

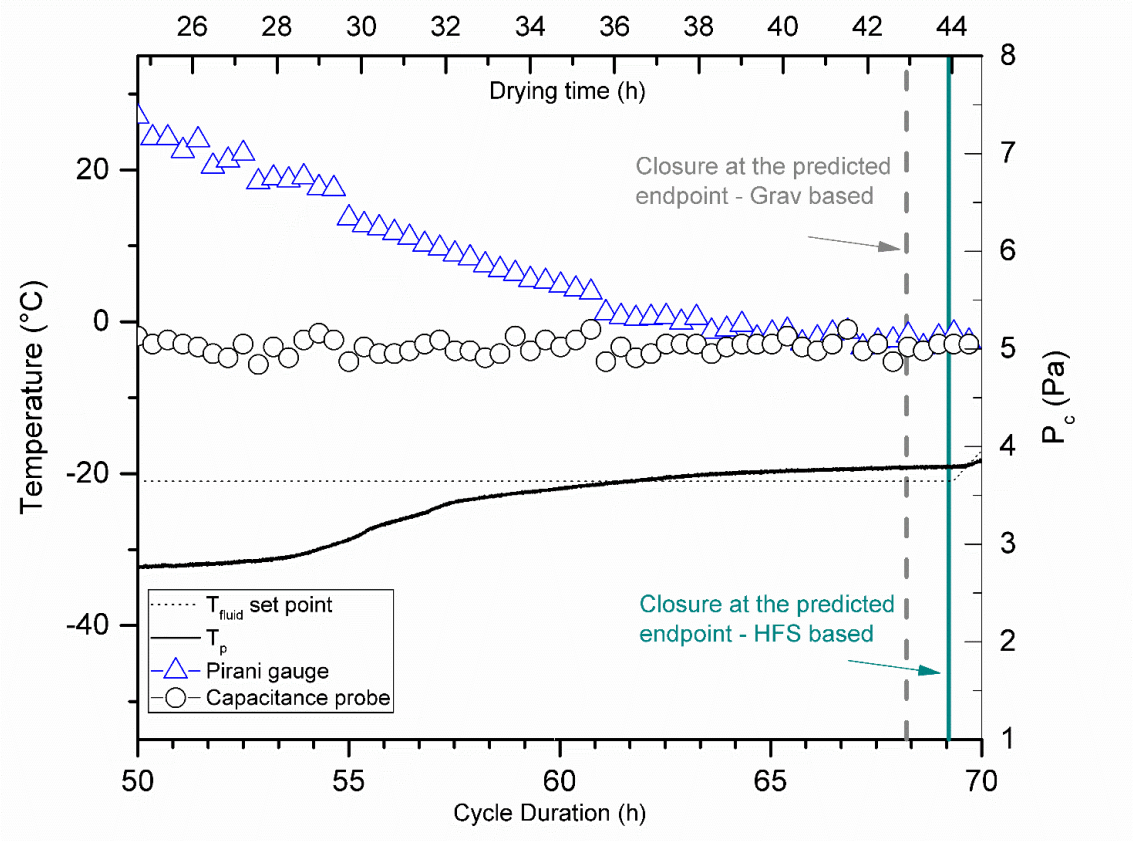

Figure 6. Verification cycle on FD02 – Zoom in to the end of primary drying showing the comparative pressure measurement.

In order to confirm the end of the primary drying, residual moisture was determined for two groups of vials closed at the two predicted time points (gravimetric- and HFS-based). The residual moisture levels are in the expected range for amorphous materials at the end of the primary drying phase [49, 50]. and the two vial groups did not significantly differ (Figure 7(a)). Those results were supplemented by the headspace moisture evaluation of the whole batch. Also in this case, no difference was highlighted between vials closed after 42:40 (h : min) (gravimetric prediction) and vials closed at 43:40 (h : min) of primary drying time (HFS-based prediction) (Figure 7(b)).

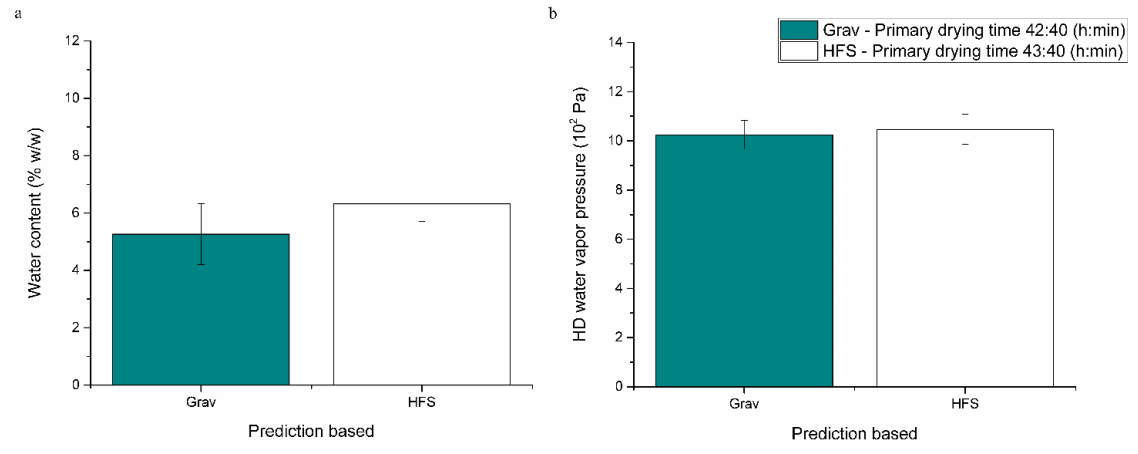

Figure 7. Verification cycle – (a) KF results for vials closed at the predicted primary drying time according the gravimetric 42:40 (h : min) (green) and the HFS method 43:40 (h : min) (white). (b) FMS results for vials closed to the predicted primary drying time according the gravimetric 42:40 (h : min) (green) and the HFS method 43:40 (h : min) (white).

The evaluation of the dried layer structure in the final products showed the absence of micro-collapses, confirming the validity of our approach (Figure A 8).

Additionally, the specific surface area (SSA) was determined as 0.78 ± 0.06 m^2/g. This result is in agreement with literature data for uncontrolled nucleation [51]. The lower standard deviation indicates a good inter-vial homogeneity, most likely resulting from the equilibration (step 3 in Table 2) in the freezing phase.

The application of HFS approach for a cycle transfer to another freeze-dryer, evidenced that the offset between the HFS and gravimetric method played a marginal role in term of drying time applying equation (7). The reason lies in equation (7): the variable term is linked to the product thermal profile, equivalent independently from the applied methods (HFS-based and gravimetric). In our experimental setup, the focus was on the heat flux sensor output and its relation with the gravimetric data for vials placed on the sensor. In this scale-up scenario, edge vials were not considered because the different design space deserves a separate investigation.

4. Conclusion

We describe for the first time an HFS-based method to develop a primary drying design space. HFS-based K_v is constantly lower than the gravimetric K_v because a P_c-independent contribution is not taken into account (most likely radiation). Nevertheless, process development can be substantially accelerated, because the HFS approach allows the determination of R_p and multiple K_v values in one single experiment by changing P_c settings within the freeze-drying cycle. The applicability of the HFS approach was confirmed with a transfer to a second freeze-dryer

using a design space generated from HFS data. Product analysis confirmed the reliability of the created design space in the case study.

Overall, the HFS methodology was successfully applied to characterize K_v and R_p. It allowed for faster analysis compared to the gravimetric approach by using a multiple-P_c experiment. Ultimately, the design space generated by HFS data compares very well with a design space developed from the gravimetric determination at low and moderate P_c. The illustrated approach presents a quick and reliable way to determine all the information for developing and safely transferring the primary drying of a lyophilization cycle, minimizing time, energy and material consumption.

Declaration of Competing Interest

The authors declare that they have no known competing financial interests or personal relationships that could have appeared to influence the work reported in this paper.

Funding

This research his research did not receive any specific grant from funding agencies in the public, commercial, or not-for-profit sectors.

Acknowledgments

The authors acknowledge Millrock Technology Inc. (Kingston, New York, USA) for the technical support. Furthermore, we want to thank Dr. Daniel Weinbuch (Coriolis Pharma) and Adam Grabarek (Coriolis Pharma) for the valuable discussions during the review of this manuscript.

5. Abbreviations and Nomenclature

A_v	cross sectional area of vial (m^2)
BET	Brunauer-Emmett-Teller
CQA	critical quality attribute
DSC	Differential scanning calorimetry
ΔH_s	sublimation heat ($J\ kg^{-1}$)
Δm	sublimed mass (kg)
Δt	considered drying time (s)
FD	freeze-dryer
FMS	frequency modulated spectroscopy
grav	gravimetric
HFS	heat flux sensor
J_w	sublimation flux ($kg\ m^{-2}\ s^{-1}$)
$J_{w\ max}$	maximum sublimation flux ($kg\ m^{-2}\ s^{-1}$)
k_{frozen}	thermal conductivity of frozen product ($W\ m^{-1}\ K^{-1}$)
KF	Karl Fischer
K_v	vial heat transfer coefficient ($W\ m^{-2}\ K^{-1}$)
L_{dried}	thickness of dried layer (m)
L_{frozen}	thickness of frozen layer (m)
l_v	average distance between vial bottom to the shelf (m^{-1})
λ_0	thermal conductivity of the gas at ambient pressure
PAT	process analytical technology
P_c	chamber pressure (Pa)
P_i	pressure at the sublimating interface (Pa)
PRT	pressure rise test
PSS	pseudo steady state
PVDF	polyvinylidene difluoride
Q_{HFS}	heat measured from heat flux sensor ($W\ m^{-2}$)
Q_{total}	total heat received by a vial ($W\ m^{-2}$)
QbD	quality by design

R^2	correlation coefficient
R_p	product resistance (m s^{-1})
t	time (s)
TDLAS	tunable diode laser absorption spectroscopy
T_{crit}	critical product temperature (K)
T_{fluid}	shelf fluid temperature (K)
T_i	temperature at the sublimating interface (K)
T_p	product temperature (K)
$T_{shelf\ surface}$	shelf surface temperature as measured by heat flux sensor (K)

6. References

[1] Deloitte, 2016 Global life sciences outlook – Moving forward with cautious optimism, (2016).

[2] F. Thomas, Changing Perceptions_ An Understanding of Lyophilization Advancements, Pharmaceutical Technology, 43 (2019) 32-34.

[3] J. Kasper, G. Winter, W. Friess, Recent advances and further challenges in lyophilization, 2013.

[4] L. Rey, J.C. May, Freeze-Drying/Lyophilization Of Pharmaceutical & Biological Products, Revised and Expanded, CRC Press, 2004.

[5] M. Pikal, Use of laboratory data in freeze drying process design: heat and mass transfer coefficients and the computer simulation of freeze drying, PDA Journal of Pharmaceutical Science and Technology, 39 (1985) 115-139.

[6] I.C. Trelea, S. Passot, F. Fonseca, M. Marin, An interactive tool for the optimization of freeze-drying cycles based on quality criteria, Drying Technology, 25 (2007) 741-751.

[7] D. Fissore, R. Pisano, A.A. Barresi, Advanced approach to build the design space for the primary drying of a pharmaceutical freeze-drying process, Journal of pharmaceutical sciences, 100 (2011) 4922-4933.

[8] E. Meister, H. Gieseler, Freeze-dry microscopy of protein/sugar mixtures: drying behavior, interpretation of collapse temperatures and a comparison to corresponding glass transition data, Journal of pharmaceutical sciences, 98 (2009) 3072-3087.

[9] S.L. Nail, S. Jiang, S. Chongprasert, S.A. Knopp, Fundamentals of freeze-drying, in: Development and manufacture of protein pharmaceuticals, Springer, 2002, pp. 281-360.

[10] S. Rambhatla, M.J. Pikal, Heat and mass transfer scale-up issues during freeze-drying, I: atypical radiation and the edge vial effect, Aaps Pharmscitech, 4 (2003) 22-31.

[11] M. Pikal, M. Roy, S. Shah, Mass and heat transfer in vial freeze-drying of pharmaceuticals: Role of the vial, Journal of pharmaceutical sciences, 73 (1984) 1224-1237.

[12] A. Hottot, S. Vessot, J. Andrieu, Determination of mass and heat transfer parameters during freeze-drying cycles of pharmaceutical products, PDA Journal of Pharmaceutical Science and Technology, 59 (2005) 138-153.

[13] M. Brülls, A. Rasmuson, Heat transfer in vial lyophilization, International Journal of Pharmaceutics, 246 (2002) 1-16.

[14] W.Y. Kuu, L.M. Hardwick, M.J. Akers, Rapid determination of dry layer mass transfer resistance for various pharmaceutical formulations during primary drying using product temperature profiles, International journal of pharmaceutics, 313 (2006) 99-113.

[15] A. Giordano, A.A. Barresi, D. Fissore, On the use of mathematical models to build the design space for the primary drying phase of a pharmaceutical lyophilization process, Journal of Pharmaceutical Sciences, 100 (2011) 311-324.

[16] S.M. Patel, M.J. Pikal, Lyophilization process design space, Journal of pharmaceutical sciences, 102 (2013) 3883-3887.

[17] X.Y. Lawrence, Pharmaceutical quality by design: product and process development, understanding, and control, Pharmaceutical research, 25 (2008) 781-791.

[18] M. Galan, Monitoring and control of industrial freeze-drying operations: the challenge of implementing quality-by-design (QbD), Freeze Drying/Lyophilization of Pharmaceutical and Biological Products, (2016) 441-459.

[19] I.H.T. Guideline, Pharmaceutical development Q8, Current Step, 4 (2005) 11.

[20] S.L. Nail, J.A. Searles, Elements of quality by design in development and scale-up of freeze-dried parenterals, BioPharm International, 21 (2008) 44.

[21] S.A. Velardi, A.A. Barresi, Development of simplified models for the freeze-drying process and investigation of the optimal operating conditions, Chemical Engineering Research and Design, 86 (2008) 9-22.

[22] V.R. Koganti, E.Y. Shalaev, M.R. Berry, T. Osterberg, M. Youssef, D.N. Hiebert, F.A. Kanka, M. Nolan, R. Barrett, G. Scalzo, Investigation of design space for freeze-drying: use of modeling for primary drying segment of a freeze-drying cycle, AAPS PharmSciTech, 12 (2011) 854-861.

[23] N. Milton, M.J. Pikal, M.L. Roy, S.L. Nail, Evaluation of manometric temperature measurement as a method of monitoring product temperature during lyophilization, PDA Journal of Pharmaceutical Science and Technology, 51 (1997) 7-16.

[24] P. Chouvenc, S. Vessot, J. Andrieu, P. Vacus, Optimization of the freeze-drying cycle: a new model for pressure rise analysis, Drying Technology, 22 (2004) 1577-1601.

[25] S.A. Velardi, V. Rasetto, A.A. Barresi, Dynamic parameters estimation method: advanced manometric temperature measurement approach for freeze-drying monitoring of pharmaceutical solutions, Industrial & Engineering Chemistry Research, 47 (2008) 8445-8457.

[26] S. Schneid, H. Gieseler, W. Kessler, M. Pikal, Tunable diode laser absorption spectroscopy (TDLAS) as a residual moisture monitor for the secondary drying stage of freeze drying, in: Proceedings of AAPS Annual Meeting, San Diego, CA, USA, 2007.

[27] D. Fissore, R. Pisano, A.A. Barresi, On the methods based on the Pressure Rise Test for monitoring a freeze-drying process, Drying Technology, 29 (2010) 73-90.

[28] X.C. Tang, S.L. Nail, M.J. Pikal, Freeze-drying process design by manometric temperature measurement: design of a smart freeze-dryer, Pharmaceutical research, 22 (2005) 685-700.

[29] X. Tang, S.L. Nail, M.J. Pikal, Evaluation of manometric temperature measurement, a process analytical technology tool for freeze-drying: Part I, product temperature measurement, AAPS PharmSciTech, 7 (2006) E95-E103.

[30] X.C. Tang, S.L. Nail, M.J. Pikal, Evaluation of manometric temperature measurement, a process analytical technology tool for freeze-drying: part II measurement of dry-layer resistance, AAPS PharmSciTech, 7 (2006) E77-E84.

[31] X.C. Tang, S.L. Nail, M.J. Pikal, Evaluation of manometric temperature measurement (MTM), a process analytical technology tool in freeze drying, part III: heat and mass transfer measurement, AAPS PharmSciTech, 7 (2006) E105-E111.

[32] V.M. Meyer, B. Keller, A new heat flux sensor: From microvolts to millivolts, sensors and Materials, 8 (1996) 345-356.

[33] I. Vollrath, V. Pauli, W. Friess, A. Freitag, A. Hawe, G. Winter, Evaluation of heat flux measurement as a new process analytical technology monitoring tool in freeze drying, Journal of pharmaceutical sciences, 106 (2017) 1249-1257.

[34] B. Scutellà, A. Plana-Fattori, S. Passot, E. Bourlès, F. Fonseca, D. Flick, I.-C. Trelea, 3D mathematical modelling to understand atypical heat transfer observed in vial freeze-drying, Applied Thermal Engineering, 126 (2017) 226-236.

[35] B. Scutellà, S. Passot, E. Bourlés, F. Fonseca, I.C. Tréléa, How vial geometry variability influences heat transfer and product temperature during freeze-drying, Journal of pharmaceutical sciences, 106 (2017) 770-778.

[36] W.Y. Kuu, S.L. Nail, G. Sacha, Rapid determination of vial heat transfer parameters using tunable diode laser absorption spectroscopy (TDLAS) in response to step-changes in pressure set-point during freeze-drying, Journal of Pharmaceutical Sciences, 98 (2009) 1136-1154.

[37] D. Fissore, R. Pisano, A.A. Barresi, Model-based framework for the analysis of failure consequences in a freeze-drying process, Industrial & Engineering Chemistry Research, 51 (2012) 12386-12397.

[38] D. Fissore, A.A. Barresi, Scale-up and process transfer of freeze-drying recipes, Drying Technology, 29 (2011) 1673-1684.

[39] H. Gieseler, W.J. Kessler, M. Finson, S.J. Davis, P.A. Mulhall, V. Bons, D.J. Debo, M.J. Pikal, Evaluation of tunable diode laser absorption spectroscopy for in-process water vapor mass flux measurements during freeze drying, Journal of Pharmaceutical Sciences, 96 (2007) 1776-1793.

[40] S. Hibler, H. Gieseler, Heat transfer characteristics of current primary packaging systems for pharmaceutical freeze-drying, Journal of pharmaceutical sciences, 101 (2012) 4025-4031.

[41] M. Pikal, W. Mascarenhas, H. Akay, S. Cardon, C. Bhugra, F. Jameel, S. Rambhatla, The nonsteady state modeling of freeze drying: in-process product temperature and moisture content mapping and pharmaceutical product quality applications, Pharmaceutical development and technology, 10 (2005) 17-32.

[42] S. Hibler, C. Wagner, H. Gieseler, Vial freeze-drying, part 1: new insights into heat transfer characteristics of tubing and molded vials, Journal of pharmaceutical sciences, 101 (2012) 1189-1201.

[43] R. Pisano, D. Fissore, A.A. Barresi, Heat transfer in freeze-drying apparatus, Heat Transfer, 1 (2011) 91-114.

[44] S.M. Patel, F. Jameel, M.J. Pikal, The effect of dryer load on freeze drying process design, Journal of pharmaceutical sciences, 99 (2010) 4363-4379.

[45] D.E. Overcashier, T.W. Patapoff, C.C. Hsu, Lyophilization of protein formulations in vials: Investigation of the relationship between resistance to vapor flow during primary drying and small-scale product collapse, Journal of pharmaceutical sciences, 88 (1999) 688-695.

[46] W.Y. Kuu, K.R. O'Bryan, L.M. Hardwick, T.W. Paul, Product mass transfer resistance directly determined during freeze-drying cycle runs using tunable diode laser absorption spectroscopy (TDLAS) and pore diffusion model, Pharmaceutical development and technology, 16 (2011) 343-357.

[47] B. Scutellà, I.C. Trelea, E. Bourlès, F. Fonseca, S. Passot, Determination of the dried product resistance variability and its influence on the product temperature in pharmaceutical freeze-drying, European Journal of Pharmaceutics and Biopharmaceutics, 128 (2018) 379-388.

[48] E. Meister, Methodology Data Interpretation and Practical Transfer of Freeze-Dry Microscopy, PhD dissertation, (2009).

[49] S.M. Patel, T. Doen, M.J. Pikal, Determination of end point of primary drying in freeze-drying process control, Aaps Pharmscitech, 11 (2010) 73-84.

[50] D. Zasypkin, T.C. Lee, Extracellular ice nucleators from Pantoea ananas: effects on freezing of model foods, Journal of food science, 64 (1999) 473-478.

[51] S.M. Patel, C. Bhugra, M.J. Pikal, Reduced pressure ice fog technique for controlled ice nucleation during freeze-drying, Aaps Pharmscitech, 10 (2009) 1406.

7. Appendix

7.1.Scanning Electron Microscopy

The morphology of the dried powder was analyzed by using a scanning electron microscope (Phenom, Phenom-World B.V., Eindhoven, the Netherlands). Glass vials were cut horizontally in the middle of the vial, above the freeze-dried cake and the product was removed. Slices of the freeze-dried material were placed on carbon conductive cement on a sample holder. The samples were analyzed under vacuum between 150x and 700x at 5 kV acceleration voltages.

7.2.BET

The specific surface area of the three freeze-dried products was analyzed by using a Quadrasorb-Evo (3P Instruments, Odelzhausen, Germany). Approximately 100 mg were placed in the measuring cell and degassed for a minimum of 16 hours at room temperature. After filling the cells with helium (0.7 – 1.0 bar) for about 5 seconds, krypton sorption measurement was performed at -195.8 °C. Six data points covering a p/p_0 (respectively p adsorbate equilibrium pressure / p_0 adsorbate saturation pressure) region of 0.05 to 0.35 were collected. The data points were evaluated according to the multipoint BET theory. Data were considered acceptable when the correlation coefficient © of linear regression was ≥ 0.9975.

7.3.Calculation of T_i

The model applied in this study relies on the energy balance at the sublimating interface described from the following equation:

heat supplied from freeze-dryer = heat removed by sublimation

$$\left(\frac{1}{K_v}+\frac{L_{frozen}}{k_{frozen}}\right)^{-1} * \left(T_{shelf} - T_i\right) = \Delta H_s * J_w$$

rearranged:

$$T_i = T_{shelf} - \Delta H_s * J_w * \left(\frac{1}{K_v}+\frac{L_{frozen}}{k_{frozen}}\right)$$

The thickness of frozen layer (L_{frozen}) is extremely small (i.e., 10-3 m) and it can be approximated $\left(\frac{1}{K_v}+\frac{L_{frozen}}{k_{frozen}}\right)$ as $\left(\frac{1}{K_v}\right)$ and equation can be written also as:

$$T_i = constant_1 - constant_2 * J_w * \left(\frac{1}{K_v}\right)$$

In this case study J_w (inversely proportional to R_p) and K_v present the same offset from the gravimetric calculation and the T_i , the estimated temperature at the sublimating interface, is comparable for both methods (gravimetric- and HFS-based). As pointed out, three different types of vials, different shelf temperatures (T_{fluid}) and chamber pressures (P_c) were assessed and same offset was obtained between gravimetric and HFS method.

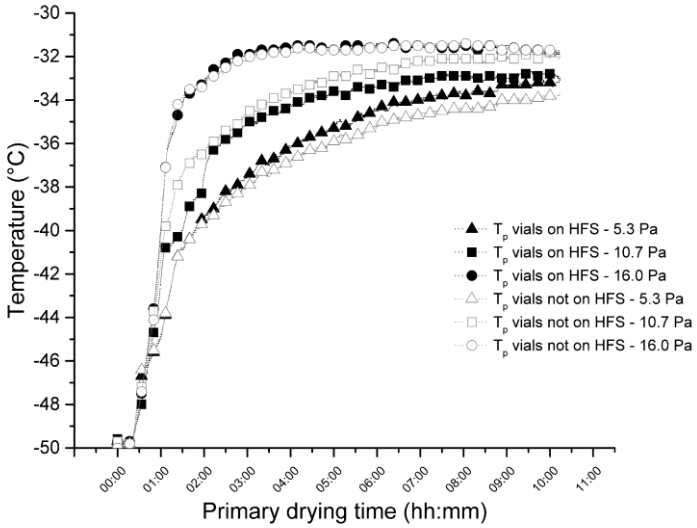

Figure A 1. T_P for vials placed on (filled symbols) and not (empty symbols) on the HFS at different P_c.

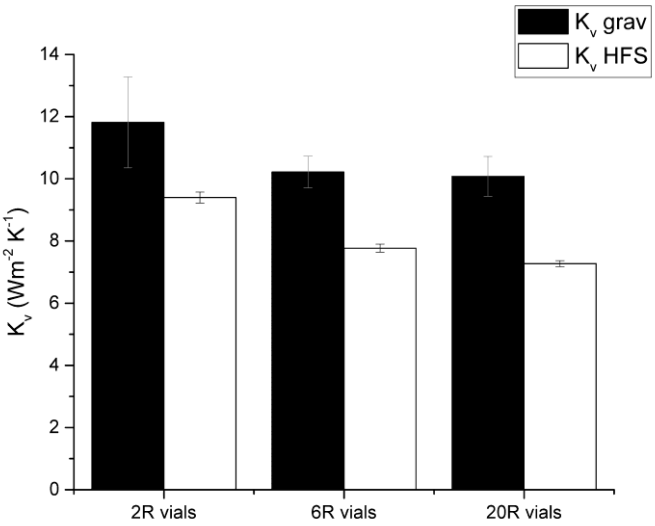

Figure A 2. K_v grav and K_v HFS for different vial types.

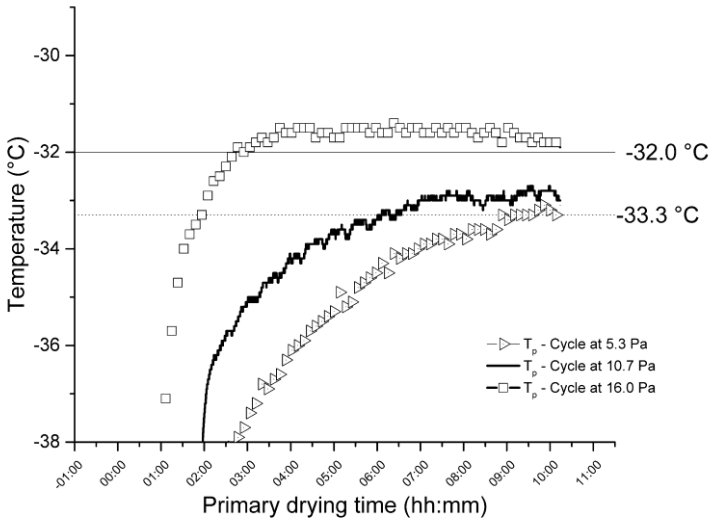

Figure A 3. T_p in cycles performed at different P_c including T_g' (-33.3 °C) and T_c (-32.0 °C) for the considered formulation.

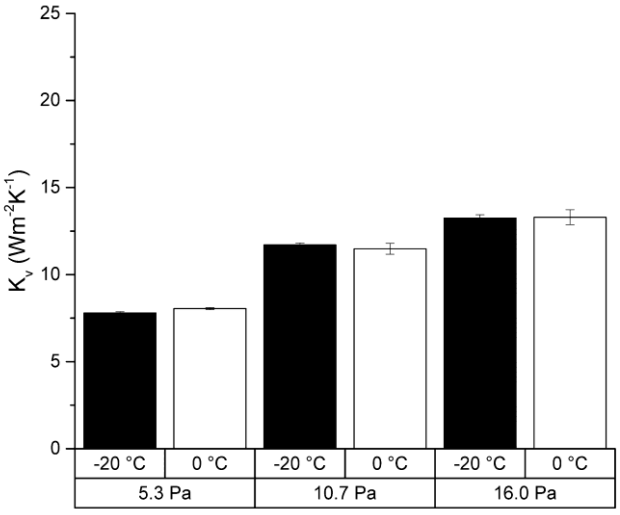

Figure A 4. K_v HFS at different T_{fluid}.

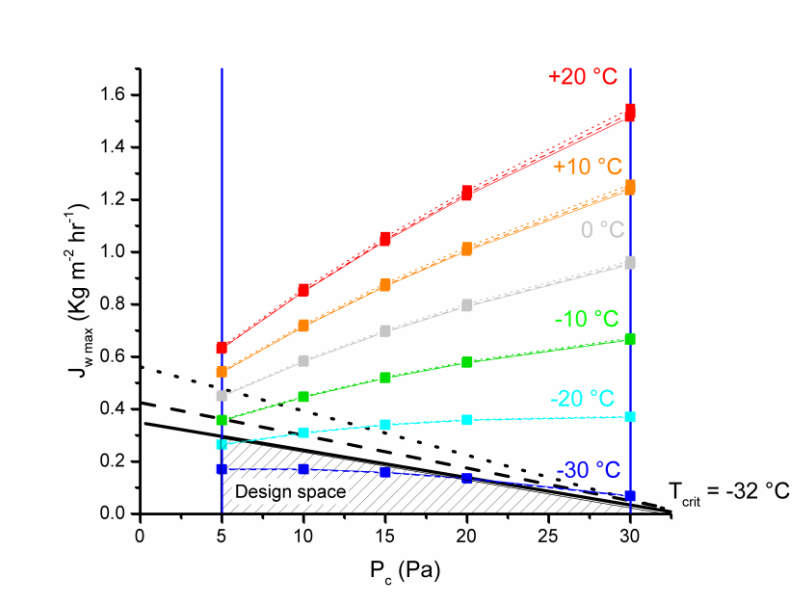

Figure A 5. Design space generated from HFS data. Black lines indicate the design space derived from R_P obtained at different P_c (___5.3 Pa, _ _ _ 10.7 Pa, ….. 16.0 Pa)

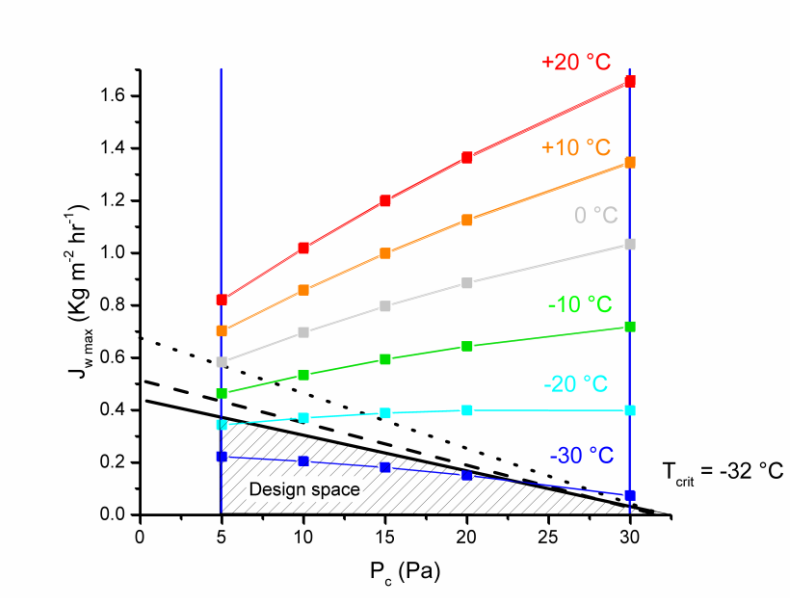

Figure A 6. Design space generated from gravimetric data. Black lines indicate the design space derived from R_P obtained at different P_c (___5.3 Pa, _ _ _ 10.7 Pa, ….. 16.0 Pa)

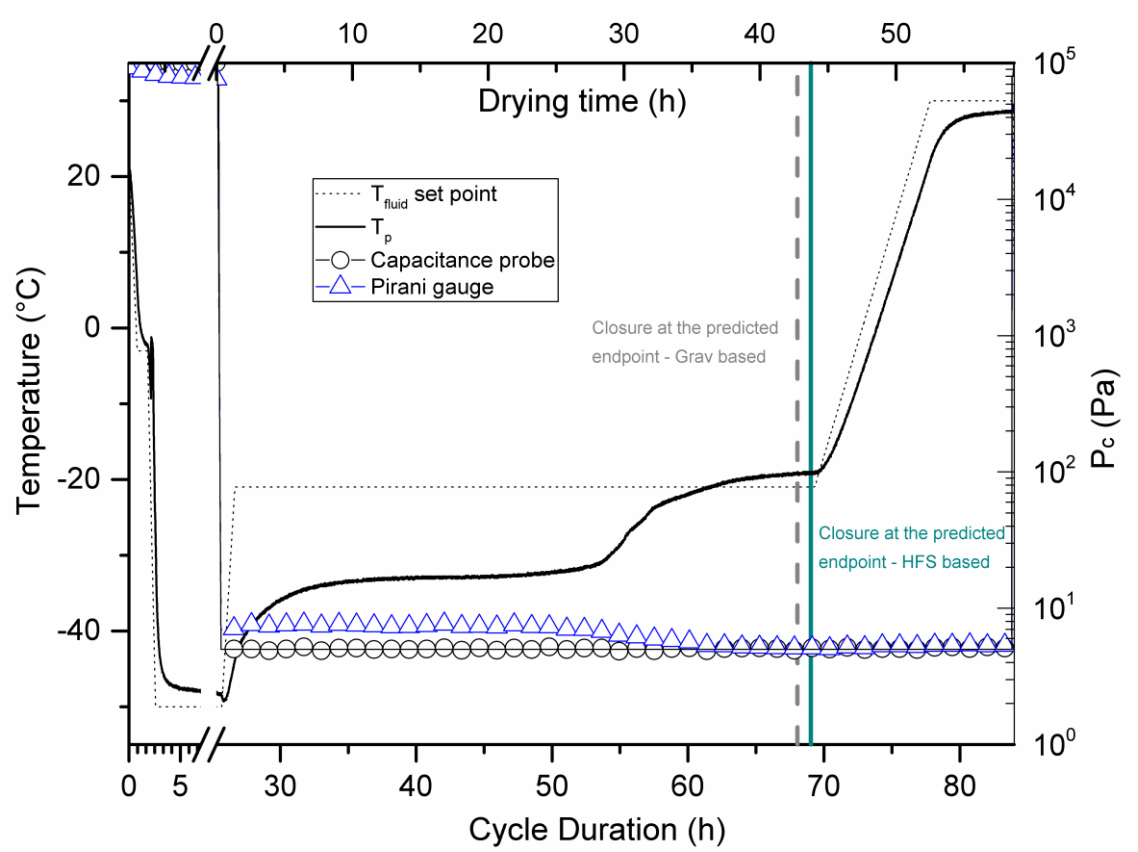

Figure A 7. Verification cycle – process readouts.

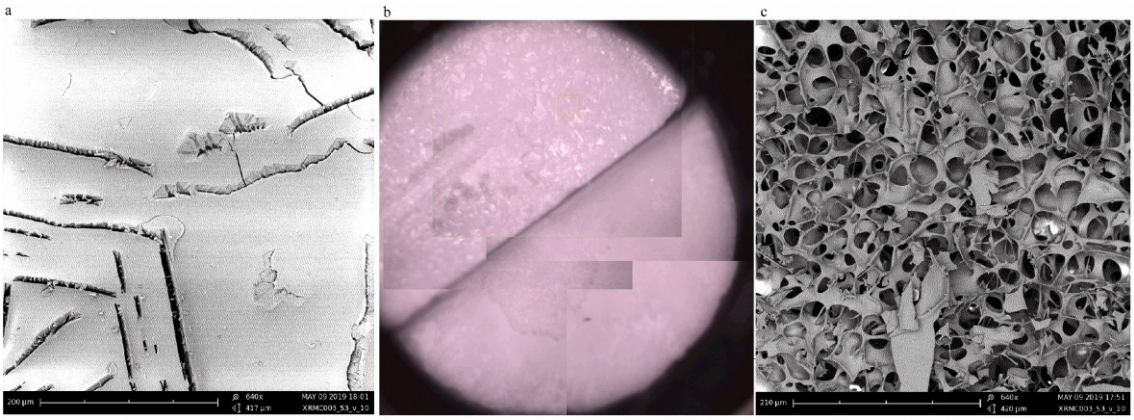

Figure A 8. Verification cycle – SEM pictures ((a) – Zoom on top of the lyophilized product / (b) – Top and bottom view of the lyophilized product / (c) – Zoom on bottom part of the lyophilized product).

Chapter IV: Design of freeze-drying cycles: the determination of heat transfer coefficient by using heat flux sensor and MicroFD

Marco Carfagna[1, 2], Monica Rosa[1], Andrea Hawe[1]*, Wolfgang Frieß[2]

[1] Coriolis Pharma Research GmbH, Fraunhoferstrasse 18 b, 82152 Martinsried, Germany;

[2] Department of Pharmacy, Pharmaceutical Technology and Biopharmaceutics, Butenandt Strasse 5, Ludwig-Maximilians-Universitaet Muenchen, D-81377 Munich, Germany;

* Corresponding author: Andrea Hawe, Coriolis Pharma Research GmbH, Fraunhoferstraße 18 b, 82152 Martinsried, Germany; e-mail: andrea.hawe@coriolis-pharma.com; Tel.: +49(0)89 41 77 60 -251

The following chapter has been published in the International Journal of Pharmaceutics as:

Design of freeze-drying cycles: The determination of heat transfer coefficient by using heat flux sensor and MicroFD

Marco Carfagna, Monica Rosa, Andrea Hawe, Wolfgang Frieß,

International Journal of Pharmaceutics,

Volume 621, 2022,121763, ISSN 0378-5173, https://doi.org/10.1016/j.ijpharm.2022.121763.

Abstract

The complexity of biopharmaceuticals requires often the freeze-drying as stabilizing process. Inadequate parameters in the primary drying phase can impair product quality, besides, increasing time and costs. Therefore, the process requires a thorough characterization and with this purpose, heat flux sensor (HFS) and miniaturized freeze-dryers conceived to emulate larger equipment, were recently introduced. Our study investigates, for the first time, the use of HFS and miniaturized freeze-dryer (MicroFD) in combination to obtain the heat transfer coefficient (K_v) for two formulation types and freezing protocols. First, as the MicroFD presents the possibility to set the temperature of vial surrounding (LyoSIM), it was determined which set-up was representative for a lab-scale freeze drying process. Additionally, the HFS-based results were compared with the data obtained by the most accurate, but time-consuming and invasive gravimetric method. Second, the role of atypical heat transfer was evaluated for HFS and gravimetric methodology with gold-coated and un-coated vials. Obtained results revealed the HFS and the MicroFD can be used in combination to obtain K_v real-time with much less effort that gravimetrically, to study different vial scenarios, and to design lyophilization processes with a limited amount of material and experiments.

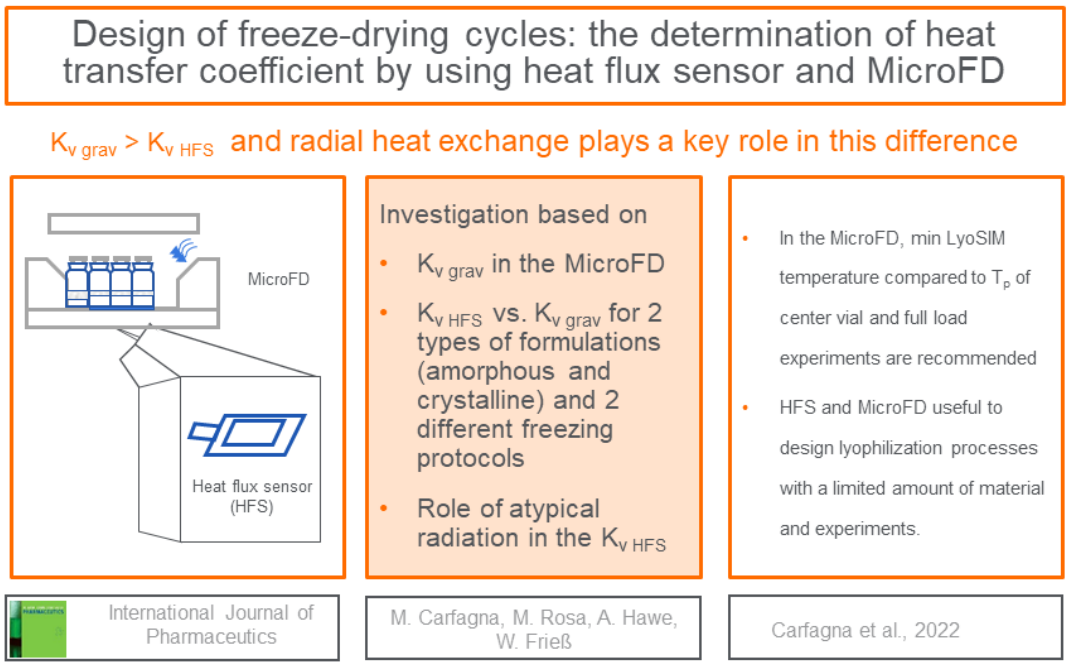

1. Introduction

Pharmaceutical development costs on average $ 1.8 billion (USD) and requires 13.5 years from molecule discovery to market [1,2]. One of the challenges, especially in early-stage formulation screening, is the limited availability of drug substance [3]. According to the quality by design (QbD) approach, a good process understanding and subsequent control of the input variables (e.g., process parameters) are essential to ensure that a product meets the critical quality attributes (cQAs) [4]. A fast determination of optimal process parameters during the early development phase helps to reduce the development time and to meet QbD expectations.

Freeze-drying is the most common stabilizing strategy for biologic drug products in case of instability in the liquid state. More than 30% of protein products newly registered within the last 5 years are marketed in the freeze-dried state and only in 2019, the U.S. FDA approved a total of 47 lyophilized drug [5,6]. During freeze-drying cycle development, the primary drying step requires particular attention, as an inappropriate choice of shelf temperature and pressure can impair product quality substantially [7]. A prerequisite for rational parameter selection is the determination of the heat received by the vial and the mass of water leaving the product [8,9]. Both fluxes (heat flux indicated as Q and sublimation flux as J_w) can be obtained respectively by following equations (1) and (2) [10]:

$$Q = K_v \left(T_{fluid} - T_p\right) \quad (1)$$

$$J_w = (P_i - P_c) \left(R_p\right)^{-1} \quad (2)$$

As shown in equation (1), Q is directly proportional to the driving force, the temperature difference between fluid circulating in the shelf (T_{fluid}) and product in the vial (T_p), and to the heat transfer coefficient (K_v). The latter was introduced to measure the impact of the vial and of the equipment on the freeze-drying process, and depends on the position of the vial within the dryer. As stated in equation (2), J_w is directly proportional to the driving force, the pressure difference between sublimating interface (P_i) and chamber (P_c), and is inversely proportional to the product resistance (R_p). Considering the same frozen solvent temperature and type, R_p describes the effect of the formulation composition and the freezing conditions on sublimation [11].

In recent years, heat flux sensors (HFSs) have been introduced as process analytical technology (PAT) for freeze-drying [12]. An HFS transduces the difference between the temperature above and below its surface into a voltage output, which is then converted into a heat flux output. In our previously published study, we have assessed the ability of the HFS to determine the coefficients necessary to obtain primary drying parameters and consequently a design space for an amorphous formulation [13]. Additionally, the HFS can monitor the freezing

step detecting nucleation and end of crystal growth [14], and can be applied to support secondary drying modelling [15].

The potential of HFS to generate key data without affecting the process is extremely interesting, especially if the available amount of material is limited, e.g., in early phase development. Up to now, HFSs has not been evaluated to obtain K_v directly comparing different formulations, specifically amorphous and crystalline. Gravimetric determination of K_v is well established and can be applied independently of the formulation type. It is reliable, but invasive based on the fact it is necessary to stop lyophilization cycle before the end of primary drying and time-consuming because it requires at least 3 separate experiments as well as the interruption of the freeze-drying cycles. We wanted to assess if and how HFS can be applied as a routine PAT tool to design and control the cycle without any limitations regarding formulation type. Furthermore, in previous work, the K_v values based on the HFS were underestimated as compared to the state-of-the-art gravimetric method [13,14]. We aimed to obtain to a better understanding of HFS output, provide an explanation for the observed differences and ultimately obtain K_v / R_p values by HFS suitable to predict the lyophilization process.

Our present work, which was conducted in a miniaturized freeze-drying equipment (Micro FD) was divided into three parts:

a. Investigation of gravimetric-based K_v in the Micro FD
b. Assessment of HFS-based K_v and comparison to K_v gravimetric for two types of formulations (amorphous and crystalline) and two different freezing protocols
c. Investigation on the role of atypical radiation in the HFS output

2. Materials and methods

2.1 Formulations and primary packaging

Experiments were carried out with 10% w/v solutions of sucrose (Ph. Eur. grade; Merck, Darmstadt, Germany) and 5% w/v solutions of mannitol (Ph. Eur. grade; Roquette, Lestrem, France) in highly purified water (Milli-Q integral water purification system, Merck Millipore, Hertfordshire, United Kingdom). Both formulations were filtered by using 0.22 µm PVDF membrane filters (Merck, Darmstadt, Germany) prior to filling. 5 ml solution were filled in 6R TopLyo glass vials (Schott, Müllheim-Hügelheim, Germany) and the vials were partially closed with 20-mm bromobutyl single vent lyophilization stoppers (Westar RS, FluoroTec B2-40 coating; West, Eschweiler, Germany).

2.2 Freeze-drying equipment and heat flux sensor (HFS)

Freeze-drying experiments were performed in a MicroFD (Millrock Technology, Kingston, NY) which holds a temperature-controlled ring called LyoSIM in close contact with the vials [16,17]. The user can set a LyoSIM offset compared to T_p (range ± 15°C) or regulate it within ± 60°C independent of T_p. A maximum of 19 vials was used in the study configuration. The MicroFD is equipped with only one shelf of 0.07 m^2 surface area. Pressure is controlled by a capacitance manometer and the unit has an additional Pirani gauge. Temperature is measured by T-type copper-constantan thermocouples (TCs) in combination with thermocouple holders (Millrock Technology, Kingston, NY). One HFS is located in the center of the shelf. HFS-based K_v (K_v HFS) values are calculated from the sensor readout (Q_{HFS}) according to:

$$K_v\ HFS = Q_{HFS}\left(T_{shelf\ surface} - T_p\right)^{-1} \quad (3)$$

where $T_{shelf\ surface}$ is the temperature of the shelf surface as measured from the built-in thermocouple of the HFS, and T_p is the product temperature measured at the vial bottom from the TC. T_{fluid} is the shelf fluid temperature set in the MicroFD.

2.3 Determination of K_v: gravimetric and HFS experiments

Based on two different processes (Table 1) a list of freeze-drying experiments varying in freezing protocol,

Table 1. Freeze-drying protocols.

Process Nomenclature	No.	Step	Time [hh:mm:ss]	T_{fluid} [°C]	P_c [Pa]	Ramp [°C/min]
A	1	Loading	00:00:00	20	100,000	
	2	Freezing	00:46:00	-3	100,000	0.50
	3		01:00:00	-3	100,000	
	4		00:47:00	-50	100,000	1.00
	5		02:00:00	-50	100,000	
B	2	Freezing	00:46:00	-3	100,000	0.50
	3		01:00:00	-3	100,000	
	4		00:54:00	-30	100,000	0.50
	5		02:00:00	-30	100,000	
	6		00:40:00	-10	100,000	0.50
	7		02:00:00	-10	100,000	
	8		00:40:00	-50	100,000	1.00
	9		02:00:00	-50	100,000	
A/B	6/10	Primary drying	00:15:00	-50	As indicated in Table 2	
	7/11		01:00:00	-20		0.50
	8/11		09:00:00	-20		

LyoSIM setting, P_c, number of vials used and formulation was performed (Table 2).

Table 2. Freeze-drying experiments.

No.	Process	LyoSIM offset compared to T_p [°C]	P_c [Pa]	No. vials	Formulation
1/2/3	A	0	5 / 11 / 16	19	Sucrose
4/5/6		-4			
7/8/9		-6			
10/11/12		-8			
13/14/15		-15			
16/17		-15		7	
18	A with freezing duration (step 5) as total duration of B	-15	5		
19	B	-15		19	
20		-15			Mannitol

Water loss (Δm) was measured by weighing all 19 filled vials placed in the MicroFD before the start of the process and after circa 10 hours of primary drying on an analytical balance (Genius ME – Sartorius, Gottingen, Germany). In this time frame, T_p is consistently reliable because thermocouple keeps the contact with the material as the drying is prematurely stopped. K_v was calculated according to the following equation:

$$K_v\ grav = \frac{\Delta m\ \Delta H_s}{A_v \int_0^{\Delta t} \left(T_{fluid} - T_p\right) dt} \tag{4}$$

where ΔH_s is the sublimation heat of ice, and A_v is the cross-sectional area of the vial.

2.4 Mathematical description of the HFS-based heat transfer coefficient

Non-linear fitting of K_v was performed by applying the Levenberg–Marquardt algorithm with Origin 2016 (OriginLab Corporation, Northampton, MA). The following equation was used for K_v calculation:

$$K_v = A_{Kv} + \frac{B_{Kv}\ P_C}{1 + l_v \frac{B_{Kv}}{\lambda_0}\ P_C} \tag{5}$$

The first summand (A_{Kv}) describes heat contributions related to vial-to-shelf contact and to uncontrolled radiation. The second summand represents the gas conduction according the Smoluchowsky theory. B_{Kv} is a coefficient proportional to gas temperature and gas composition in the chamber, l_v is the average distance between vial bottom and shelf, and λ_0 is the thermal conductivity of gas in the chamber at ambient pressure [18]. l_v was estimated using an imprint test [19], while λ_0 was adopted from literature ($1.8\ 10^{-2}$ $Wm^{-1}K^{-1}$)[11].

2.5 Radiation contribution in HFS output: gold plated vials

A gilding kit including a gold leaf (KVP Kölner Vergolderprodukte GmbH, Dresden, Germany) was used for plating vials. A base for glass preparation and, subsequently, an activator, were applied with a synthetic brush. After drying of the reagents, a gold leaf was pressed onto the vial with a soft cloth to ensure a smooth application.

2.6 Emissivity measurements

Vial temperature was measured with an infrared thermometer PeakTech 4980 (PeakTech Prüf- und Messtechnik GmbH, Ahrensburg, Germany) and a resistance temperature detector (Pt100 – Martin Christ, Osterode, Germany). The emissivity value (ε) input of the infrared thermometer was adjusted to achieve a temperature.

2.7 Data analysis

Throughout the manuscript, wherever not stated differently, gravimetric values K_v are based on experimental mean (calculated on n = 6 for center vials / n = 11 for edge vials) ± standard deviation.

3. Results and discussion

3.1. K_v determination in the MicroFD by using the gravimetric approach

In freeze-drying, two vial populations can be distinguished, center vials which are confined by other vials and edge vials which are closer to the chamber wall and not fully surrounded by other vials. Edge vials are exposed to a higher heat flux due to atypical radiation and to less cooling effect by neighboring vials [20,21]. The MicroFD contains a higher proportion of edge vials relative a lab-scale freeze-dryers and its walls and door are closer to the edge vials boosting the radiation impact [20,22].

Preliminary experiments using water for K_v evaluation demonstrated an extremely curved sublimation front and conical ice shape with pronounced shrinkage (Figure S1). This was even the case when the LyoSIM temperature offset compared to T_p was set to the minimum value of -15°C. The mathematical model for K_v calculation assumes a constant sublimation area and the absence of a radial thermal gradient [23]. Therefore, we used a sucrose solution in our study to ensure at least contact of the drying product with the container walls and to reduce cone formation. The heat transfer experiments for vials in contact, edge vials, and vials not in contact with the LyoSIM (center vials) were conducted at 5, 11, and 16 Pa and at different LyoSIM temperature settings. The lowest P_c represents the lower end of values for manufacturing freeze-dryer. At the highest value, pressure is the predominant factor in the heat transfer and 11 Pa were selected as midpoint in between [24,25]. The LyoSIM temperature offset was regulated based on T_p of the vial in the very center reflecting the ultimate center vial.

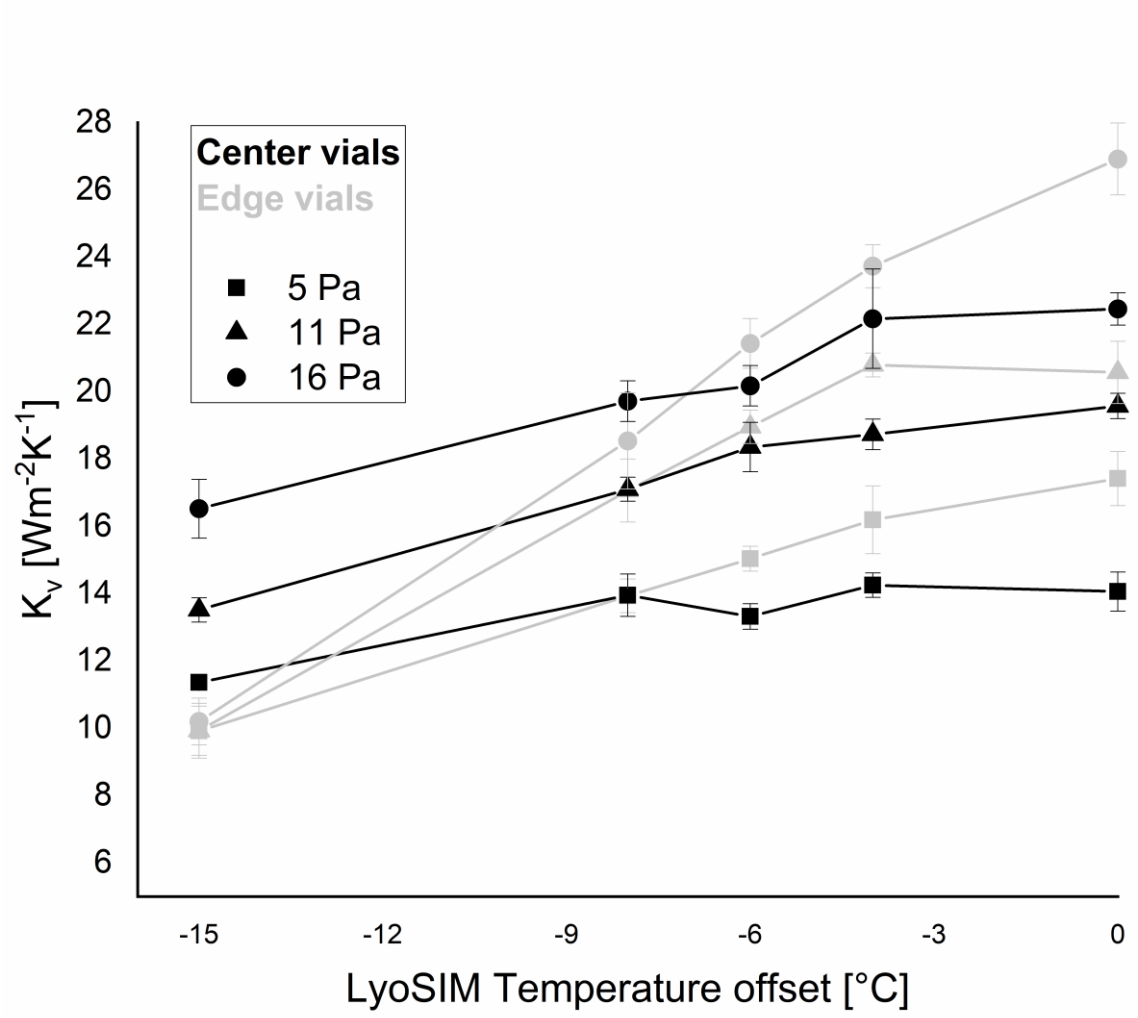

Figure 1: K_v gravimetric obtained for different LyoSIM setting (offset compared to product temperature) in the MicroFD for center and edge vials, depending on the chamber pressure during primary drying – for 10%w/v sucrose.

In Figure 1, the heat transfer results, expressed by K_v, are plotted against the set LyoSIM temperature. The presented K_v results were determined based on vials without TC. Therefore, mass flux was unaffected. Bosca et al. found similar T_p profiles, R_p and K_v values in a non-GMP environment for vials with and without TC [26]. For both vial populations, rather high K_v values were determined at the lowest LyoSIM offset value of 0°C. These K_v values give an estimation of the heat surplus for this small-size equipment compared to traditional lab-scale freeze-dryers. The difference in K_v between center and edge vials is more pronounced at higher P_c with 4.5 and 3.4 $Wm^{-2}K^{-1}$ at 16 and 5 Pa, respectively. K_v becomes the same for center and edge vials when the LyoSIM temperature offset is -7°C at 16 Pa or -8°C at 5 and 11 Pa. This finding is relevant if one wants to obtain a homogenous batch in terms of heat transfer in the MicroFD. In contrast, setting a -15°C LyoSIM offset allows to emulate the heat transfer for center vials in the lab-scale freeze-dryer. Accordingly, the K_v of 10.4 ± 1.0 $Wm^{-2}K^{-1}$ obtained in the

MicroFD corresponds well to 10.2 ± 0.8 $Wm^{-2}K^{-1}$ obtained in a lab-scale freeze dryer equipped with an HFS, applying 5 Pa and a T_{fluid} of -20°C [19]. Thus, it is possible to distinguish the behavior of edge and center vials. When the temperature offset is set to the minimum of -15°C, K_v is independent of P_c for edge vials at ~10 $Wm^{-2}K^{-1}$ as the predominant heat transfer mechanisms are contact and radiation contribution (Figure 1). In contrast, at this minimum temperature offset, the heat transfer of center vials is influenced by gas conduction and comparable to lab-scale freeze-dryers.

Heat transfer in freeze-drying includes pressure related gas conduction between vial and shelf and non-pressure related radiation and direct vial to shelf contact [27]. To define the role of the different mechanisms, we performed a non-linear fit according to Equation 5. The results are summarized in Table 3 and Figure 2.

Table 3. Contact / radiation (A_{Kv}) and gas-related (B_{Kv}) parameters calculated by fitting of K_v gravimetric.

Parameter	**LyoSIM offset compared to Tp [°C]**	**K_v grav –edge vials**	**K_v grav – center vials**
A_{Kv} [$Wm^{-2}K^{-1}$]	0	12.19	10.33
B_{Kv} [$Wm^{-2}K^{-1}Pa^{-1}$]		0.98	0.85
A_{Kv} [$Wm^{-2}K^{-1}$]	-4	11.87	8.76
B_{Kv} [$Wm^{-2}K^{-1}Pa^{-1}$]		0.99	1.16
A_{Kv} [$Wm^{-2}K^{-1}$]	-6	10.87	8.80
B_{Kv} [$Wm^{-2}K^{-1}Pa^{-1}$]		0.87	0.96
A_{Kv} [$Wm^{-2}K^{-1}$]	-8	10.97	10.48
B_{Kv} [$Wm^{-2}K^{-1}Pa^{-1}$]		0.60	0.71
A_{Kv} [$Wm^{-2}K^{-1}$]	-15	9.72	8.69
B_{Kv} [$Wm^{-2}K^{-1}Pa^{-1}$]		0.28	0.52

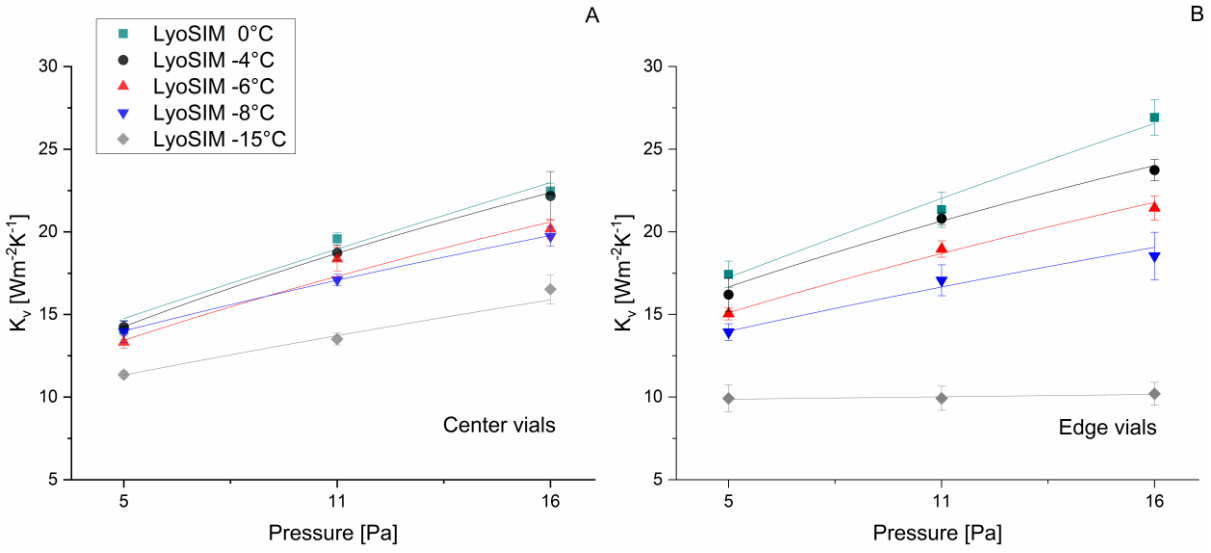

Figure 2: K_v grav vs. P_c for different LyoSIM offset for center vials (A) and edge vials (B). Lines indicate the fit of data sets to describe related mechanism based on classical K_v equation (for all fits $R^2 > 0.985$).

The slope of K_v versus P_c is the same for center vials for different LyoSIM settings but the intercept at $P_c = 0$, obtained by extrapolation, decreases with increasing offset (Figure 2A). This suggests that LyoSIM mainly impacts the gas independent contributions, radiation and contact, for the center vials and helps to estimate the change of K_v that can occur in the different vial populations.

3.2.K_v HFS for different types of formulations

After having found a LyoSIM set-up to match K_v gravimetric in the MicroFD with the one in the lab-scale FD, we evaluated the K_v based on HFS in more detail. K_v values based on HFS are overall lower than the gravimetric values (Figure 3), confirming the previous findings [17].

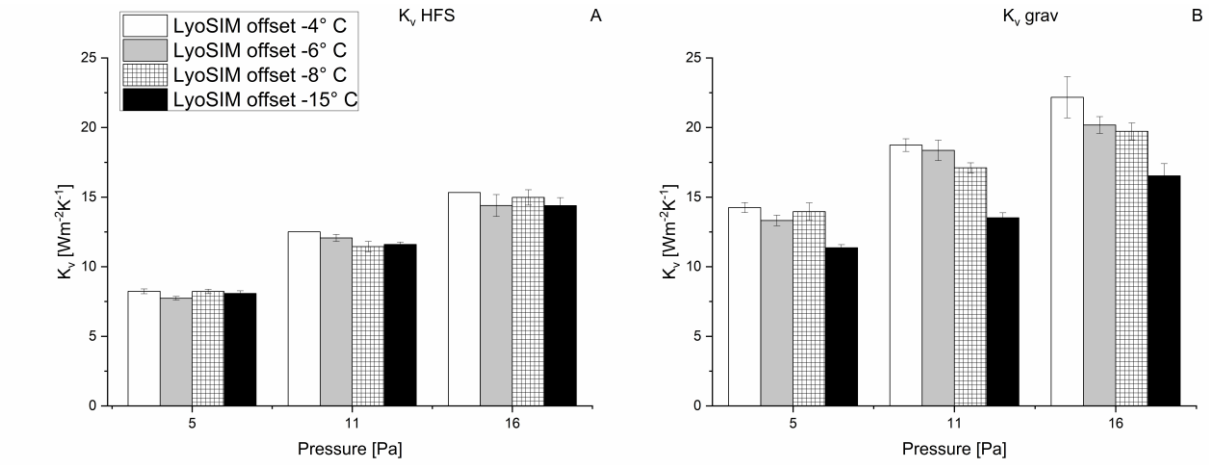

Figure 3: Impact of the LyoSIM offset on K_v HFS (A) and comparison with corresponding K_v grav (B) for 10% w/v sucrose.

Additionally, LyoSIM temperatures have little influence on the HFS-based K_v values. The difference in K_v between the two methodologies becomes less with increasing LyoSIM offset. Decreasing the LyoSIM temperature exclusively lowers the gravimetric K_v.

To further evaluate the deviation between gravimetric and HFS-based K_v, we studied a 5% mannitol solution besides sucrose solutions. For mannitol, the freezing protocol was adapted to assure mannitol crystallization and to reduce the risk of vial breakage [28] but, the primary drying conditions were kept.

The vapor flow rates for sucrose without annealing, with annealing as well as for mannitol with annealing were 204, 259 and 238 $gh^{-1}m^{-2}$ respectively. Given same vials and primary drying conditions, the formulation only marginally impacts the gravimetric K_v [29] but annealing increases the sublimation rate [30]. This is supported by a lower T_p during primary drying of sucrose frozen with annealing compared to frozen without annealing reflecting a lower R_p.

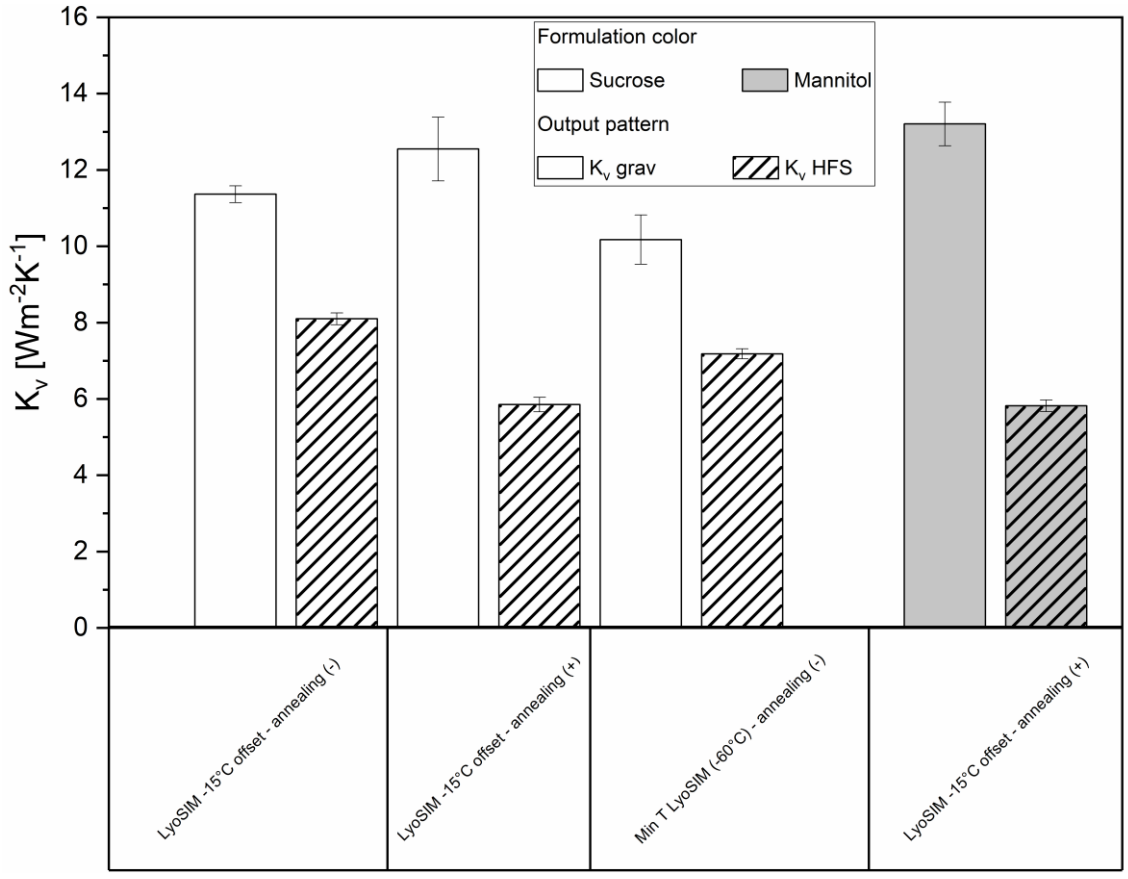

Figure 4: K_v grav (filled columns) and K_v HFS (patterned columns) for sucrose (white columns) and mannitol (gray columns). LyoSIM and freezing protocols (FP) indicated below columns [with (+) /without annealing (-). P_c = 5 Pa

Nevertheless, the K_v values for annealed product (Figure 4), both gravimetric and HFS-based K_v, were not affected by the formulation, but K_v HFS became markedly lower with annealing. Overall, we suggest that in order to obtain

a homogenous batch with respect to the heat transfer, the LyoSIM temperature should be set according to an offset to the T_p of the most shielded vial of -8 °C for Pc ≤ 11 Pa and -7 °C at P_c =16 Pa, and in order to obtain results comparable to a lab-scale FD to -15 °C.

3.3.Investigations on heat transfer mechanisms affecting the HFS output

To explain the difference between gravimetric and HFS-based K_v values, we initially hypothesized that the HFS-based K_v is influenced exclusively by heat mechanisms related to the shelf, contact and gas conduction between vial bottom and shelf. However, with annealing the divergence between the two methods increased. Therefore, we closely investigated the impact of radiation conducting a series of experiments with gold-coated vials. The gold-coated vials showed an emissivity ε of 0.53 compared to 0.95 for clear vials which is in line with literature [20,31,32]. We considered the extreme offsets of -15°C and +15°C between LyoSIM and T_p. and, if not stated differently, only 7 vials was placed in the center of the freeze-drying chamber to reduce shielding by a surrounding row of vials.

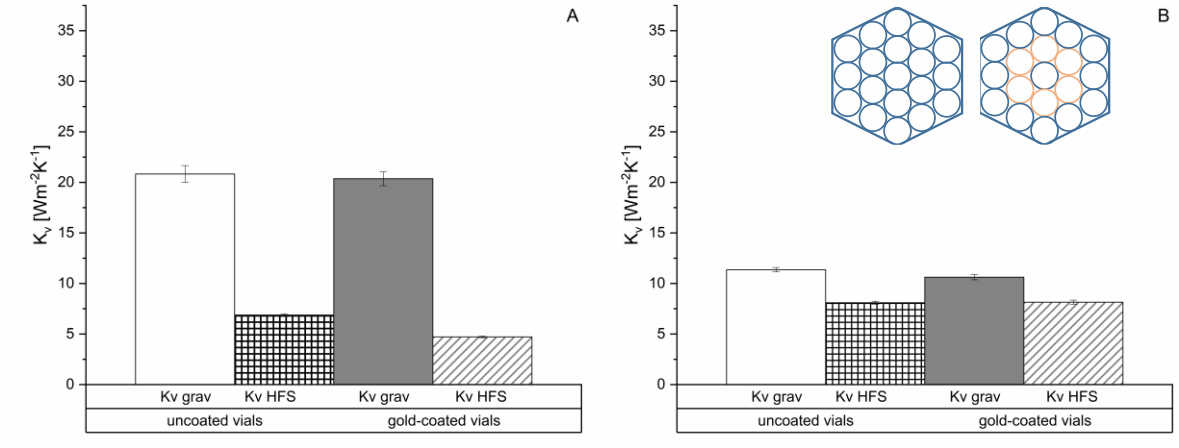

Figure 5: K_v and radiation effect: LyoSIM -15°C offset on different type of vials – partial load (7 vials) (A) and full load (19 vials) (B). Loading scheme (blue – uncoated vial / orange – gold-coated vials). P_c = 5 Pa

As shown in Figure 5A, independently of the type of vials used, the partial load with only 7 vials results in rather high gravimetric K_v values whereas the HFS-based K_v is hardly influenced. Gold-coating does not significantly impact K_v in these setups, indicating that radiation is not a key element (Figure 5B). Consequently, the increase of K_v gravimetric with HFS-based K_v unaffected, points to the cooling effect by the neighboring vials [21]. In the partial load, the absence of the surrounding row of vials results in higher T_p, a smaller difference between T_p and T_{fluid} and thus reduces the amount of heat detected by the sensor despite accelerated sublimation.

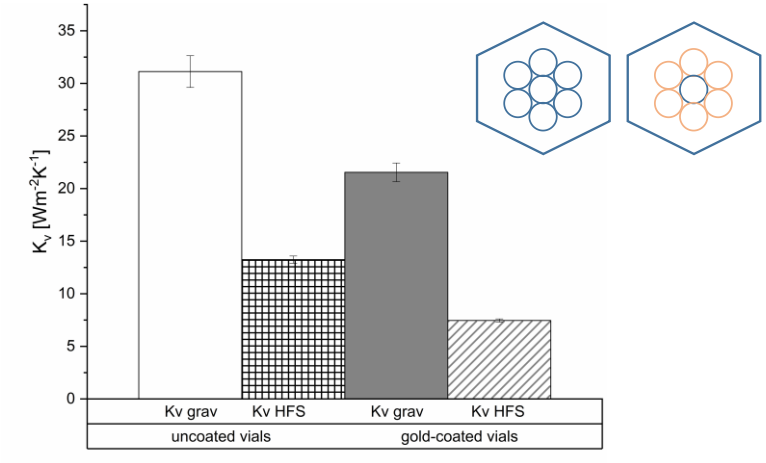

Figure 6: K_v and radiation effect: LyoSIM +15°C offset on different type of vials – partial load (7 vials). Loading scheme (blue – uncoated vial / orange – gold-coated vials). P_c = 5 Pa

With a LyoSIM offset of +15°C gold-coating leads to a remarkable reduction of K_v gravimetric by approx. 30% (Figure 6). With this elimination of radiation by gold coating, the K_v gravimetric became similar for the two offset settings. Nevertheless, the neighboring vial effect is still present, with the K_v values being markedly lower for shielded center vials. The reduced size of the freeze-drying chamber could amplify the atypical heat transfer effect.

In 2003 Rambhatla and Pikal carried out a series of experiments on gold-coated vials, resulting in sublimation rate values of 0.09 g/h and 0.18 g/h for gold-coated and clear vials, respectively [33]. In their work, primary drying investigations were performed in a lab-freeze-dryer at different shelf temperatures (-25/ -15 / 0 °C) and with a chamber pressure of ca. 20 Pa (0.15 mmHg). We obtained 0.14 g/h and 0.18 g/h for gold-coated and clear vials, respectively in the most radiation-driven scenario. A direct comparison of the results is not straightforward, due to differences in T_{fluid}, P_c and freeze-dryer type. In particular the chamber pressure, as main factor for K_v, differs by ca. 15 Pa and with it the resulting sublimation rate values.

Overall, the cooling effect by the neighboring vials by radial heat exchange causes the substantial discrepancy between the gravimetric and HFS-based K_v results for edge vials. Annealing leads to a lower R_p and consequently a sublimation rate which is reflected in the K_v gravimetric but not in the HFS-based K_v. Additionally, the cooling effect by neighboring vials is not reflected in the HFS-based K_v.

4. Conclusions

We investigated the gravimetric and the HFS based K_v in a miniaturized freeze-dryer for two types of formulations, amorphous and crystalline, and two different freezing protocols. Additionally, the role of atypical

radiation in the HFS output was assessed by studying vials with low- and normal emissivity at different LyoSIM settings, loading settings and comparing K_v gravimetric and HFS-based. The HFS-based K_v values are markedly lower than the gravimetric K_v values. This can only partially be attributed to radiation. We found that the radial heat exchange plays a key role in this difference in between HFS-based and gravimetric K_v.

To mimic conditions representative for a lab-scale freeze drying process in the MicroFD, the LyoSIM temperature has to be set to the minimum offset of -15 °C compared to the most shielded vials, to achieve a reduction of atypical heat transfer, and it is important to perform full load experiments with the MicroFD. In case of partial load, atypical heat transfer substantially speeds up drying in the MicroFD which is well reflected in the gravimetric K_v but not in the HFS-based K_v. Consequently, the HFS-based K_v in the MicroFD can be misleading also considering that K_v is process-, vial positioning- and equipment-related [29].

Overall, the HFS and the MicroFD with the LyoSIM can be used in combination to obtain K_v real-time with much less effort that gravimetrically, to study different vial scenarios, and to design lyophilization processes with a limited amount of material and experiments. Nevertheless, our studies also point to the limitations and potentially substantial differences between K_v gravimetric and HFS-based e.g., when comparing annealed with non-annealed products. Future works should address if the combination of K_v and R_p, both HFS-based, have the potential to generate a valid design space for center vials and establish HFS as routine method for freeze-drying scientists.

Declaration of Competing Interest

The authors declare that they have no known competing financial interests or personal relationships that could have appeared to influence the work reported in this paper.

Funding

This research did not receive any specific grant from funding agencies in the public, commercial, or not-for-profit sectors.

Acknowledgments

The authors want to thank Zarah Schaal for her experimental support during the period at Coriolis Pharma, as well as Dr. Matthias Lucke and Dr. Constanze Helbig (Coriolis Pharma) for the valuable discussions during the review of the manuscript.

5. Abbreviations and Nomenclature

A_v	cross sectional area of vial (m^2)
cQA	critical quality attribute
ΔH_s	sublimation heat ($J\ kg^{-1}$)
Δm	sublimed mass (kg)
Δt	considered drying time (s)
ε	emissivity
FD	freeze-dryer
grav	gravimetric
HFS	heat flux sensor
J_w	sublimation flux ($kg\ m^{-2}\ s^{-1}$)
K_v	vial heat transfer coefficient ($W\ m^{-2}\ K^{-1}$)
l_v	average distance between vial bottom to the shelf (m^{-1})
λ_0	thermal conductivity of the gas at ambient pressure
PAT	process analytical technology
P_c	chamber pressure (Pa)
P_i	pressure at the sublimating interface (Pa)
PVDF	polyvinylidene difluoride
Q	heat received by a vial ($W\ m^{-2}$)
QbD	quality by design
Q_{HFS}	heat measured from heat flux sensor ($W\ m^{-2}$)
R^2	correlation coefficient
R_p	product resistance ($m\ s^{-1}$)
t	time (s)
T_{fluid}	temperature of fluid circulating in the shelf (°C)
T_i	temperature at the sublimating interface (°C)
T_p	product temperature (°C)
$T_{shelf\ surface}$	shelf surface temperature as measured by heat flux sensor (°C)
TC	thermocouple

6. References

[1] S.M. Paul, D.S. Mytelka, C.T. Dunwiddie, C.C. Persinger, B.H. Munos, S.R. Lindborg, A.L. Schacht, How to improve RD productivity: The pharmaceutical industry's grand challenge, Nat Rev Drug Discov. 9 (2010) 203–214. https://doi.org/10.1038/nrd3078.

[2] J.A. DiMasi, H.G. Grabowski, R.W. Hansen, Innovation in the pharmaceutical industry: New estimates of R&D costs, J Health Econ. 47 (2016) 20–33. https://doi.org/10.1016/j.jhealeco.2016.01.012.

[3] V. I. Razinkov, M. J. Treuheit, G. W. Becker, Methods of High Throughput Biophysical Characterization in Biopharmaceutical Development, Curr Drug Discov Technol. 10 (2013) 59–70. https://doi.org/10.2174/1570163811310010008.

[4] A.S. Rathore, H. Winkle, Quality by design for biopharmaceuticals, Nat Biotechnol. 27 (2009) 26–34. https://doi.org/10.1038/nbt0109-26.

[5] J. Gray, Lyophilization in Review 2019, (2020).

[6] 2017-2027 Lyophilization Services for Biopharmaceuticals, Lyophilization Services for Biopharmaceuticals, 2017-2027, (2017) 239. https://www.reportbuyer.com/product/4886788/lyophilization-services-for-biopharmaceuticals.html (accessed March 22, 2022).

[7] D. Fissore, R. Pisano, Computer-Aided Framework for the Design of Freeze-Drying Cycles: Optimization of the Operating Conditions of the Primary Drying Stage, Mdpi.Com. 3 (2015) 406–421. https://doi.org/10.3390/pr3020406.

[8] M. Rosa, J.M. Tiago, S.K. Singh, V. Geraldes, M.A. Rodrigues, Improving Heat Transfer at the Bottom of Vials for Consistent Freeze Drying with Unidirectional Structured Ice, AAPS PharmSciTech. 17 (2016) 1049–1059. https://doi.org/10.1208/s12249-015-0437-3.

[9] D. Fissore, R. Pisano, A.B.-J. of pharmaceutical sciences, undefined 2011, Advanced approach to build the design space for the primary drying of a pharmaceutical freeze-drying process, Elsevier. (n.d.).

[10] M.J. Pikal, M.L. Roy, S. Shah, Mass and heat transfer in vial freeze-drying of pharmaceuticals: Role of the vial, J Pharm Sci. 73 (1984) 1224–1237. https://doi.org/10.1002/jps.2600730910.

[11] M.J. Pikal, M.L. Roy, S. Shah, Mass and heat transfer in vial freeze-drying of pharmaceuticals: Role of the vial, J Pharm Sci. 73 (1984) 1224–1237. https://doi.org/10.1002/jps.2600730910.

[12] I. Vollrath, V. Pauli, W. Friess, A. Freitag, … A.H.-J. of, undefined 2017, Evaluation of heat flux measurement as a new process analytical technology monitoring tool in freeze drying, Elsevier. (n.d.).

[13] M. Carfagna, M. Rosa, M. Lucke, A. Hawe, W. Frieß, Heat flux sensor to create a design space for freeze-drying development, European Journal of Pharmaceutics and Biopharmaceutics. 153 (2020) 84–94. https://doi.org/10.1016/j.ejpb.2020.05.028.

[14] C. Moino, E. Bourlés, R. Pisano, B. Scutellà, In-Line Monitoring of the Freeze-Drying Process by Means of Heat Flux Sensors, Ind Eng Chem Res. 60 (2021) 9637–9645. https://doi.org/10.1021/acs.iecr.1c00536.

[15] K. Yoon, V. Narsimhan, Understanding Heat Transfer During the Secondary Drying Stage of Freeze Drying: Current Practice and Knowledge Gaps, J Pharm Sci. 111 (2022) 368–381. https://doi.org/10.1016/j.xphs.2021.09.032.

[16] I. Vollrath, V. Pauli, W. Friess, A. Freitag, A. Hawe, G. Winter, Evaluation of Heat Flux Measurement as a New Process Analytical Technology Monitoring Tool in Freeze Drying, J Pharm Sci. 106 (2017) 1249–1257. https://doi.org/10.1016/j.xphs.2016.12.030.

[17] M. Carfagna, M. Rosa, M. Lucke, A. Hawe, W. Frieß, Heat flux sensor to create a design space for freeze-drying development, European Journal of Pharmaceutics and Biopharmaceutics. 153 (2020) 84–94. https://doi.org/10.1016/j.ejpb.2020.05.028.

[18] D. Fissore, R. Pisano, A.A. Barresi, Model-based framework for the analysis of failure consequences in a freeze-drying process, Ind Eng Chem Res. 51 (2012) 12386–12397. https://doi.org/10.1021/ie300505n.

[19] M. Carfagna, M. Rosa, M. Lucke, … A.H.-E.J. of, undefined 2020, Heat flux sensor to create a design space for freeze-drying development, Elsevier. (n.d.).

[20] S. Rambhatla, M.J. Pikal, Heat and mass transfer scale-up issues during freeze-drying, I: Atypical radiation and the edge vial effect, AAPS PharmSciTech. 4 (2003) 22–31. https://doi.org/10.1208/pt040214.

[21] S. Ehlers, R. Schroeder, W. Friess, Trouble with the neighbor during freeze-drying: rivalry about energy, J Pharm Sci. 110 (2021) 1219–1226. https://doi.org/10.1016/j.xphs.2020.10.024.

[22] D. Fissore, A.A. Barresi, Scale-up and process transfer of freeze-drying recipes, Drying Technology. (2011). https://doi.org/10.1080/07373937.2011.597059.

[23] S.A. Velardi, A.A. Barresi, Development of simplified models for the freeze-drying process and investigation of the optimal operating conditions, Chemical Engineering Research and Design. 86 (2008) 9–22. https://doi.org/10.1016/j.cherd.2007.10.007.

[24] B. Scutellà, S. Passot, E. Bourlés, F. Fonseca, I.C. Tréléa, How Vial Geometry Variability Influences Heat Transfer and Product Temperature During Freeze-Drying, J Pharm Sci. 106 (2017) 770–778. https://doi.org/10.1016/j.xphs.2016.11.007.

[25] S.M. Patel, M.J. Pikal, Lyophilization process design space, J Pharm Sci. (2013). https://doi.org/10.1002/jps.23703.

[26] S. Bosca, A.A. Barresi, D. Fissore, Use of a soft sensor for the fast estimation of dried cake resistance during a freeze-drying cycle, Int J Pharm. 451 (2013) 23–33. https://doi.org/10.1016/j.ijpharm.2013.04.046.

[27] R. Pisano, D. Fissore, A.A. Barresi, Heat transfer in freeze-drying apparatus, in: Developments in Heat Transfer, InTech Rijeka, Croatia, 2011: pp. 91–114.

[28] N.A. Williams, Y. Lee, G.P. Poll, T.A. Jennings, The Effects of Cooling Rate on Solid Phase Transitions and Associated Vial Breakage Occurring in Frozen Mannitol Solutions, PDA J Pharm Sci Technol. 40 (1986).

[29] P. Sane, Identification and Quantification of Heterogeneity in Freezing and Primary Drying Steps of Lyophilization, Doctoral Dissertations. (2016). http://opencommons.uconn.edu/dissertations/1099%0Ahttp://opencommons.uconn.edu/dissertations/1099/.

[30] J. Andrieu, S. Vessot, A review on experimental determination and optimization of physical quality factors during pharmaceuticals freeze-drying cycles, Drying Technology. 36 (2018) 129–145. https://doi.org/10.1080/07373937.2017.1340895.

[31] T.L. Bergman, F.P. Incropera, A.S. Lavine, D.P. Dewitt, Introduction to heat transfer, John Wiley \& Sons, 2011.

[32] Engineering ToolBox, No Title, (n.d.). www.engineeringtoolbox.com/emissivity-coefficients-d_447.html (accessed July 15, 2020).

[33] S. Rambhatla, M.J. Pikal, Heat and mass transfer scale-up issues during freeze-drying, I: atypical radiation and the edge vial effect., AAPS PharmSciTech. 4 (2003) E14. https://doi.org/10.1208/pt040214.

Chapter V: Lyophilization cycle design for highly concentrated protein formulations supported by micro freeze-dryer and heat flux sensor

Marco Carfagna[1, 2], Monica Rosa[1], Andrea Hawe[1*], Wolfgang Frieß[2]

[1] Coriolis Pharma Research GmbH, Fraunhoferstrasse 18 b, 82152 Martinsried, Germany;

[2] Department of Pharmacy, Pharmaceutical Technology and Biopharmaceutics, Butenandtstrasse 5, Ludwig-Maximilians-Universitaet München, D-81377 Munich, Germany;

* Corresponding author: Andrea Hawe, Coriolis Pharma Research GmbH, Fraunhoferstrasse 18 b, 82152 Martinsried, Germany; e-mail: Andrea.Hawe@coriolis-pharma.com;

The following chapter has been published in the International Journal of Pharmaceutics as:

Lyophilization cycle design for highly concentrated protein formulations supported by micro freeze-dryer and heat flux sensor

Marco Carfagna, Monica Rosa, Andrea Hawe, Wolfgang Frieß,

International Journal of Pharmaceutics,

Volume 643, 2023,123285, ISSN 0378-5173, https://doi.org/10.1016/j.ijpharm.2023.123285.

Abstract

High-concentration protein formulations (HCPFs) represent a common strategy and freeze-drying can mitigate the stability challenges of HCPFs. In general, an in-depth characterization of the lyophilization process is essential to not impair the product quality by inappropriate process parameters. The aim of this study was to create a primary drying design space for lyophilized HCPFs by utilizing the heat flux sensor (HFS) integrated in a MicroFD with a minimum number of cycles and product vials. All the necessary data to obtain the design space were determined starting from only two lyophilization cycles, each holding 19 vials. The vial heat transfer coefficient (Kv) was determined by the HFS and compared to gravimetric values. The results indicate a consistent offset between the HFS and the gravimetry based values for annealed samples with higher protein content. This work highlights a possibility of integrating new technologies, the HFS and the MicroFD to generate a design space for lyophilization of HCPFs, which enables to implement a QbD approach at minimal material and time investment.

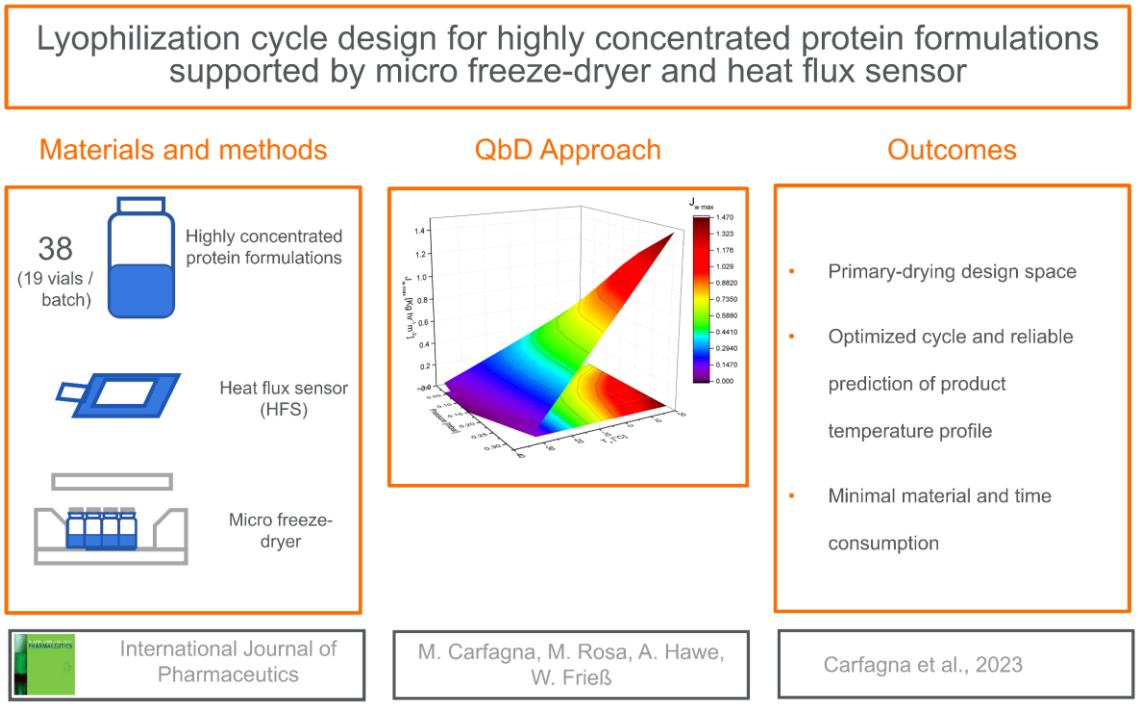

1. Introduction

The subcutaneous administration of biopharmaceuticals represents a valuable alternative compared to the intravenous route, especially for chronic diseases [1]. In fact, it presents the advantages of home medication in addition to a higher patient compliance. The injectable volume is usually in the range of 1-2 ml to avoid pain for the patients and difficulties in administration [2,3]. In the case of antibodies this may lead to formulations with high protein concentration between 100 and 200 mg/ml [1,4]. At such high concentrations, challenges of increased viscosity, limited solubility and reduced protein stability arise [4]. In the case of limited protein stability, converting the liquid formulation into a lyophilizate can be an appropriate route of choice [5].

Lyophilization of high-concentration protein formulations (HCPFs) brings multiple challenges. The product resistance to the sublimation flow is usually higher and this can result in longer drying times [6,7]. On the other hand, the collapse temperature increases with higher protein concentrations [8], which allow a drying under harsher conditions. Overall, it is important to find a good balance in reducing the primary drying time at higher temperatures without affecting product quality [9,10]. Especially considering that the overall cost of a HCPF batch can be extremely high, i.e., 30,000 lyophilized vials filled with 100 mg/ ml recombinant protein value on average ca. $ 1.5 million [11]. The key fluxes governing the lyophilization process are the heat (Q), received by the vial, and the mass of sublimed water (J_w) which are both indirectly regulated by the temperature of the shelf, the circulating shelf fluid resp. (T_{fluid}) and the chamber pressure (P_c) [12]. To mathematically describe the relation between these fluxes (Q and J_w) and the related input parameters (T_{fluid} and P_c), the vial heat transfer coefficient (K_v) and the product resistance (R_p) were introduced [13,14]. Both are essential elements of the Quality by Design (QbD) approach in lyophilization and for a scientific process transfer [15]. K_v represents the impact of the vial and equipment on Q and depends mainly on P_c and position of the vial within the dryer [13,16]. R_p depicts the impact of the formulation on J_w and is affected by the freezing conditions and the drying progression [13,17]. The most reliable and classical way to obtain K_v is the gravimetric method based on determination of water loss after certain sublimation times during primary drying. This approach enables differentiation between center or edge vials on different shelves. Based on K_v, R_p can be obtained and the evolution of the dried layer thickness can be followed [18]. The gravimetric method has some limitations. It requires the abortion of the process during primary drying, it is rather time-consuming, and results are not available in real-time for process monitoring and control [19]. Another option for K_v determination is pressure rise test (PRT) methods, where the chamber pressure increases due to isolation between the lyophilization chamber and the condenser for a variable time (3-30s), which feeds

different algorithms based on the specific methods. PRT requires a fast-closing valve to isolate the lyophilization chamber, which is not available for all freeze-dryers. Furthermore, PRT may offer unreliable results for high solid content amorphous products due to re-adsorption effects (total solid content >150 mg/ml) [20]. An additional method for K_v determination is tunable diode laser absorption spectroscopy (TDLAS) that measures the flow and composition of the gas in the duct connecting drying chamber and the condenser. TDLAS is costly and can only be retro-fitted in freeze-dryers with a duct between chamber and condenser. PRT and TDLAS provide an average K_v, for the whole batch and cannot differentiate between edge and center vials [21].

Recently, heat flux sensors (HFSs) have been evaluated as a PAT tool to monitor the overall process in-line [22,23]. Published studies highlighted the capabilities of HFS in detecting the end of ice crystal growth during the freezing and as the end point in primary drying [22,23].

It is of major interest to gain process knowledge transferable to manufacturing equipment to mitigate the risk for commercial batches. In this regard, we have previously assessed the feasibility by obtaining key process parameters and consequently in creating a design space for a placebo formulation by using an HFS in a standard lab-scale freeze-dryer [24]. More recently, a miniaturized freeze-dryer equipped with HFS and has been introduced onto the market. As suggested by the commercial name, MicroFD, the equipment has a smaller size. The shelf can accommodate a limited number of vials (e.g., a maximum of 19 6R vials) with the aim of saving material and efforts during lyophilization cycle development. Besides other standard components, this equipment includes the HFS and a component named LyoSIM which can emulate different heat transfer scenarios (Figure 1).

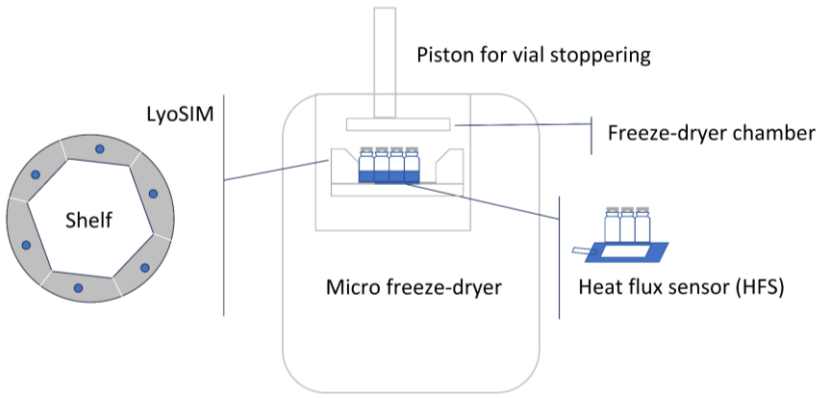

Figure 1 Schematic representation of the MicroFD and key components. Top-view of the LyoSIM is shown.

As HCPFs present many technical challenges from manufacturability to stability, obtaining in-depth knowledge about the lyophilization process with a minimum amount of material and time is of high interest. In this context,

the combined use of the HFS and MicroFD to generate and select a valid design space for HCPF have been explored.

Therefore, the aim of our study was to verify if HFS / MicroFD can be applied for HCPF and to confirm their potential for design space creation. To this end, we determined K_v and R_p of HCPF in a MicroFD. Subsequently, we generated a design space for the primary drying process and confirmed its validity experimentally by estimation of primary drying time, product temperature profile whilst additionally considering cake appearance and water content.

2. Materials and methods

2.1 Formulations and primary packaging

Experiments were carried out with 50 and 150 mg/ml solution of Bovine Serum Albumin (BSA) (Sigma-Aldrich, Munich, Germany) with 10 % w/v sucrose (Ph. Eur. grade; Merck, Darmstadt, Germany) in 10 mM sodium phosphate buffer pH 7.4. The BSA concentration of both formulations was checked after filtration through 0.22 µm PVDF membrane filters (Merck, Darmstadt, Germany) by using a Nanodrop 2000 UV photometer (Thermo Fisher Scientific, Wilmington, USA). 2.6 ml solution were filled in 6R TopLyo glass vials (Schott, Müllheim-Hügelheim, Germany) unless differently specified. The vials were partially closed with 20-mm bromobutyl single vent lyophilization stoppers (Westar RS, FluoroTec B2-40 coating; West, Eschweiler, Germany).

2.2 Freeze-drying equipment and heat flux sensor (HFS)

19 vials were processed in a 0.07 m^2 shelf area MicroFD (Millrock Technology, Kingston, NY) equipped with an HFS located at the center of the shelf. Vials were surrounded by the LyoSIM ring, the temperature of which can be regulated with an offset to T_p (range ± 15°C) or between -60 and + 60°C independently of T_p [25,26]. This component is a temperature-regulated ring composed of 6 metallic blocks on the edge of the shelf surface. The size of the LyoSIM blocks is adjusted to the vial diameter which results in a hexagonal array of vials when the full capacity is reached. Thereby, the wall of vials at the edge come into contact with the blocks (Figure 1). In this study, the LyoSIM temperature had an offset to the center vial T_p of 0 °C during freezing and -15 °C during drying. These parameters were selected based on previous work [26]. Pressure was controlled by a capacitance manometer and monitored in addition with a Pirani gauge. Product temperature was measured by T-type copper-constantan thermocouples in combination with thermocouple holders (Millrock Technology, Kingston, NY).

2.3 Determination of K_v and R_p and their mathematical description

The following freezing protocols were evaluated:

- 1-step freezing (F) by ramping down to -50 °C at 1°C/min
- 2-step freezing (2F) by equilibrating the samples at -3 °C for 60 minutes followed by ramping down to -50 °C at 1°C/min
- 2-step freezing and annealing (2FA) by equilibrating the samples at -3 °C for 60 minutes followed by ramping down to -50 °C at 1°C/min followed by a ramp to -10°C at 1°C/min, a 260 minutes hold at -10 °C followed another ramp to -50 °C at 1°C/min

For each protocol, the final freezing temperature was held for at least 2 hours. Primary drying was conducted at 5 Pa and -20 °C as T_{fluid}. Water loss (Δm) was measured by weighing all 19 filled vials placed in the MicroFD before the start of the process and after approximately 10 hours of primary drying on an analytical balance (Genius ME – Sartorius, Gottingen, Germany). In this time frame, T_p is consistently reliable because the thermocouple keeps contact with the material as the drying is prematurely stopped. K_v grav and K_v HFS were calculated according to the following equations:

$$K_{v\,grav} = \frac{\Delta m\, \Delta H_s}{A_v \int_0^{\Delta t} (T_{fluid} - T_p)\, dt} \quad (1)$$

where ΔH_s is the sublimation heat of ice, and A_v is the cross-sectional area of the vial.

The HFS-based K_v (K_v HFS) is related to the sensor readout (Q_{HFS}) as by the following equation:

$$K_{v\,HFS} = \frac{Q_{HFS}}{(T_{shelf\ surface} - T_p)} \quad (2)$$

where $T_{shelf\ surface}$ is the temperature of the shelf surface as measured from the built-in thermocouple of the HFS, and T_p is the product temperature measured at the vial bottom from the thermocouple. T_{fluid} is the shelf fluid temperature set in the MicroFD. To generate K_v at three different chamber pressures a 3-pressure experiment (3PE) was performed for the 150 mg/ml BSA formulation. A 2FA protocol with annealing at -10°C was followed to a temperature decrease of T_{fluid} until -50°C. For primary drying the shelf temperature was set at -20°C and chamber pressure was initially set at 5 Pa, then increased at 11 Pa and finally at 16 Pa. The LyoSIM was set at -15°C offset compared to T_p, as in the single pressure experiments. For the comparison between $K_{v\,grav}$ and $K_{v\,HFS}$, the average of gravimetric values was considered. More specifically, the data from vials placed above the HFS, were included in the calculation, with the exception of the one containing the thermocouple.

The product resistance (R_p) was obtained by the following equation:

$$R_p = \frac{(P_i - P_c)}{J_w} \quad (3)$$

where J_w is the sublimation flux as obtained from equations 4-5, and P_i is the pressure at the sublimating interface determined from the Goff-Gratch equation and, T_i, the temperature at the sublimating interface that can be approximated to T_p.

$$Q = K_v(T_{fluid} - T_p) \quad (4)$$

$$J_w = \frac{Q}{\Delta H_s} \quad (5)$$

K_v and R_p were mathematically described by non-linear fitting by the following equations:

$$K_v = A_{Kv} + \frac{B_{Kv}\, P_C}{1 + l_v \frac{B_{Kv}}{\lambda_0}\, P_C} \quad (6)$$

$$R_p = R_{p0} + \frac{A_{Rp}\, L_{dried}}{1 + B_{Rp}\, L_{dried}} \quad (7)$$

Details on equations coefficients and physical constant can be found in previous publications [26,27]. A_{Kv}, B_{Kv} are obtained from the best fit of K_v vs. P_c variation while R_{p0}, A_{Rp} and B_{Rp} from the best fit of R_p vs. dried layer (L_{dried}) evolution.

2.4 Analysis of collapse temperature (T_c)

The collapse temperature (T_c) of the formulations was analyzed with a Linkam microscope equipped with an FDCS 196 freeze-drying stage (Linkam Scientific Instruments, Surrey, UK). 2 µl of formulation were pipetted on a quartz crucible and a cover slip was placed above the droplet with a 25-µm spacer. The sample was frozen at 1 K/min to -50°C. Afterwards, two alternative protocols were executed:

a) vacuum was applied to start the drying
b) sample was annealed to -10°C, cooled again at -50°C with holding times in both cases of 10 min and then vacuum applied

Once the vacuum level reached 10 Pa, the sample was heated at 1 K/min to -40°C and the sample was kept for 10 min at that temperature to obtain a suitable dried layer. The sample was heated to 5°C using a heating rate

of 1°C/min and images were taken every second. Collapse temperature of the frozen solution was determined from the appearance of translucent dots or fissures behind the ice sublimation interface.

2.5 Design space creation and verification of the optimized cycle

A design space for each formulation (50 and 150 mg/ml) was created based on the mathematical model proposed by Velardi and Barresi [28] for the freezing protocols 2F and 2FA. The algorithm was applied to estimate the evolution of dried material thickness, temperature at the sublimating interface (T_i) and primary drying time. In particular, the evolution of the frozen layer (L_{frozen}), reciprocal of the dried layer, is calculated based on the sublimation flux (equation 3):

$$\frac{dL_{frozen}}{dt} = \frac{1}{\rho_{frozen} - \rho_{dried}} \frac{(P_i - P_c)}{R_p} \tag{8}$$

where ρ_{frozen} and ρ_{dried} indicate the density of the frozen and the apparent density of the dried product respectively. The relation between T_p, T_{fluid} and T_i is expressed as

$$T_p = T_{fluid} - \frac{1}{K_v} \frac{(T_{fluid} - T_i)}{\left(\frac{1}{K_v} + \frac{L_{frozen}}{k_{frozen}}\right)} \tag{9}$$

where k_{frozen} is the thermal conductivity of the frozen layer. Based on this equation and that all heat received by the frozen product is used for sublimation (equation 5) and pseudo-stationary conditions that allow process evolution to be described as in equation 8, at the sublimating interface, the energy balance can be written as:

$$\frac{(P_i - P_c)}{R_p} \Delta H_s = T_{fluid} - \frac{(T_{fluid} - T_i)}{\left(\frac{1}{K_v} + \frac{L_{frozen}}{k_{frozen}}\right)} \tag{10}$$

The optimized verification cycle parameters are summarized in Table 1.

Table 1. Parameters for the verification freeze-drying cycle.

No.	Step	Time [hh:mm:ss]	Cumulative Process Time [hh:mm:ss]	T_{fluid} [°C]	P_c [Pa]	Cooling / heating rate [°C/min]
1	Loading	00:10:00	-	20	100,000	
2	Freezing	00:46:00	00:56:00	-3	100,000	0.50
3		01:00:00	01:56:00	-3	100,000	
4		00:47:00	02:43:00	-50	100,000	1.00
5		02:00:00	04:43:00	-50	100,000	
6		00:40:00	05:23:00	-10	100,000	0.50
7		06:00:00	11:23:00	-10	100,000	
8		00:40:00	12:03:00	-50	100,000	0.50
9		02:00:00	14:03:00	-50	100,000	
10	Primary drying	00:15:00	14:18:00	-50	11	
11		02:40:00	16:58:00	30	11	0.50
12		06:24:00	23:22:00	30	11	
13	Secondary drying	06:00:00	29:22:00	30	11	

The transition from primary to secondary drying was defined in advance and not on the comparative pressure Pirani / Capacitance. Time of desorption in secondary drying was set to 6 hours.

2.6 Optical evaluation of the freeze-dried product

The freeze-dried cakes were visually evaluated for compactness, contact to walls of vial, shape, color and overall appearance. Furthermore, photos were taken. Scanning electron microscope (SEM) images were generated with a bench top SEM (Phenom-World B.V., Eindhoven, The Netherlands) after transferring samples in a glove box under controlled humidity conditions (<10% relative humidity) and preparing a slice from the cross section of the center part of the lyophilizates.

2.7 Residual moisture analysis

The residual moisture content of the lyophilizates was analyzed by Karl Fischer titration with an Aqua 40.00 (Analytik Jena, Jena, Germany) using a head space module. The samples were prepared in a glovebox at ≤ 10% relative humidity. Approximately 50 - 80 mg sample was weighed into an empty 2R vial and stoppered. Blank

values were obtained from empty vials. The vials were heated to 120 °C in the oven connected to the reaction vessel via a tubing system. The titration occurred until water evaporation was no longer detectable.

2.8 Data analysis

Throughout the manuscript, if not stated differently, values are given as mean ± standard deviation. Gravimetric K_v was calculated on n = 6 and Karl Fischer results are based on n = 3.

3. Results and discussion

3.1.HFS-based parameters for HCPF

The heat transfer coefficient K_v is a key factor to consider when designing freeze-drying cycles. It is used to predict the product temperature and therefore the primary drying time. We investigated the impact of the freezing protocol on the determination of HFS-based and gravimetric K_v (Figure 2).

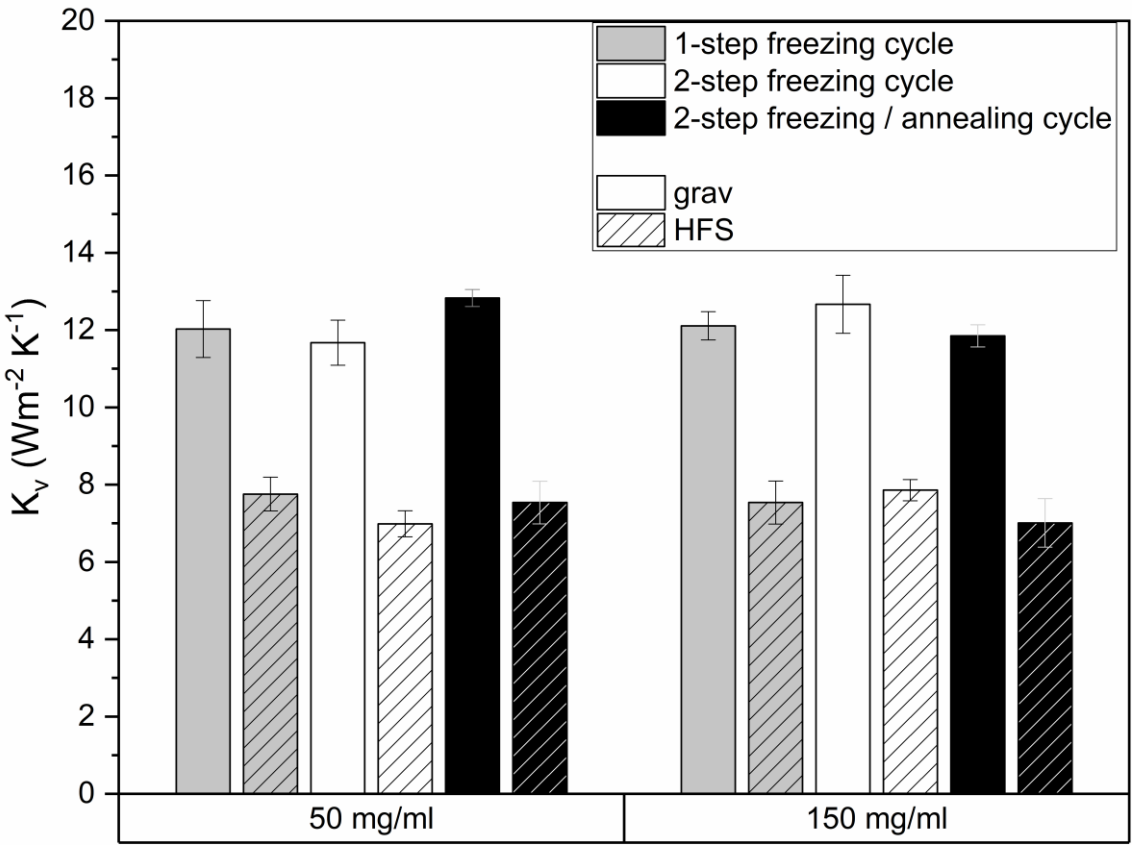

Figure 2: Comparison of gravimetric and HFS based Kv for 50 and 150 mg/ml BSA formulation for three different freezing protocols.

It was deemed appropriate to incorporate different freezing protocols for two main reasons. Firstly, we wanted to assess the constant corrective factor between gravimetric and HFS-based. Secondly, we sought to also evaluate whether it was possible to screen the freezing protocol ad-hoc for a product, with the aim of determining drying time / process time, T_p and design space before the freeze-dying cycle is potentially transferred to another equipment. Additionally, the knowledge of the necessary process parameters and applicable ranges in the freeze-dryer where the product will be transferred will minimize the risks of the transfer / scale-up. More specifically, the 2F protocol with the -3°C hold phase was included as a soak step so that all product vials were equilibrated before initiating the freezing to reduce vial-to-vial variability. The annealing phase in the 2FA protocol and the single-

step freezing, the 1F protocol, were studied to understand the impact on product resistance when compared to the 2F protocol.

In accordance with the literature, the obtained K_v values were independent of the freezing protocol and the gravimetric K_v was consistently higher than the HFS-based K_v [26,29]. The delta between HFS-based and gravimetric K_v was 4.5 $Wm^{-2}K^{-1}$ ± 0.3, except for the annealed 50 mg/ml BSA formulation. In this specific cycle, the cooling system showed a slower cooling rate post annealing with 0.4 vs. 1 °C/min (Figure S1) which, in combination with the delayed vacuum application, caused a higher T_p for the center vials and consequently a warmer LyoSIM. Therefore, the center vials were 5°C warmer than edge vials in contact with the LyoSIM, and the resulting effect was a higher delta of 5.7 $Wm^{-2}K^{-1}$ for this specific cycle. The other experiments showed edge and center vials have a comparable temperature at a protein concentration of 150 mg/ml (Figure S1) confirming the optimal selection of LyoSIM setting. This aspect is highly relevant as the MicroFD presents the possibility to save time and material in the process design phase due to the reduced size and the availability of the HFS. These advantages can be exploited if the equipment can simulate the lab-scale freeze-dryer scenario and counteract atypical heat transfer, which is exacerbated in such a small freeze-dryer chamber. According to the manufacturer's claim, the LyoSIM simulates surrounding sublimating vials and acts as heat sink. Hence, edge vials should dry slower and be representative of center vials in a classic lab-scale equipment. A previous study examined the LyoSIM settings and the effect on the heat transfer coefficient [26]. Based on a step-wise decrease of the offset compared to T_p, an optimal set-up of -15°C was found. The current results confirmed that also for HCPFs the selected LyoSIM temperature offset is applicable.

To exclude any filling volume effect on K_v, additional experiments with a 1 ml instead of standard 2.6 ml filling volume were carried out for the 50 mg/ml BSA formulation. The T_p of the vials filled with less volume confirmed the finding that edge and center vials temperatures overlap (Figure S2).

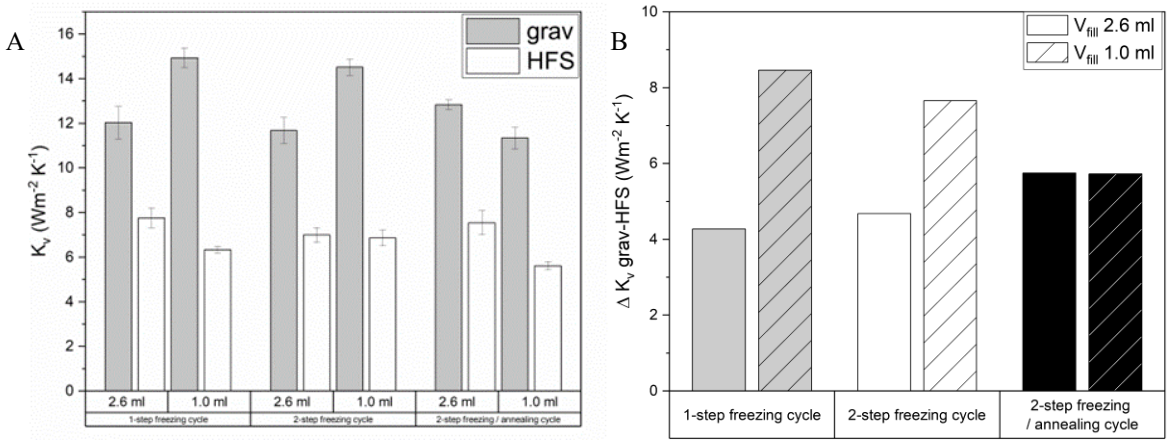

Figure *3*: Comparison of Kv grav and Kv HFS results by considering three freezing protocols and two filling volumes (A) Focus on the difference between gravimetric and HFS-based values (B) – 50 mg/ml BSA formulation

The delta between $K_{v\,grav}$ and $K_{v\,HFS}$ was higher with 1-ml fill volume in case of non-annealed samples (Figure 3), whereas no difference could be observed for annealed products. This indicates that a good batch homogeneity, which is improved by annealing [7,30], is essential for K_v based modeling approaches, specifically when using $K_{v\,HFS}$. At higher concentration of 150 mg/ml the delta between the K_v techniques is less indicating a higher inter-vial homogeneity.

To verify the applicability of $K_{v\,HFS}$, the pressure dependence was investigated at three different P_c values. We performed a run covering three different P_c settings (3-PE) at 5, 11 and 16 Pa comparable to our previous work [26] and calculated the corresponding K_v HFS at each pressure [24]. The obtained $K_{v\,HFS}$ values can be plotted against the P_c rendering the parameters A_{Kv} and B_{Kv} of a non-linear fit. While the previous gravimetric results were 8.7 Wm^{-2}K^{-1} for A_{Kv} and 0.5 Wm^{-2}K^{-1} Pa^{-1} for B_{Kv}, the current results HFS-based were 4.0 Wm^{-2}K^{-1} for A_{Kv} and 0.5 Wm^{-2}K^{-1} Pa^{-1} for B_{Kv}. The nonlinear fit is described by the parameter A_{Kv} that reflects well the highlighted offset of 4.5 Wm^{-2}K^{-1} ± 0.3 and the B_{Kv} that expresses the same P_c dependency of gravimetric data. Based on the collected data, we consider this offset applicable in case of annealed HPCFs. The factors that mainly influence this offset are the filling volume (V_{fill}), the freezing protocol and, partially, the overall solid content. The first variable, V_{fill}, seems to have a bigger impact when small volumes are used where the K_v HFS is not able to detect the total heat received by the vial, specifically the portion of radial heat [26]. At the same filling volume, annealing increases the difference between gravimetric and HFS based K_v. This can be explained considering that a lower R_p, and therefore a higher sublimation rate, is reflected in the K_v gravimetric, but not in the HFS-based K_v. This aspect is consistent with the same observation made on an amorphous excipient, which we previously published [26].

However, this effect becomes less pronounced as the solid content increases. In case of 150 mg/ml despite the annealing effect, the amount of heat detected by the sensor, and consequently reflected by K_v HFS, is aligned to other freezing protocols and equal to 4.5 $Wm^{-2}K^{-1}$ ± 0.3. It is also interesting to note, that when V_{fill} is lower, annealing leads to higher batch homogeneity compared to other freezing protocols. This effect is beneficial an offset between the gravimetric and the HFS-based technique as in the case of higher solid content / higher V_{fill}.

After the focus on K_v, we evaluated R_p. As solid content affects product resistance, the HCPFs have a higher R_p value and hence a longer drying time. A common strategy to accelerate drying is to induce structural changes to the frozen matrix through the freezing protocol, mainly by annealing. The impact on specific surface area of the product is reflected in the drying time. The MicroFD allows a screening of freezing protocols and in this study, we exploited this potential. Overall, the heat transfer determinations impact considerably R_p calculations: HFS-based R_p is higher than the gravimetric R_p. The product resistance results are comparable in both formulations with higher values for 1F protocol for the lowest concentration. Our hypothesis is that this phenomenon is caused by increased inhomogeneity in the freezing phase. As expected, the obtained data confirm that annealing reduces the product resistance.

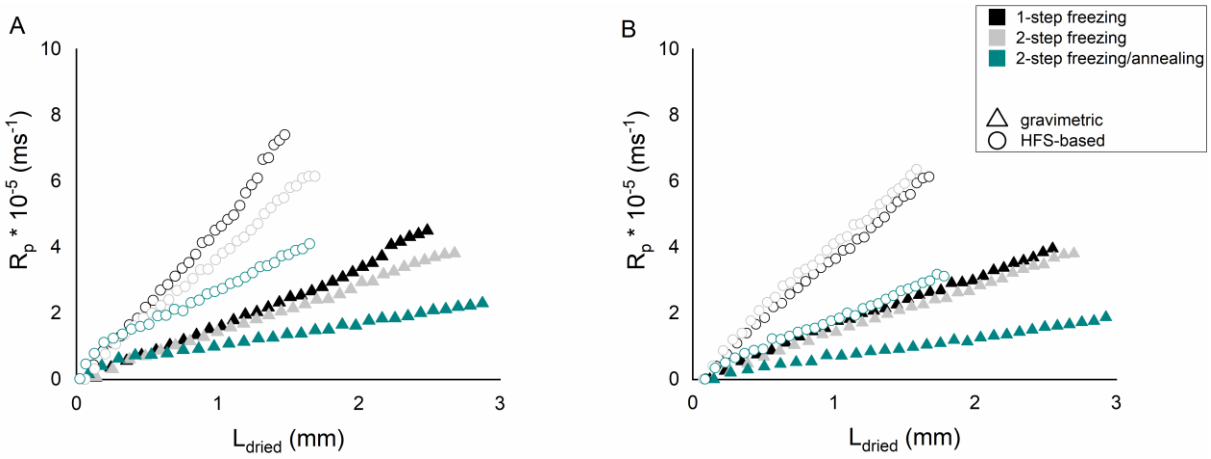

Figure 4: R_p data for 50 mg/ml (A) and 150 mg/ml formulation (B) determined by using gravimetric and HFS-based Kv data determined for the different freezing protocols.

More specifically, for both 50 and 150 mg/ml BSA, independently of the applied methodology, the annealing protocol results in a lower product resistance enabling faster drying compared to the one or two-step freezing approach, which appear equivalent in term of R_p (Figure 4). Following the explanation highlighted in the K_v discussion, once we corrected the HFS-based K_v for the offset, we calculated the real R_p based on the "offset-corrected" K_v that is equivalent to the gravimetric K_v.

3.2.Design space assessment – impact of freezing protocols and protein content

We used the combination of MicroFD and HFS for the first time to create a design space applied to HCPFs. This was achieved with only two lyophilization cycles, each of 19 vials that represent the full capacity of the MicroFD chamber for the studied primary packaging. The aim was to obtain a reliable procedure based on minimal experimental activities and material consumption. Therefore, the following steps were conceived:

a) K_v HFS-based
b) R_p estimation with K_v adjustment based on the determined offset
c) Determination of equipment constraints - in case of the MicroFD no equipment constrains were applied, due to the very low number of vials involved; determination of formulations constraints - in our case the T_c increases with protein concentration and annealing (T_c 50 mg/ml non-annealed: -16°C, annealed: -14°C; 150 mg/ml non-annealed: -13°C, annealed: -10.5°C – Figure S3)
d) Creation of design spaces for different R_p

The purpose of the design space is to visually depict which T_{fluid} and P_c can be applied without overcoming the collapse temperature (T_c) of the processed formulation. Product temperature varies during the drying process: as the thickness of the dried layer (L_{dried}) increases, resistance to sublimation flow changes. Therefore, when building the design space, we considered the product temperature at the sublimating interface (T_i) when ice thickness (L_{frozen}) is at its minimum. As drying is almost completed, this temperature is the maximum T_i reached for the selected inputs (T_{fluid} and P_c). The design spaces were created by mathematical simulations in a T_{fluid} range between -30 and +30°C and P_c from 5 to 30 Pa. The input variables were kept constant over the complete primary drying phase. The in-silico determination was based on the assumptions that all heat received by the frozen product is used for sublimation (equation 5) and pseudo-stationary conditions that allow process evolution to be described as in equation 8. Additionally, considering that T_p can be described as function of T_i (equation 9), the whole process can be summarized in equation 10. Hence, the model considering the K_v- P_c / R_p-dried layer description allows the determination of T_i, sublimation flow, and consequently Tp and drying time when L_{frozen} is equal to 0. Among the different options to present the design space, we chose to plot the max T_i versus the P_c. in order to highlight which combination T_{fluid} / P_c were part of the design space by imposing the formulation constraint (T_c) (Figure 5).

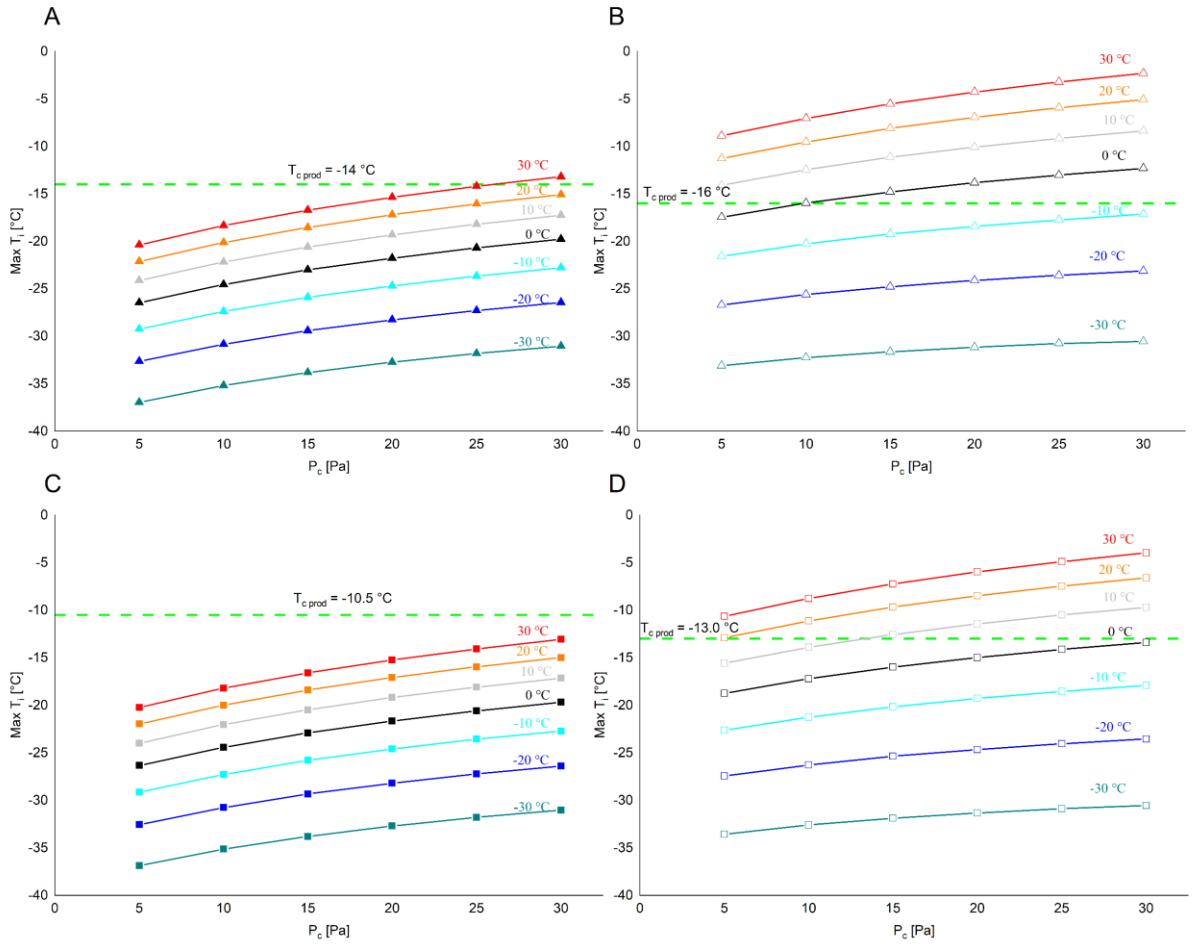

Figure 5: Design spaces for difference formulations and freezing options. The maximum values of T_i based on the input parameters (T_{fluid}, P_c) are plotted versus P_c. T_c (dashed line) is superimposed on the chart. Formulation 50 mg/ml 2-step freezing annealing (A) and 2-step freezing (B) and formulation 150 mg/ml 2-step freezing annealing (C) and 2-step freezing (D)

The first element of attention is the role of protein content that influences one of the design space borders, represented by the T_c. A second point is the influence of the different R_p on the shrinkage of the design space: a lower R_p, as in the case of annealing, creates a situation in which the freeze-dryer inputs (T_{fluid} and P_c.) have less influence on T_p and therefore can be set to higher values with a consequent shorter drying time. The collected data represent a valuable set of information that can accelerate the in-depth knowledge of the process and guide to a rational design of the freeze-drying cycle.

3.3.Verification of the freeze-drying cycle selected based on the design space

The generated design spaces were taken as a basis to experimentally verify the predicted parameters for the 150 mg/ml formulation. The verification cycle was planned at the highest considered T_{fluid} of +30°C and with a P_c of 11 Pa as midpoint of the tested range. According to our predictions, T_p should be in a range of -19.3 °C to -14 °C, respectively at the beginning and at the end of the primary drying (PD) holding phase respectively. The PD time was estimated in a range between 9.5 and 10.0 hours based on K_v variability.

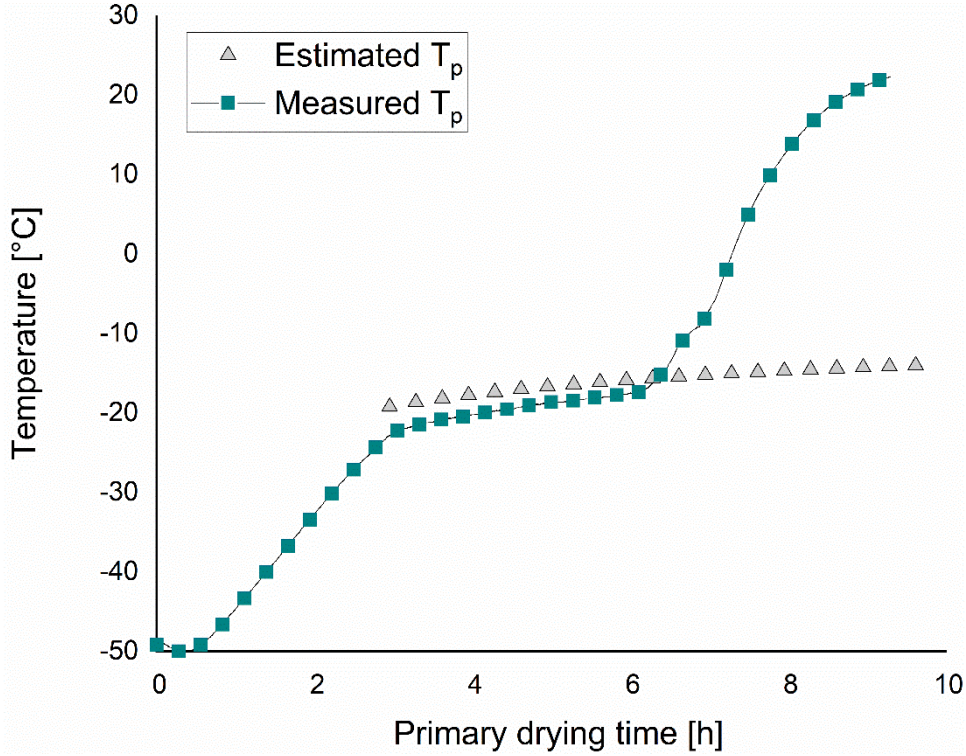

Figure 6: Comparison between T_P measured during verification freeze-drying cycle and T_P estimated from our mathematical simulation

For the verification cycle, T_p was in a range of -22 °C and -15 °C at the beginning and until the thermocouple ceased to provide a reliable output, respectively (Figure 6). The comparison between the measured and the estimated T_p was in good agreement.

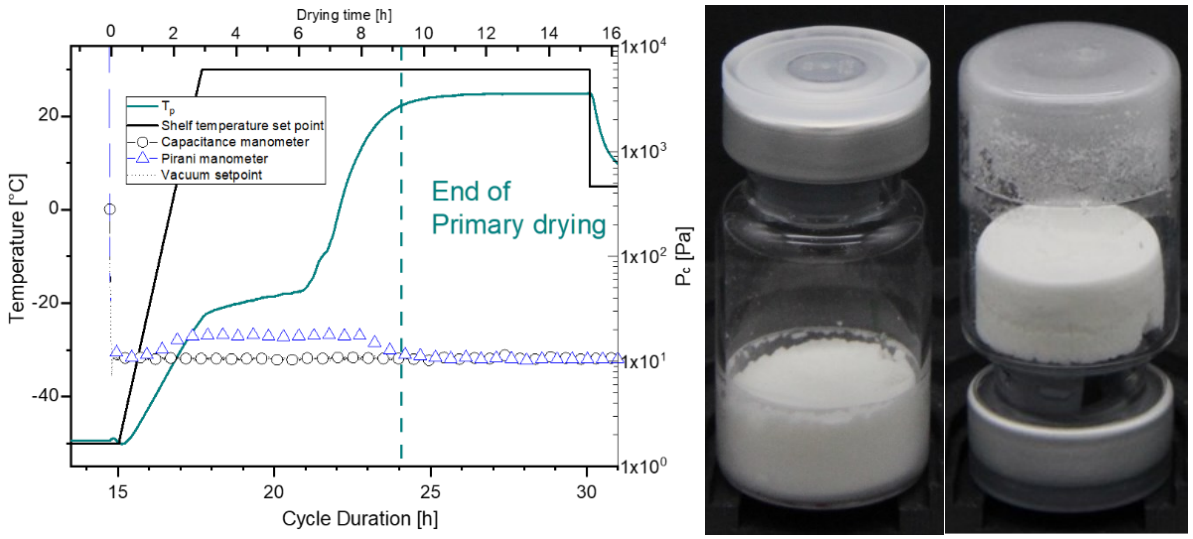

Figure 7: Drying phases (primary/secondary drying) of the verification freeze-drying cycle [150 mg / ml BSA formulation – 2FA protocol] (A) - Cake appearance of exemplary final product from verification freeze-drying cycle (B)

Additionally, the PD time equal to 9.3 hours in the verification cycle, was consistent with the expected range based on the design space. In fact, it must be considered that the PD endpoint was experimentally determined by the alignment between the capacitance probe and the Pirani gauge (Figure 7A) and an uncertainty of 12 min can be considered negligible due to the detection point and the limited amount of cycles performed.

The alignment between estimated and experimental results were corroborated by the characterization of the final lyophilized products. Macroscopically, pharmaceutically elegant cakes without signs of collapse were obtained with little vial to vial variability (Figure 7B). SEM demonstrated a crust-like layer with the presence of pores and cracks homogenously-distributed at the top and a central part characterized by pores of approx. 50 µm in diameter (Figure 8).

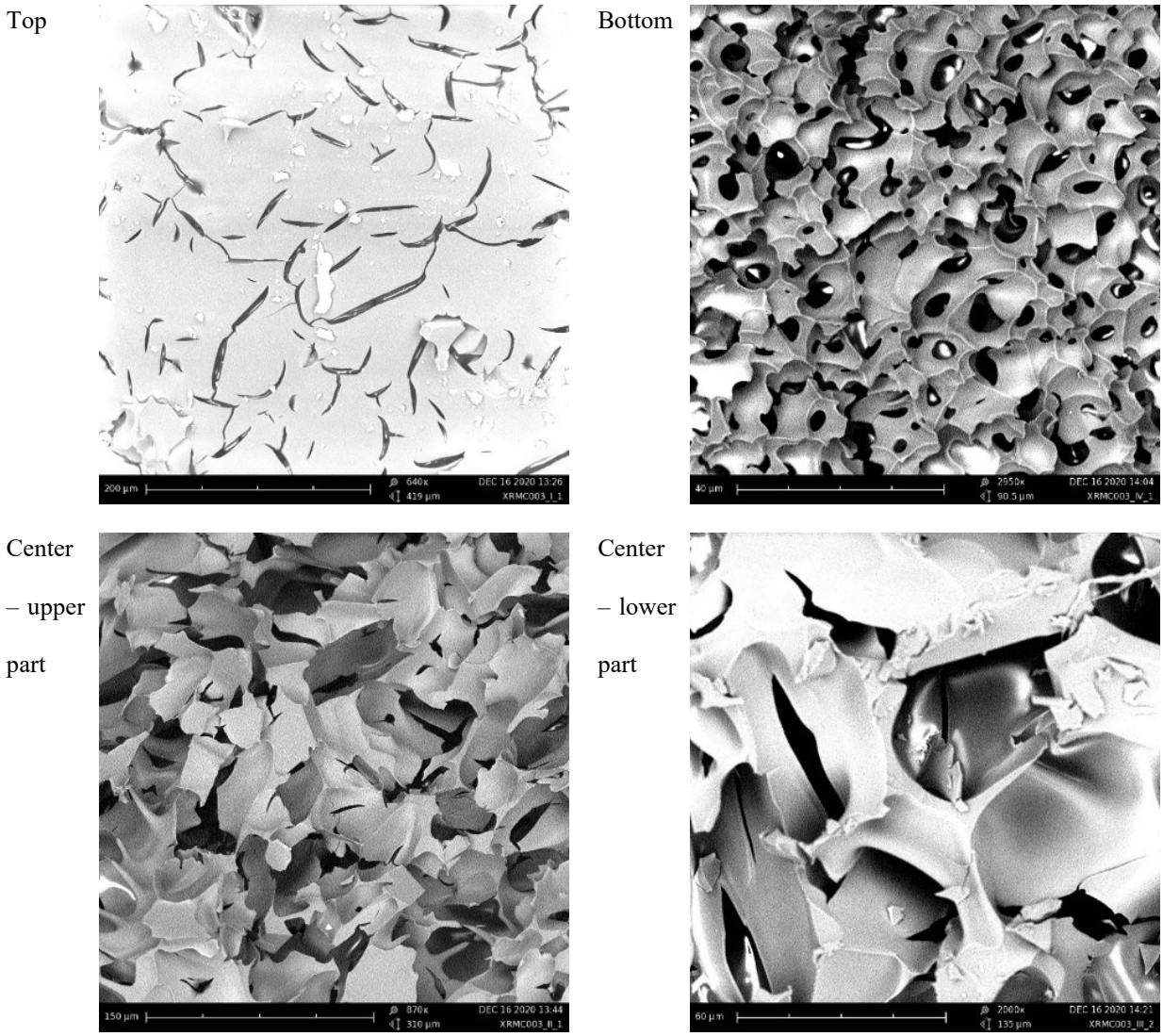

Figure 8: Scanning electron microscopy (SEM) exemplary images from final product of the verification freeze-drying cycle

The moisture level was low with 0.3 % ± 0.02 for center vials and 0.6 % ± 0.02 for edge vials. Thus, appearance and moisture level indicate that primary drying proceeded below T_c.

The verification was performed based on the data obtained in the Micro FD at minimal material and resource consumption considering the previously performed equipment characterization [26]. The suitability of the combination of MicroFD and HFS to create a primary drying design space for HCPFs was confirmed based on product characteristics, product temperature profiles and primary drying duration. A general work flow would be:

a. Definition of the T_{fluid} in the target freeze-dryer involved in the transfer (indicated as FD02), starting from the data obtained in the MicroFD (indicated as FD01)

$$T_{fluid\ FD02} = \frac{K_{v\ FD02}\left(\frac{1}{K_{v\ FD02}} + \frac{L_{frozen\ FD01}}{k_{frozen}}\right)T_{p\ FD01} + T_{i\ FD01}}{K_{v\ FD02}\left(\frac{1}{K_{v\ FD02}} + \frac{L_{frozen\ FD01}}{k_{frozen}}\right) - 1} \quad (11)$$

considering the heat transfer coefficients of FD02 for edge and center vials and the previous Micro FD characterization [24].

b. Process simulation to set drying time and expected product thermal profile.

4. Conclusions

In summary, we present an approach to define a primary drying design space for lyophilization of high concentration protein formulations utilizing the HFS integrated into a MicroFD with only two lyophilization cycles, each of 19 vials. T_p and end of PD could be predicted well, and a collapse-free and low moisture content product was obtained. Furthermore, a correction of the HFS-based K_v by a constant offset is required but it allows a reliable R_p determination in this case study. Using a design space fed by HFS-based inputs in a MicroFD enables rapid assessment of the impact of operating parameters on product quality and process efficiency by optimization of the drying time. A drawback of the HFS-based K_v determination is the necessity to correct for a constant in the case of higher protein content. Nevertheless, future investigations should focus on quantifying the role of key variables such as the filling volume and the intra-batch homogeneity in affecting the offset between the gravimetric and the HFS-based technique, especially for lower protein content formulations. This work highlights the possibility of integrating the new HFS and MicroFD technologies in a design space application to fully implement a QbD approach whilst minimizing material usage and invested time.

Acknowledgement

The authors acknowledge Millrock Technology Inc. (Kingston, NY, USA) for the helpful technical support.

Declaration of Competing Interest

The authors declare that they have no known competing financial interests or personal relationships that could have appeared to influence the work reported in this paper.

Funding

This research did not receive any specific grant from funding agencies in the public, commercial, or not-for-profit sectors.

5. Abbreviations and Nomenclature

A_v	cross sectional area of vial (m^2)
BSA	bovine serum albumin
ΔH_s	sublimation heat ($J\ kg^{-1}$)
Δm	sublimed mass (kg)
Δt	considered drying time (s)
F	1-step freezing
FD	freeze-dryer
grav	gravimetric
HCPF	high-concentration protein formulation
HFS	heat flux sensor
J_w	sublimation flux ($kg\ m^{-2}\ s^{-1}$)
K_v	vial heat transfer coefficient ($W\ m^{-2}\ K^{-1}$)
$K_{v\ grav}$	vial heat transfer coefficient ($W\ m^{-2}\ K^{-1}$) gravimetric-based
$K_{v\ HFS}$	vial heat transfer coefficient ($W\ m^{-2}\ K^{-1}$) HFS-based
k_{frozen}	thermal conductivity of the frozen layer ($W \cdot m^{-1} \cdot K^{-1}$)
L_{frozen}	thickness of frozen layer (m)
l_v	average distance between vial bottom to the shelf (m^{-1})
λ_0	thermal conductivity of the gas at ambient pressure ($W \cdot m^{-1} \cdot K^{-1}$)
P_c	chamber pressure (Pa)
P_i	pressure at the sublimating interface (Pa)
PVDF	polyvinylidene difluoride
Q	heat received by a vial ($W\ m^{-2}$)
QbD	Quality by Design
Q_{HFS}	heat measured from heat flux sensor ($W\ m^{-2}$)
RH	relative humidity
R_p	product resistance ($m\ s^{-1}$)
ρ_{dried}	apparent density of the dried product ($kg\ m^{-3}$)
ρ_{frozen}	density of the frozen product ($kg\ m^{-3}$)

t	time (s)
T_{fluid}	temperature of fluid circulating in the shelf (°C)
T_i	temperature at the sublimating interface (°C)
T_p	product temperature (°C)
$T_{shelf\ surface}$	shelf surface temperature as measured by heat flux sensor (°C)
T_c	collapse temperature (°C)
V_{fill}	filling volume (ml)
2F	2-step freezing
2FA	2-step freezing and annealing
3-PE	3-pressure experiment

6. References

[1] K.R. Ward, P. Matejtschuk, Lyophilization of Pharmaceuticals and Biologicals: New Technologies and Approaches, Humana Press, 2019. http://www.springer.com/series/7653.

[2] C. Narasimhan, H. MacH, M. Shameem, High-dose monoclonal antibodies via the subcutaneous route: Challenges and technical solutions, an industry perspective, Ther Deliv. 3 (2012) 889–900. https://doi.org/10.4155/tde.12.68.

[3] F. Cilurzo, F. Selmin, P. Minghetti, M. Adami, E. Bertoni, S. Lauria, L. Montanari, Injectability evaluation: An open issue, AAPS PharmSciTech. 12 (2011) 604–609. https://doi.org/10.1208/s12249-011-9625-y.

[4] S.J. Shire, Z. Shahrokh, J.U.N. Liu, Challenges in the Development of High Protein Concentration Formulations, J Pharm Sci. 93 (2004) 1390–1402.

[5] J.C. Kasper, W. Friess, The freezing step in lyophilization: Physico-chemical fundamentals, freezing methods and consequences on process performance and quality attributes of biopharmaceuticals, European Journal of Pharmaceutics and Biopharmaceutics. 78 (2011) 248–263. https://doi.org/10.1016/j.ejpb.2011.03.010.

[6] P. Garidel, I. Presser, Lyophilization of high-concentration protein formulations, Lyophilization of Pharmaceuticals and Biologicals: New Technologies and Approaches. (2019) 291–325.

[7] X.C. Tang, M.J. Pikal, M.P.-P. research, undefined 2004, M.J. Pikal, Design of Freeze-Drying Processes for Pharmaceuticals: Practical Advice, Springer. 21 (2004) 191–200. https://doi.org/10.1023/B:PHAM.0000016234.73023.75.

[8] J.S.; Colandene, James D.; Maldonado Linda M.; Creagh, Alam T.; Vrettos, T.M.; Goad, Keneeth G.; Spitznagel, Lyophilization cycle development for a high-concentration monoclonal antibody formulation lacking a crystalline bulking agent, J Pharm Sci. 96 (2007) 1598–1608. https://doi.org/10.1002/jps20812.

[9] A. Butreddy, N. Dudhipala, K.Y. Janga, R.P. Gaddam, Lyophilization of Small-Molecule Injectables: an Industry Perspective on Formulation Development, Process Optimization, Scale-Up Challenges, and Drug Product Quality Attributes, AAPS PharmSciTech. 21 (2020). https://doi.org/10.1208/s12249-020-01787-w.

[10] D. Fissore, R. Pisano, A.A. Barresi, Advanced approach to build the design space for the primary drying of a pharmaceutical freeze-drying process, J Pharm Sci. 100 (2011) 4922–4933. https://doi.org/10.1002/jps.22668.

[11] S. Cullen, E. Walsh, V. Gervasi, D. Khamar, T.R. McCoy, Technical transfer and commercialisation of lyophilised biopharmaceuticals — application of lyophiliser characterisation and comparability, AAPS Open. 8 (2022). https://doi.org/10.1186/s41120-022-00059-0.

[12] B. Scutellà, I.C. Trelea, E. Bourlès, F. Fonseca, S. Passot, Determination of the dried product resistance variability and its influence on the product temperature in pharmaceutical freeze-drying, European Journal of Pharmaceutics and Biopharmaceutics. 128 (2018) 379–388. https://doi.org/10.1016/j.ejpb.2018.05.004.

[13] M.J. Pikal, M.L. Roy, S. Shah, Mass and heat transfer in vial freeze-drying of pharmaceuticals: Role of the vial, J Pharm Sci. 73 (1984) 1224–1237. https://doi.org/10.1002/jps.2600730910.

[14] A. Giordano, A.A. Barresi, D. Fissore, On the use of mathematical models to build the design space for the primary drying phase of a pharmaceutical lyophilization process, J Pharm Sci. 100 (2011) 311–324.

[15] H. Kawasaki, T. Shimanouchi, Y. Kimura, Recent Development of Optimization of Lyophilization Process, J Chem. 2019 (2019). https://doi.org/10.1155/2019/9502856.

[16] S. Hibler, C. Wagner, H. Gieseler, Vial freeze-drying, part 1: New insights into heat transfer characteristics of tubing and molded vials, J Pharm Sci. 101 (2012) 1189–1201. https://doi.org/10.1002/jps.23004.

[17] R. Pisano, D. Fissore, A.A. Barresi, P. Brayard, P. Chouvenc, B. Woinet, Quality by design: Optimization of a freeze-drying cycle via design space in case of heterogeneous drying behavior and influence of the freezing protocol, Pharm Dev Technol. 18 (2013) 280–295. https://doi.org/10.3109/10837450.2012.734512.

[18] W.Y. Kuu, K.R. Obryan, L.M. Hardwick, T.W. Paul, Product mass transfer resistance directly determined during freeze-drying cycle runs using tunable diode laser absorption spectroscopy (TDLAS) and pore diffusion model, Pharm Dev Technol. 16 (2011) 343–357. https://doi.org/10.3109/10837451003739263.

[19] S. Bosca, A.A. Barresi, D. Fissore, Use of soft sensors to monitor a pharmaceuticals freeze-drying process in vials, Pharm Dev Technol. 19 (2014) 148–159. https://doi.org/10.3109/10837450.2012.757786.

[20] H. Gieseler, T. Kramer, M.J. Pikal, Use of manometric temperature measurement (MTM) and SMART™ freeze dryer technology for development of an optimized freeze-drying cycle, J Pharm Sci. 96 (2007) 3402–3418.

[21] A. Kauppinen, Raman and near-infrared spectroscopic methods for in-line monitoring of freeze-drying process, University of Eastern Finland, 2015.

[22] C. Moino, E. Bourles, R. Pisano, B. Scutella, In-line monitoring of the freeze-drying process by means of heat flux sensors, Ind Eng Chem Res. 60 (2021) 9637–9645.

[23] I. Vollrath, W. Friess, A. Freitag, A. Hawe, G. Winter, Comparison of ice fog methods and monitoring of controlled nucleation success after freeze-drying, Int J Pharm. 558 (2019) 18–28. https://doi.org/10.1016/j.ijpharm.2018.12.056.

[24] M. Carfagna, M. Rosa, M. Lucke, A. Hawe, W. Frieß, Heat flux sensor to create a design space for freeze-drying development, European Journal of Pharmaceutics and Biopharmaceutics. 153 (2020) 84–94. https://doi.org/10.1016/j.ejpb.2020.05.028.

[25] J.M. Goldman, X. Chen, J.T. Register, V. Nesarikar, L. Iyer, Y. Wu, N. Mugheirbi, J. Rowe, Representative Scale-Down Lyophilization Cycle Development Using a Seven-Vial Freeze-Dryer (MicroFD ®), J Pharm Sci. 108 (2019) 1486–1495. https://doi.org/10.1016/j.xphs.2018.11.018.

[26] M. Carfagna, M. Rosa, A. Hawe, W. Frieß, Design of freeze-drying cycles: The determination of heat transfer coefficient by using heat flux sensor and MicroFD, Int J Pharm. 621 (2022) 121763. https://doi.org/10.1016/j.ijpharm.2022.121763.

[27] D. Fissore, R. Pisano, A.A. Barresi, Model-based framework for the analysis of failure consequences in a freeze-drying process, Ind Eng Chem Res. 51 (2012) 12386–12397. https://doi.org/10.1021/ie300505n.

[28] S.A. Velardi, A.A. Barresi, Development of simplified models for the freeze-drying process and investigation of the optimal operating conditions, Chemical Engineering Research and Design. 86 (2008) 9–22. https://doi.org/10.1016/j.cherd.2007.10.007.

[29] P. Sane, Identification and Quantification of Heterogeneity in Freezing and Primary Drying Steps of Lyophilization, Doctoral Dissertations. (2016). http://opencommons.uconn.edu/dissertations/1099%0Ahttp://opencommons.uconn.edu/dissertations/1099/.

[30] S.L. Nail, S. Jiang, S. Chongprasert, S.A. Knopp, Fundamentals of freeze-drying, Development and Manufacture of Protein Pharmaceuticals. (2002) 281–360.

7. Appendix

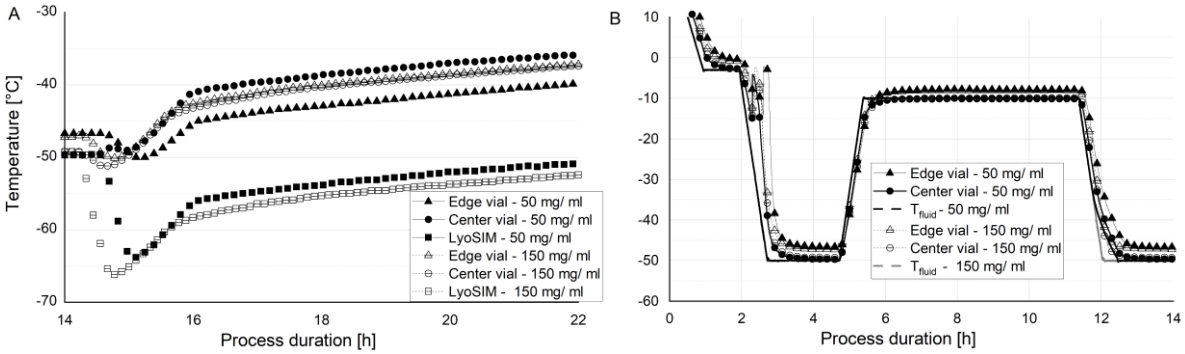

Figure S1: Comparison of temperature profiles of product temperature and LyoSIM for freeze-drying by using the 2-step freezing / annealing protocol during primary drying (A) and during freezing phase (B)

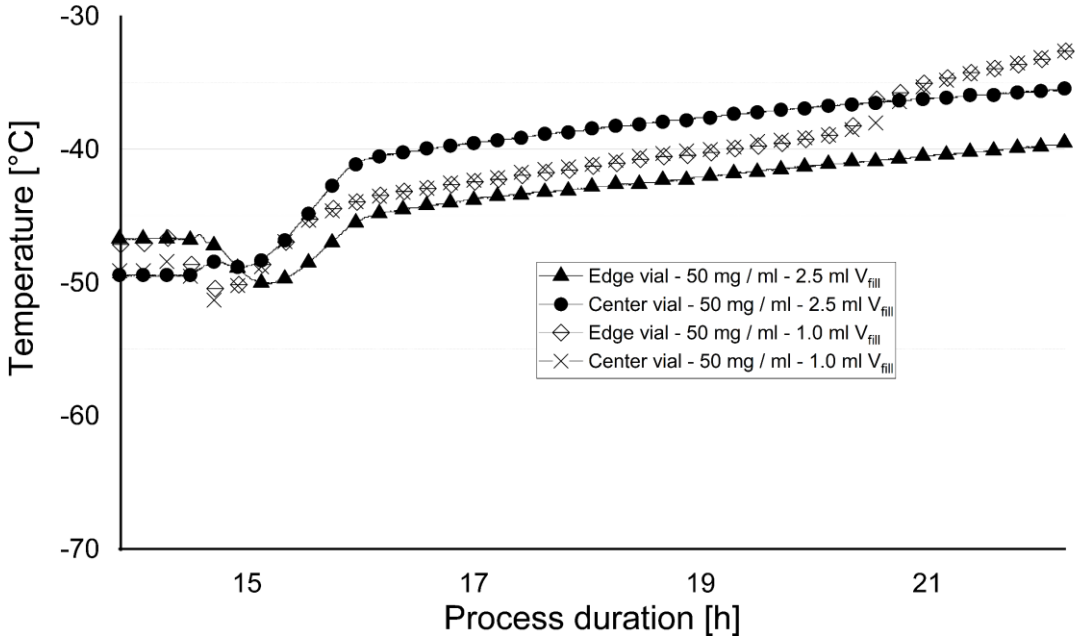

Figure S2: Comparison of temperature profiles for freeze-drying with 2-step freezing / annealing protocol 50 mg / ml formulation (△ edge vial, ○ center vial with a filling volume of 2.5 ml, ◊ edge vial, X center vial with a filling volume of 1.0 ml) during primary drying

Chapter VI: Final summary

In the last two decades, based on FDA and ICH initiatives, the quality by design (QbD) approach has gained a central role in the product development and manufacturing of the pharmaceutical sector. Simultaneously, the increasing number of biologics in the market raised the attention on the lyophilization, the main stabilizing technique.

The QbD approach with its process understanding and control can be implemented through process analytical technology (PAT) tools. The general goal of the thesis was to assess two innovative solutions in the hands of freeze-drying scientists, the heat flux sensor and the miniaturized equipment in the frame of the transfer of freeze-drying cycles.

Chapter I introduces the process considering main components of typical equipment and the three main phases. Subsequently, it is illustrated the difference between the traditional and the more recent approach represented by the QbD. The focus is then moved to the main PAT tools applied in the freeze-drying field with a classification according to the monitoring focus and the parameter of interest. Finally, a brief description of challenges related to the transfer of lyophilization.

One of the objectives of the thesis was the application of the heat transfer sensor to the transfer of freeze-drying cycle. Therefore, as described in **Chapter III**, we developed for the first time an HFS-based method to build a primary drying design space in a laboratory-scale equipment. Starting from the heat flux measured between shelf and vial, it was determined an HFS-based K_v. This allowed the possibility to obtain product resistance evolution during the process. The integration of this novel PAT tool with a mathematical model describing the process give the opportunity to predict product thermal profiles under different shelf temperatures and chamber pressures to create a design space. Consequently, lyophilization design can be substantially accelerated, even because the HFS approach allows the determination of R_p and multiple K_v values in one single experiment. To confirm HFS approach validity a freeze-drying transfer was performed by applying the design space generated from HFS data. The attractiveness of this PAT tools was strengthened by the final and IPC analyses of the transferred product. Nevertheless, HFS-based K_v was found constantly lower than the gravimetric K_v because a P_c-independent contribution is not considered.

To tackle this aspect and to exploit the potentialities of novel equipment, as next step, we characterized a miniaturized freeze-dryer, named as MicroFD, in **Chapter IV**. Besides the reduced size of the lyophilization

chamber, in our setup suitable for 19 vials (6R-type), this equipment presents a peculiar component, named LyoSIM, with the purpose to simulate larger freeze-dryer. The investigation was focused on the heat transfer and carried out with the state-of-the-art technique, the gravimetric, and the HFS based for two types of formulations, amorphous and crystalline. The LyoSIM is temperature-controlled ring that can be set according to an offset linked T_p or in absolute way. Therefore, we perform a screening of suitable temperature to simulate heat transfer as in the laboratory-scale. The minimum offset of -15 °C, compared to the most shielded vials, and the full load of the equipment were required to obtain satisfying results with a pronounced reduction in atypical heat transfer. This allowed an investigation on the role of atypical radiation in the HFS output by considering vials with low- and normal emissivity at different LyoSIM settings. The gained information confirmed that the HFS-based K_v are lower than the gravimetric K_v. Interestingly, the results in case of partial load of the equipment can only partially ascribed to radiation. The radial heat exchange appears to play a key role in the delta between HFS-based and gravimetric K_v.

Finally, the applicability of the combined use HFS and MicroFD to design a freeze-drying cycle was applied to high concentration protein formulations in **Chapter V**. The goal was to minimize the effort in term of material, invested time in order to have a successful design space and expected CQAs with an optimized primary drying time. Two protein concentrations and three different freezing protocols were investigated to highlight the effects on HFS output and its relation with the gravimetric technique. Additionally, a verification on the filling volume was performed for the lowest protein concentration. In our case study, annealing not only increased the intra-batch homogeneity, as expected, but also allowed a constant offset between HFS and gravimetric K_v. Thus, future studies should quantify the impact of freezing / filling volume in affecting the offset between the gravimetric and the HFS-based technique, especially for lower protein content formulations. Nevertheless, based only on two lyophilization cycles, each of 19 vials, a design space and a verification cycle were generated. Hence, by applying them, T_p and the end of the primary drying were well predicted, and a collapse-free and low moisture content product could be obtained. In summary, despite the highlighted sensor pitfall, it was the first time that the integration of HFS, MicroFD and design space was achieved with excellent product results by minimizing material, invested time and full implementation of QbD approach.

In conclusion, this thesis presented two extremely useful tools for designing and transfer freeze-drying cycles: the HFS and the MicroFD. Both sensor and miniaturized equipment combined with in-silico simulation can allow to study different scenarios with a limited amount of material and experiments. Additionally, the study on radiation

effect highlighted the contribution of radial heat exchange in the “edge” vials. Overall, this work represents a key contribution to establish HFS and MicroFD as routine techniques for freeze-drying scientists.

Appendix

List of publications

Heat flux sensor to create a design space for freeze-drying development

Marco Carfagna, Monica Rosa, Matthias Lucke, Andrea Hawe, Wolfgang Frieß,

European Journal of Pharmaceutics and Biopharmaceutics,

Volume 153,2020, Pages 84-94, ISSN 0939-6411, https://doi.org/10.1016/j.ejpb.2020.05.028.

Design of freeze-drying cycles: The determination of heat transfer coefficient by using heat flux sensor and MicroFD

Marco Carfagna, Monica Rosa, Andrea Hawe, Wolfgang Frieß,

International Journal of Pharmaceutics,

Volume 621, 2022,121763, ISSN 0378-5173, https://doi.org/10.1016/j.ijpharm.2022.121763.

Lyophilization cycle design for highly concentrated protein formulations supported by micro freeze-dryer and heat flux sensor

Marco Carfagna, Monica Rosa, Andrea Hawe, Wolfgang Frieß,

International Journal of Pharmaceutics,

Volume 643, 2023,123285, ISSN 0378-5173, https://doi.org/10.1016/j.ijpharm.2023.123285.